REMARKS/ARGUMENTS

After entry of this amendment, claims 11-19, 21-25, and 58-73 are pending. Claims 11-19, 21-25, and 58-73 are under consideration, claims 1-10 and 20 having been canceled, and new claims 58-73 having been added.

The term "preventing" has been replaced with "prophylaxis" in the claims. Previous claim 11 referred to "treating" and "preventing" in the same claim. Because "prophylaxis" is a noun and "treating" is a verb, it is grammatically awkward to refer to both in the same claim. Accordingly, treating and prophylaxis are now claimed in two independent claims 11 and 58, respectively. New independent claim 58 corresponds to previously presented claim 11. New claims 59-71, which depend from claim 58, correspond to claims 11-19 and 21-25, respectively. Support for new claims 72 and 73 is provided at *e.g.*, p. 50, line 11. Support for prophylaxis is provided at *e.g.*, p. 51, lines 17-19. Applicant addresses the Examiner's comments using the paragraph numbering of the office action.

¶3. The references cited by the information disclosure statements filed September 21, 2001 and August 16, 2002 include all the elements required to comply with 37 C.F.R. §§ 1.97-98 which are known to Applicant. A copy of citation number 187 is submitted herewith.

¶10. A petition for withdrawal of the restriction requirement is submitted herewith under separate cover.

¶¶11-27. Rejections under 35 USC 112, first paragraph. Due to the length of the rejection, applicants will address the Examiner's comments by paragraph number.

¶¶11-13. The Examiner summarizes the previous rejection, applicant's response, and the claims. No response is needed.

¶14. The Examiner alleges that Examples in the specification showing administration of Aβ42 with adjuvant reduces levels of Aβ in the brains of transgenic mice are not predictive of treatment of ATTR disease. The Examiner states that there are no examples directed to ATTR or art accepted ATTR models.

In response, it is submitted that the Examiner appears not to have considered much of the available evidence noted in the last response. The available evidence includes not only the Examples in the specification describing use of AB42. The specification also shows successful results for AB1-5 fragment and several monoclonal antibodies to Aβ. The specification also describes an example in which antibodies to various epitopes of Aβ and antibodies to synuclein were tested in an *ex vivo* assay for capacity to clear amyloid deposits from brain tissue in the presence of phagocytic cells (*see* pp. 113-117). The antibodies to Aβ were also tested in the PDAPP mouse model. The results from the *ex vivo* model show excellent correlation with those *in vivo*: antibody to Aβ that cleared deposits *ex vivo* also cleared deposits *in vivo*. Because antibodies to synuclein were found to clear amyloid deposits characteristic of Alzheimer's disease *ex vivo* and because of the excellent correlation between *ex vivo* and *in vivo* results, one would reasonable expect that antibodies to synuclein would also clear amyloid deposits *in vivo*. Thus, administration of synuclein with an adjuvant is reasonable expected to clear amyloid deposits in similar fashion to Aβ. Likewise, as the Examiner is aware, closely analogous results have been reported for administration of PrP or antibodies thereto. (*see* Sigurdsson *et al.*, *Am. J. Pathol.* 161, 13-17 (2002) (active administration); and, Sigurdsson *et al.*, *Neuroscience Letters* 336, 185-187 (2003) (passive administration), both of which are of record). Activity of other combinations of amyloid peptide and adjuvant can likewise be shown in analogous animal models of amyloid disease. Animal models of transthyretin-based disease were available in the early 1990's. (*See* Kohno *et al.*, *Am J. Pathol.*, 150[4]:1497-508 [1997]; Murakami *et al.*, *Am. J. Pathol.*, 141[2]:451-6 [1992]; and, Yi *et al.*, *Am. J. Pathol.*, 138[2]:403-12 [1991], copies of which are attached hereto.)

The available evidence also includes a high degree of similarity in amyloid deposits formed in different disease. Although the precursor proteins in different amyloid diseases do not share sequence homology or related native structure, the morphology and

properties of all amyloid fibrils are remarkably similar *see* Sunde *et al., J. Mol. Biol.*, 273:729-739 [1997]). All give similar high-resolution X-ray fiber diffraction patterns, consistent with a helical array of beta-sheets parallel to the fiber long axis, with the strands perpendicular to this axis irrespective of the nature of their precursor proteins (*Ibid*).

The burden is on the PTO to show lack of enablement, not for the applicant to prove enablement. *In re Marzocci*, 169 USPQ 367, 370 (CCPA 1971). If the evidence is in "equipoise," an inventor is "entitled to a patent." *In re Oetiker,* 24 USPQ2d 1443, 1447 (Fed. Cir. 1992) (Plager, J., concurring). Here, given the common structure of amyloid deposits in different diseases, the likelihood that immunization of any amyloid peptide with an adjuvant in an appropriate regime will generate antibodies, and the demonstration that antibodies to three different amyloid peptides (Aβ, synuclein, and PrP) have clearing activity against amyloid deposits, it is likely that what has been observed for Aβ in treatment of Alzheimer's disease is generally true for other amyloid peptides in treatment of other amyloidogenic diseases. In the circumstances, it is insufficient for the Examiner to allege unpredictability. Rather, the Examiner must provide a showing why notwithstanding the above evidence, it is more likely than not that the claimed methods would not be effective for other amyloidogenic diseases.

¶¶15-16. The Examiner alleges the specification is not enabling for prevention of ATTR disease or other amyloidogenic disease. In the context of preventive medicine, it is submitted that a regime does not have to achieve complete and total stoppage of disease in every patient to be considered a preventive treatment. Nevertheless, to speed prosecution, applicants have replaced reference to prevention in the claims with "prophylaxis."

¶¶17-18. The Examiner again alleges that results obtained using Aβ are not predictive of treatment of transthyretin-based disease. Applicants respond as above.

¶19. The Examiner again alleges that the methods are not enabled for prevention. Applicants respond as above.

¶20. The Examiner alleges that the specification does not provide guidance or examples that would enable use of fragments of transthyretin. The Examiner alleges that deletions, insertions or substitutions of amino aids can lead to structural and functional changes in biological activity and immunological properties (citing to Skolnick & Fetrow and Jobling & Holmes). The Examiner alleges that biological function and immunological recognition are unpredictable properties which must be experimentally determined. The Examiner also says that for small peptides, conjugation appears to be required for promoting an effective immune response.

It is respectfully submitted that the Examiner is giving undue emphasis to the alleged unpredictability of mutations on protein structure and function. The effect of mutations may in some instances be unpredictable, but this is not detrimental to enablement if it can be determined which agents have the desired effect by even a considerable amount of experimentation that is routine or based on the guidance of the specification.

> [E]xperimentation needed to practice the invention must not be undue experimentation. The key word is 'undue,' not 'experimentation.' The determination of what constitutes undue experimentation in a given case requires the application of a standard of reasonableness, having due regard for the nature of the invention and the state of the art...The test is not merely quantitative, since a considerable amount of experimentation is permissible, if it is merely routine, or if the specification in question provides a reasonable amount of guidance with respect to the direction in which the experimentation should proceed.
>
> *In re Wands*, 8 USPQ2d 1400, 858 F.2d 731, 737 (Fed. Cir. 1988).

The issue in *Wands* was whether the specification of the *Wands* patent enabled production of a class of antibodies having IgM isotype and a binding affinity of at least 10^9 M^{-1} using Kohler Milstein technology. As the Examiner is aware, Kohler Milstein technology is a classical technique that involves individualized screening of hybridomas to identify a subset with desired binding characteristics. Until the hybridomas have been screened, it is unpredictable which will have the desired characteristics. Nevertheless, the court found that "practitioners of

this art are prepared to screen negative hybridomas in order to find one that makes the desired antibody" (858 F.2d at 740). The *Wands* patent was held to be enabled.

Here, fragments and mutants of transthyretin can be screened using analogous methods and endpoints to those noted in the specification of Aβ. It is noted that animal models of transthyretin-based disease were available at the first priority date of the application. The number of fragments of transthyretin is not infinite and because many of the various possible fragments have overlapping sequences, the key regions of peptide needed for pharmacological activity can be determined by screening only a relatively small proportion of the total number of peptides. For example, if it is found that deletion of 20 amino acids from the C-terminus has no lowering of activity, then one can infer that deletions of fewer amino acids from the C-terminus will also not lower activity. Thus, by testing only a few of the possible fragments of transthyretin, one can predict whether any other fragment will have pharmacological activity. Other agents could be screened using the same transgenic animal model with an initial preliminary screen to show the antibody can elicit antibodies that bind to transthyretin (*see* specification at paragraph bridging pp. 31-32).

With respect to carrier molecules, the specification provides general guidance that carriers are likely to be required for shorter peptides (*see* specification at p. 44. lines 5-7). The specification also provides particular examples in which Aβ42 was found to be effective without a carrier and Aβ1-5 with a carrier (*see* specification at p. 82). With intermediate fragments sizes, it would be a routine matter to determine whether a carrier is required. For example, one could perform an initial screen with a carrier. If the desired activity is obtained, one could repeat the experiment without the carrier to determine whether the carrier contributed to the activity.

The relevant quanta of permissible experimentation for a genetic claim cannot be the aggregate of work required to produce each and every embodiment potentially encompassed by the claims. If this were the case, it would never be possible to have a generic claim encompassing an unlimited number of species. Such claims have been upheld in numerous patents including those in unpredictable arts. *See, e.g., Ex parte Mark*, 12 USPQ2d 1904 (BPAI 1989); and, *In re Angstadt*, 190 USPQ 214 (CCPA 1976). The breadth of claims is relevant only insofar as the different species encompassed by the claims require different adaptations of an

exemplified strategy. *See In re Strahilevitz*, 212 USPQ 561 (CCPA 1982) ("Although the invention is applicable to a large variety of haptens and antigens, the Examiner offered no reasons why these compounds would require *different techniques or process parameters*." *Ibid. at* p. 563 (emphasis supplied). Here, as discussed above, the application discloses a strategy of administering an agent and an adjuvant to generate antibodies against an amyloid component and thereby reducing or effecting prophylaxis of amyloid deposits. The application also provides examples of how agents can be screened for the desired activity using a transgenic mouse model. Other agents can be identified by routine repetition of the same procedure. Routine repetition of the same basic procedures to isolate additional agents operating according to the same principles to achieve the same results may require considerable experimentation but does not constitute undue experimentation.

¶21. The Examiner cites Palla as discussing a monoclonal antibody that is reactive with certain mutagenic forms of transthyretin found in diseased patients but not with transthyretin found in healthy individuals. The Examiner alleges that it is not clear whether fragments that generate this antibody or any other would be therapeutic. Applicants reiterate the above comments regarding the routine nature of screening fragments using the principles and strategy described in the application.

¶22. The Examiner again alleges the methods are not enabling for prevention. Applicants respond as above.

¶23. The Examiner notes that there are a number of distinct transthyretin-based diseases by different mutations of transthyretin. The Examiner takes the view that undue experimentation would be required on how each individual isoform and mutation will affect the immune system of the patient.

As discussed above, the application discloses a general strategy in which pharmaceutical compositions comprising an agent and adjuvant generate an antibody response against an amyloid component and thus remove the amyloid component or reduce its further accumulation in amyloid deposits in a subject. This strategy accommodates different

amyloidogenic diseases characterized by different amyloid components by appropriate selection of the agent in the composition. For example, to treat Alzheimer's disease, one can select an agent that generates an antibody response to Aβ, and to treat a transthyretin-based disease, one can select an agent that generates an antibody response to the transthyretin component of the disease. Insofar as different transthyretin-based diseases are characterized by different mutations of transthyretin, the different subtypes of disease can similarly be accommodated, if necessary, by selection of an agent that induces antibodies to the transthyretin form present in the appropriate subtype. Mutagenic variation between different forms of transthyretin-based disease does not, however, necessarily imply that a different agent is needed for treatment of each disease subtype. Although a particular mutation in transthyretin may be critically affect the path of disease, it is less likely to change substantially the immunoreactivity of the fragment. Thus, many antibodies against one form of transthyretin are likely to react with other forms notwithstanding mutagenic variation. By analogy, the antibodies shown to have pharmacological activity against prion-based disease by Sigurdsson et al., Neuroscience Letters 336, 185-187 (2003) were all raised against normal PrP rather than the pathogenic form, AScr. For these reasons, it is submitted that general strategy for design of pharmaceutical compositions can accommodate variations between transthyretin proteins in different types of transthyretin-based disease.

¶24. No comment is needed.

¶25. The Examiner again raises the issue whether results from Aβ and PrP are predictive of transthyretin-based disease. Applicants respond as above.

¶¶26-27. The Examiner summarizes the rejection. No additional comments are needed.

If the Examiner believes a telephone conference would expedite prosecution of this application, please telephone the undersigned at 650-326-2400.

Respectfully submitted,

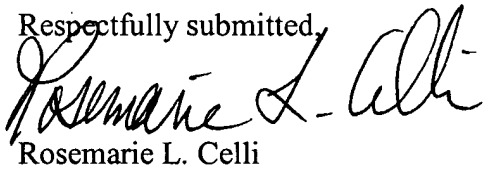

Rosemarie L. Celli
Reg. No. 42,397

TOWNSEND and TOWNSEND and CREW LLP
Two Embarcadero Center, Eighth Floor
San Francisco, California 94111-3834
Tel: 650-326-2400
Fax: 650-326-2422
Attachments (as noted)
RLC
60103238 v1

BEST AVAILABLE IMAGES

Defective images within this document are accurate representations of the original documents submitted by the applicant.

Defects in the images may include (but are not limited to):

- BLACK BORDERS
- TEXT CUT OFF AT TOP, BOTTOM OR SIDES
- FADED TEXT
- ILLEGIBLE TEXT
- SKEWED/SLANTED IMAGES
- COLORED PHOTOS
- BLACK OR VERY BLACK AND WHITE DARK PHOTOS
- GRAY SCALE DOCUMENTS

IMAGES ARE BEST AVAILABLE COPY.

As rescanning documents *will not* correct images, please do not report the images to the Image Problem Mailbox.

J. Mol. Biol. (1997) 273, 729–739

JMB

Common Core Structure of Amyloid Fibrils by Synchrotron X-ray Diffraction

Margaret Sunde*, Louise C. Serpell, Mark Bartlam, Paul E. Fraser Mark B. Pepys and Colin C. F. Blake

Laboratory of Molecular Biophysics, University of Oxford, Rex Richards Building South Parks Road, Oxford OX1 3QU, UK

**Corresponding author*

Tissue deposition of normally soluble proteins as insoluble amyloid fibrils is associated with serious diseases including the systemic amyloidoses, maturity onset diabetes, Alzheimer's disease and transmissible spongiform encephalopathy. Although the precursor proteins in different diseases do not share sequence homology or related native structure, the morphology and properties of all amyloid fibrils are remarkably similar. Using intense synchrotron sources we observed that six different *ex vivo* amyloid fibrils and two synthetic fibril preparations all gave similar high-resolution X-ray fibre diffraction patterns, consistent with a helical array of β-sheets parallel to the fibre long axis, with the strands perpendicular to this axis. This confirms that amyloid fibrils comprise a structural superfamily and share a common protofilament substructure, irrespective of the nature of their precursor proteins.

Keywords: amyloid; fibre; X-ray diffraction; protofilament; structure

Introduction

Amyloidosis is the extracellular deposition of insoluble protein fibrils leading to tissue damage and disease (Pepys, 1996; Tan *et al.*, 1995; Kelly, 1996). The fibrils form when normally soluble proteins and peptides self-associate in an abnormal manner (Kelly, 1997). Amyloid is associated with serious diseases including systemic amyloidosis, Alzheimer's disease, maturity onset diabetes, and the prion-related transmissible spongiform encephalopathies (Table 1). There is no specific treatment for amyloid deposition and these diseases are usually fatal. The subunits of amyloid fibrils may be wild-type, variant or truncated proteins, and similar fibrils can be formed *in vitro* from oligopeptides and denatured proteins (Bradbury *et al.*, 1960; Filshie *et al.*, 1964; Burke & Rougvie, 1972). The nature of the polypeptide component of the fibrils defines the character of the amyloidosis.

Despite large differences in the size, native structure and function of amyloidogenic proteins, all amyloid fibrils are of indeterminate length, unbranched, 70 to 120 Å in diameter, and display pathognomonic green birefringence when viewed in polarized light after staining with Congo Red (Pepys, 1996). Early X-ray diffraction examinations of amyloid fibrils (Bonar *et al.*, 1967; Eanes & Glenner, 1968) gave simple patterns with 4.7 to 4.8 Å meridional reflections and 10 Å equatorial reflections, arising from the molecular spacings present within the regularly repeating, ordered structural elements of the fibrils. They are characteristic of a cross-β structure (Pauling & Corey, 1951) in which the polypeptide chain is organized in β-sheets arranged parallel to the fibril axis with their constituent β-strands perpendicular to the fibril axis. This distinctive fibre diffraction pattern led to the amyloidoses being called the β-fibrilloses (Glenner, 1980a,b), and the fibril protein of Alzheimer's disease was named the β-protein before its secondary structure was known (Glenner & Wong, 1984). The characteristic cross-β diffraction pattern, together with the fibril appearance and tinctorial

Present addresses: M. Sunde, Oxford Centre for Molecular Sciences, University of Oxford, New Chemistry Laboratory, South Parks Road, Oxford OX1 3QT, UK; L. C. Serpell, Center for Research in Neurodegenerative Diseases, University of Toronto, Tanz Neuroscience Building, Queen's Park Crescent West, Toronto M5S 3H2, Canada; P. E. Fraser, Center for Research in Neurodegenerative Diseases and Department of Medical Biophysics, University of Toronto, Tanz Neuroscience Building, Queen's Park Crescent West, Toronto M5S 3H2, Canada; M. B. Pepys, Immunological Medicine Unit, Royal Postgraduate Medical School, Hammersmith Hospital, Du Cane Road, London W12 0NN, UK.

0022-2836/97/430729-11 $25.00/0/mb971348

Table 1. Diversity of amyloid fibril proteins

Clinical syndrome	Fibril subunit	Cross-β pattern	Structure of precursor	Reference to structure
Monoclonal protein systemic (AL) amyloidosis	Full-length or fragments of V_L domain of Ig light chain	*	All β	Schormann *et al.* (1995)
Reactive systemic (AA) amyloidosis	76-residue N-terminal fragment of amyloid A protein	*	α/β	Turnell *et al.* (1986b)
Familial amyloidotic polyneuropathy	Full-length or fragments of transthyretin variants	*	All β	Hamilton *et al.* (1993)
Hereditary apoAI amyloidosis	N-terminal fragments (~90 residues) of apoAI variants	*	(α/β)	Nolte & Atkinson (1992)
Hereditary lysozyme amyloidosis	Full-length lysozyme variants	*	α + β	Booth *et al.* (1997)
Type II diabetes mellitus	37-residue fragment of islet-amyloid polypeptide	*	Unknown	
Alzheimer's disease	1-39 to 43 residue Aβ protein	†	α, β or coil	Barrow *et al.* (1992)
Insulin-related amyloid	Full-length wild-type insulin	†	α + β	Adams *et al.* (1969)
Transmissible spongiform encephalopathies	Full-length or fragments of prion protein	†	α + β	Harrison *et al.* (1997)
Medullary carcinoma of the thyroid	Fragments of calcitonin	†	Unknown	
Senile systemic amyloidosis	Full-length or fragments of wild-type transthyretin	‡	All β	Blake *et al.* (1978)
Hemodialysis-related amyloidosis	Full-length, wild-type β_2-microglobulin	‡	All β	Becker & Reeke (1985)
Isolated atrial amyloidosis	Atrial natriuretic factor	‡	Unknown	
Hereditary cerebral amyloid angiopathy	110-residue fragment of variant cystatin-C	‡	α + β	Bode *et al.* (1988)
Finnish hereditary amyloidosis	71-residue fragment of gelsolin variants	‡	α/β	Burtnick *et al.* (1996)
Hereditary fibrinogen α-chain amyloidosis	Fragments of fibrinogen α-chain variants	‡	Unknown	

Key to symbols: *, this work; †, see the text for reference; ‡, no diffraction evidence; (α/β), secondary structure prediction.

properties are now the accepted diagnostic hallmarks of amyloid, and suggest that the fibrils, although formed from quite different protein precursors, share a degree of structural similarity.

In order to determine the extent and nature of this similarity we have used intense synchrotron X-ray beams to obtain the first high-resolution diffraction patterns from a range of different *ex vivo* and synthetic amyloid fibrils. Amyloid fibrils were isolated from patients with, respectively: monoclonal λ immunoglobulin light chain amyloidosis (Pepys, 1996); reactive systemic amyloid A protein amyloidosis (Pepys, 1996) and hereditary amyloidosis caused by Leu60Arg variant apolipoprotein A-I (Soutar *et al.*, 1992); Asp67His variant lysozyme (Pepys *et al.*, 1993; Booth *et al.*, 1997); and two different transthyretin variants, Val30Met and Gly47Val (Booth *et al.*, 1994). Synthetic fibrils were prepared from a peptide corresponding to residues 10 to 19 (β-strand A) of transthyretin, and from a peptide with the sequence of residues 20 to 29 of the islet-associated polypeptide (IAPP).

The high-resolution meridional X-ray pattern and a common repeat on the fibril axis

The synchrotron X-ray diffraction patterns from these different fibril preparations are shown in Figure 1 and the spacings of the reflections are listed in Table 2. These high-resolution patterns are dominated by the cross-β reflections but they also contain groups of additional reflections that have not been observed previously in other amyloid diffraction patterns. Despite the known, large differences in the lengths and folding conformations of the polypeptide chains of the precursors, the major features of the diffraction patterns from the various amyloid fibrils are clearly very similar.

The meridional diffraction pattern derives from the ordered molecular structures along the length of the amyloid fibril. The presence of reflections on the meridian out to 2 Å indicates that the individual fibrils have highly ordered internal structures along the fibre axis. The intense reflection at 4.7 to 4.8 Å that dominates the meridional diffraction patterns of amyloid fibrils is derived from the mean separation of the hydrogen-bonded β-strands that are arranged perpendicular to the fibre axis in the cross-β structure (Figure 2). In addition to this intense reflection, the synchrotron radiation has also revealed several weaker, higher-angle reflections, occurring in this range of diverse amyloids, that have not been reported previously. These reflections include a second order of the 4.7 to 4.8 spacing, at 2.4 Å.

In some of the amyloid samples (Figure 1(b), (d), (e) and (f), the intense "4.7 Å" reflection can be seen to be a close doublet, with components at 4.82 Å and 4.63 Å. In patterns where this doublet cannot be resolved its presence can be inferred from the observation that the calculated first order of the second harmonic of the 4.7 Å spacing, found at 2.39 to 2.41 Å, maps to the extreme inner edge of the intense 4.7 Å reflection, leaving space for a 4.6 Å component within the overall intensity envelope. The weaker, higher-angle reflections occur at closely similar spacings in the different samples. For example, reflections with spacings of 3.2 Å, 2.8 to 2.9 Å, 2.22 to 2.27 Å and 2.00 to 2.02 Å occur frequently, and reflections with spacings of 2.39 to 2.41 Å (the second order of the intense 4.82 Å reflection) are present in all of the amyloid samples that we have examined at high resolution. Because these reflections are very weak, even in relatively well oriented patterns, their absence from certain images may simply indicate that they are too weak to be observed above the noise level in those patterns. The observed similarity over the medium- and high-angle regions of the meridional X-ray pattern can only occur if the fibrils have well-defined and closely similar molecular structures, at least insofar as their ordered core components are concerned.

The observed meridional spacings can be fitted to the same repeat distance for each pattern, namely 115 Å (Table 2). The observed spacings for many of the reflections can also be fitted to a fundamental repeat of 28.8 to 29.9 Å to give orders of diffraction of 6 through 14 for spacings from 4.8 Å to 2.00 Å. However, this fit does not include all observed reflections. It is possible to include these if it is assumed that the 28.8 to 28.9 Å distance represents a pseudo-repeat and that the true repeat is four times as long, being 115.1 to 115.6 Å. As Table 2 indicates, all of the observed meridional reflections can be indexed on this longer repeat and this indexing can be carried out separately for the diffraction patterns from each type of amyloid fibril to give almost identical repeat distances. The ability to index the meridional spacings from each different fibril preparation to essentially the same unit cell edge indicates a close similarity in the underlying core molecular structure of all of these samples. This similarity is evidence that the protofilament structure of amyloid fibrils is common across the diverse range of fibril samples examined here, regardless of the constituent protein or the number of protofilaments making up the fibril.

The most intense features of the X-ray patterns we show here correspond to those previously reported for other amyloid fibrils (Table 1), including those from full-length (Kirschner *et al.*, 1986; Gorevic *et al.*, 1987) and fragments of the Alzheimer's disease Aβ peptide (Kirschner *et al.*, 1987; Fraser *et al.*, 1991; Inouye *et al.*, 1993), amyloid A protein (Turnell *et al.*, 1986a), calcitonin (Gilchrist & Bradshaw, 1993), insulin (Burke & Rougvie, 1972), and synthetic peptides of transthyretin (Jarvis *et al.*, 1993) and the prion protein (Come *et al.*, 1993; Tagliavini *et al.*, 1993; Nguyen *et al.*, 1995). The lack of high-resolution data, beyond the basic cross-β reflections, has limited further analysis of the molecular structures of these fibrils.

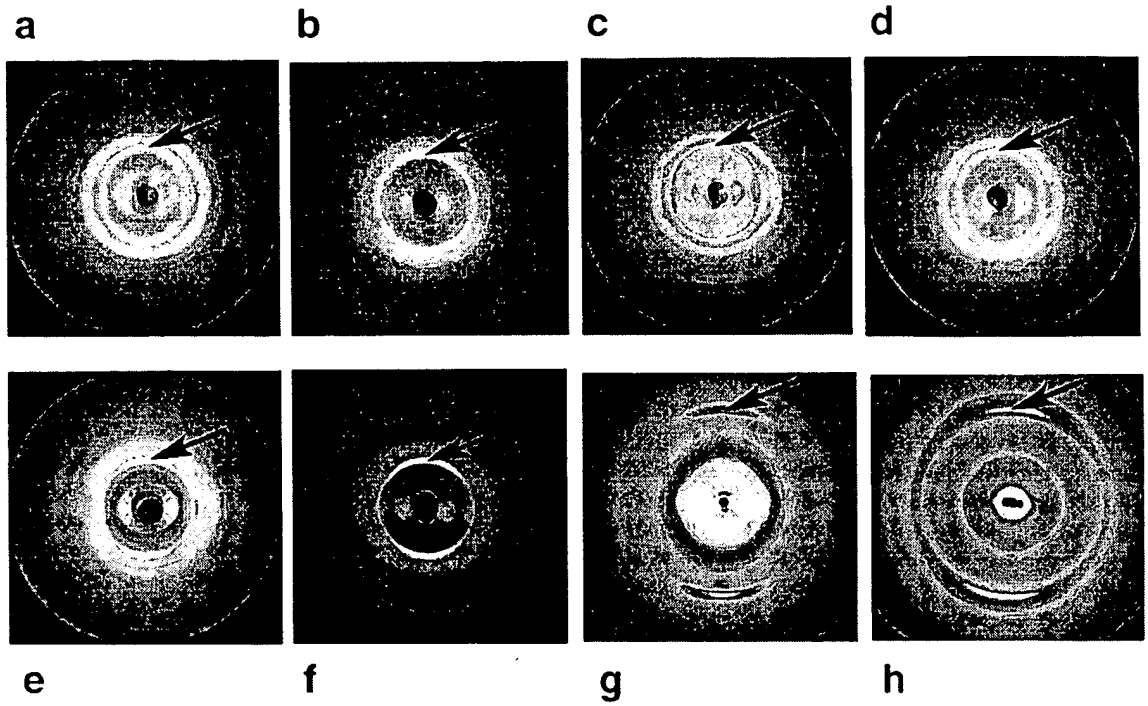

Figure 1. X-ray fibre diffraction patterns from *ex vivo* and synthetic amyloid fibrils. X-ray fibre diffraction patterns from eight different types of amyloid fibril, prepared as described below. The meridional axis (direction parallel to the fibril axis) is the vertical axis in this display. Amyloid fibril samples as follows: (a) ATTR2, Gly47Val transthyretin; (b) ATTR1, Val30Met transthyretin; (c) AAPOAI, Leu60Arg apolipoprotein A-I; (d) AL, monoclonal λ immunoglobulin light chain; (e) FTTR, peptide with the sequence of the A-strand of human transthyretin; (f) FIAPP, peptide with the sequence of residues 20 to 29 of the islet-associated polypeptide; (g) AA, amyloid A protein; (h) ALys, Asp67His lysozyme. Amyloid fibrils were isolated, as described by Nelson *et al.* (1991), from spleens of patients with different types of systemic amyloidosis and prepared for X-ray examination on a stretch frame. A droplet of fibril suspension (5 to 10 mg/ml in distilled water) was placed between two tubes and allowed to dry at room temperature, during which time the distance between the ends of the capillaries was increased slowly, by small increments, to stretch out the fibrils and encourage alignment. The peptides were synthesized by standard peptide synthesis chemistry and were dissolved in distilled water at a concentration of 10 mg/ml to produce amyloid fibrils. The solution, in a siliconized capillary tube, was then placed in a 2 T magnetic field to facilitate alignment of the fibrils during their formation and was allowed to dry at room temperature for about ten days. X-ray fibre diffraction patterns were collected at user station ID2 on beamline 4 at the European Synchrotron Research Facility (ESRF) at Grenoble, France (wavelength 0.9515 Å), at station 7.2 at the Synchrotron Radiation Source (SRS) at Daresbury, UK (wavelength 1.488 Å) or in-house using a Cu Kα Rigaku rotating-anode source (wavelength 1.5418 Å). All images were collected on MARResearch image plate X-ray detectors (180 or 300 mm diameter). Various exposure times were used for the different samples to optimize the detection of reflections. The images were collected on different beamlines, with varying wavelengths, beam-stops and sample-to-detector distances; these variations account for the differences in relative intensities and positions of the beam stop between images. The fibre diffraction patterns were analysed using the display program IPDISP, run on a Hewlett Packard workstation (ESRF) and a Digital workstation (Oxford). Spacings were measured in triplicate and on both sides of the patterns. False colour images were produced with the program PROFIDA (Lorenz & Holmes, 1993).

Differences in the equatorial reflections

The equatorial X-ray reflections relate to the fibril structure perpendicular to the fibre direction. Because the crystalline order in fibres is usually much lower in directions perpendicular to the fibre axis than parallel to the axis, the equatorial reflections from amyloid fibrils are weaker and broader than their meridional equivalents (Figure 1, Table 3). Early diffraction studies of amyloid (Bonar *et al.*, 1967; Eanes & Glenner, 1968) demonstrated a single equatorial reflection with a spacing of about 10 Å. As the intensities of the equatorial reflections are determined by the structure of the fibrils projected down the fibre axis, this reflection has been identified as representing the spacing of the β-sheets in the amyloid fibril.

The use of synchrotron radiation has revealed a more detailed equatorial diffraction pattern in which there are both additional reflections and also greater spatial resolution of the previously observed reflections. The synchrotron patterns do, however, exhibit broad maxima at around 10 Å and 5 Å, characteristic of β-sheets separated by

Table 2. Meridional reflections

σ	0.59	0.37	0.099	0.46	0.28	0.61	0.47	0.35
	ATTR1	ATTR2	AL	AApoAI	ALys	AA	FTTR	FIAPP
Order								
24	4.84	4.84	4.82	4.79	4.80	4.76	4.80	4.83
25	4.64	4.60	4.62	4.64	4.63	4.60	4.58	4.60
26				4.42	4.46			
27								
(n-i)	4.11		4.13	4.12	4.13	4.14		
28								
29								
30								
(o-m)	3.83	3.85	3.85					3.83
31				3.73	3.73	3.72	3.71	
32			3.61					
33								
34				3.40				
35								
36							3.21	
37				3.13				
38								
39								
40				2.90				
41		2.82					2.82	
42								
43								
44							2.61	
45								
46								
47								
48	2.39	2.41	2.41	2.39	2.40		2.39	2.41
49								
50								
51			2.27				2.25	
52								2.22
53				2.17				
54								
55								
56								
57								
58				2.00			2.00	
cell	115.37	115.39	115.61	115.46	115.56	115.12	115.13	115.48

Spacing (in Å) of all meridional reflections measured from diffraction patterns, with the corresponding order of the indexed reflections. Calculated cell edge dimension (along the meridian) given for each fibril sample (with standard deviation). Samples as follows: ATTR1, Val30Met variant transthyretin; ATTR2, Gly47Val variant transthyretin; AL, monoclonal λ immunoglobulin light chain; AApoAI, Leu60Arg variant apolipoprotein A-I; ALys, Asp67His variant lysozyme; AA, amyloid A protein; FTTR, peptide with the sequence of the A-strand of wild-type human transthyretin; FIAPP, peptide with the sequence of residues 20 to 29 of the islet-associated polypeptide. (o-m), off-meridional reflection; (n-i), the reflections do not index to the common cell edge dimension. There is evidence from other studies that this spacing arises from lipid contamination (Damas *et al.*, 1995).

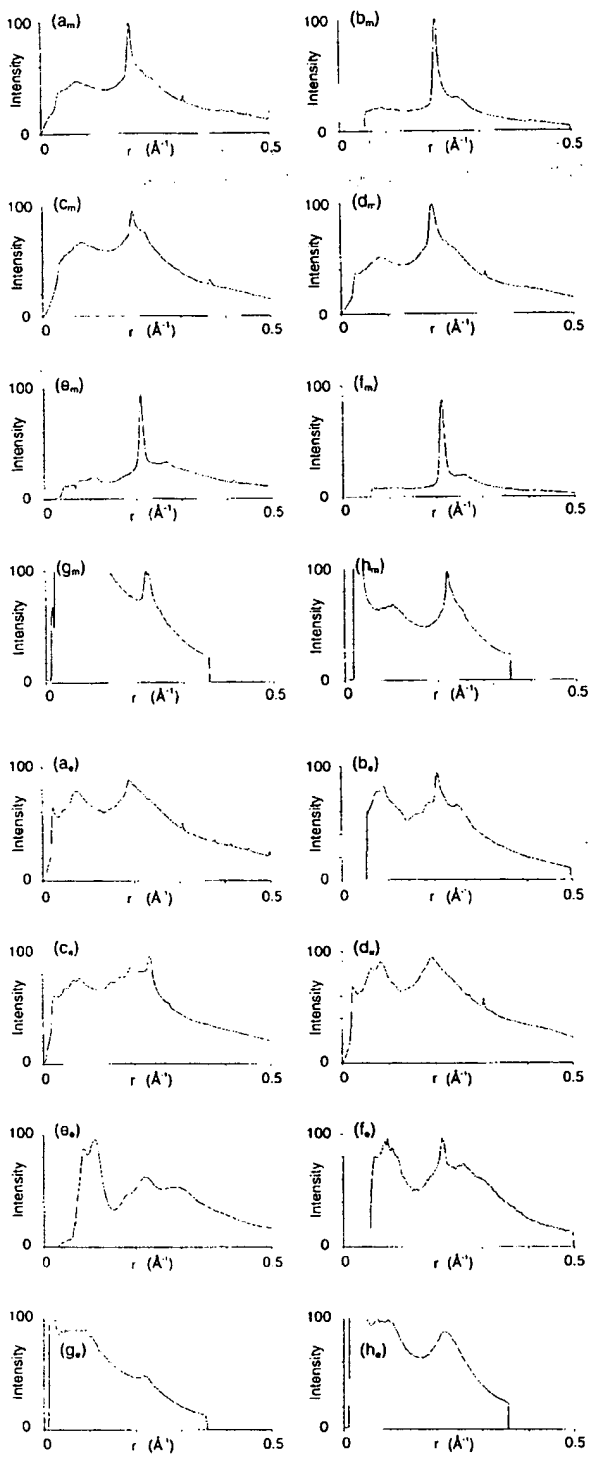

Figure 2. Comparison of the meridional and equatorial reflections. Meridional and equatorial profiles from samples of eight different amyloid fibrils, showing the close similarities in the meridonal diffraction and the large differences in the distribution of the equatorial reflections between these diverse amyloid samples. The samples, illustrated in the same order as in figure 1, are as follows; (a) ATTR2; (b) ATTR1; (c) AAPOAI; (d) AL; (e) FTTR; (f) FIAPP; (g) AA; (h) ALys (abbreviations as in legend to Figure 1). Meridional profiles are illustrated as parts (a_m) to (g_m) of the Figure and equatorial profiles are parts (a_e) to g_e). The profiles were extracted using an adapted version of PROFIDA (Lorenz & Holmes, 1993). The diffraction patterns were centred, rotated to align the meridional axis with the vertical axis of the screen, and corrected for beam polarisation. Profiles were averaged over both Δr and $\Delta\theta$, over the ranges $0 < r < 0.5$ Å^{-1}, $\Delta r = 0.000782$ Å^{-1} and $0 < \theta < 10°$, $\Delta\theta = 1°$. The profiles are plotted on the same, arbitrary, intensity scale for comparison.

approximately 10 Å, as suggested earlier. It is known that the spacing in β-sheets is dependent on the side-chain composition of the β-sheets (Arnott *et al.*, 1967; Geddes *et al.*, 1968). A recent analysis of the X-ray diffraction patterns from prion rods and fibrils formed from peptides corresponding to fragments of the prion protein has shown that the β-sheet spacings vary in these samples because of differences in sequence (Nguyen *et al.*, 1995). The present results are also in agreement with those of Jarvis and co-workers, who have reported β-sheet spacings of 8 to 10 Å in synthetic fibrils prepared from peptides that correspond to single strands of the transthyretin molecule (Jarvis *et al.*, 1993). The slight variation in the equatorial reflections observed in the series of fibrils presented here therefore presumably reflects the differences in protein sequences in these diverse types of amyloid but falls within acceptable limits for amino acid compositions found in globular proteins.

The larger number of equatorial reflections revealed by the synchrotron X-ray source suggests the presence of protofilaments in amyloid fibrils. The short-range order involved in the packing of protofilaments, within or between the fibrils, can be described by a one-dimensional interference function dependent on the centre-to centre separation (or diameter) of the protofilaments, and their arrangement in the fibrils (Burge, 1959, 1963). Electron microscopy studies of the sub-fibrillar structure of amyloid have revealed that different types of amyloid may show different numbers and arrangements of protofilaments in the fibrils (Shirahama & Cohen, 1967; Shirahama *et al.*, 1973; Cohen *et al.*, 1981). Fraser and co-workers have shown that the protofilaments formed by Aβ peptides assemble into hollow rods or ribbons of various sizes under different conditions of pH (Fraser *et al.*, 1991) and, while Aβ, amyloid A protein and immunoglobulin light chain amyloid fibrils are reported to be composed of five or six protofilaments around an electron lucent core (Cohen *et al.*, 1981; Kirschner *et al.*, 1987; Fraser *et al.*, 1991), transthyretin amyloid has been shown to be composed of four protofilaments in a square array (Serpell *et al.*, 1995). It may therefore be expected that the equatorial reflections produced by the amyloid fibrils of different types will reflect the variation in number and arrangement of protofilaments in their fibrils.

Table 3. Equatorial reflections

ATTR1	ATTR2	AL	AApoAI	ALys	AA	FTTR	FIAPP
						26.3	
16.0			15.17	14.60			
12.60		12.55	11.78	12.32		11.51	11.42
	10.62				10.96		
10.10		9.70	9.79	10.35		8.92	8.60
7.56	7.94	7.56					
6.05		6.11	5.98	5.74		5.72	5.53
5.32	5.46	5.26	5.37			4.53	
3.94			3.88	3.89		3.43	3.28

Spacing (in Å) of all equatorial reflections measured from diffraction patterns. Samples as in Table 2.

It is also possible that the diameters of the protofilaments (and therefore their centre-to-centre spacing) may vary because of the need to accommodate differently sized loops linking the β-structure core, and/or to allow for some variation in the lengths of the β-strands dependent on the nature of the precursor. These variations may account for the differences between the 25 to 35 Å diameter protofilaments seen in amyloid A protein and immunoglobulin light chain fibrils, and Alzheimer's amyloid and the 50 to 60 Å diameter protofilaments demonstrated in transthyretin amyloid (Fraser *et al.*, 1991; Cohen *et al.*, 1981; Serpell *et al.*, 1995). In view of these possible variations of structure, the observed equatorial spacings listed in Table 3 are difficult to interpret readily in more detail than is given above. Where there is a sufficient number of equatorial reflections and other information it is possible to analyze the substructure of the fibril in some detail, as for example, has been done for the transthyretin fibril (Blake & Serpell, 1996; Blake *et al.*, 1996). The number of observable equatorial reflections listed in Table 3 is insufficient to characterize all of the amyloid fibrils studied here but the similarity in the equatorial reflections displayed by the *ex vivo* fibrils on the one hand, and the synthetic peptide fibrils on the other, may reflect the fact that the protofilament packing in these two groups is related to the nature of their constituent polypeptides.

A generic fibril structure

The degree of similarity we have observed in the diffraction patterns of these different amyloid samples is indicative of a common core molecular structure at least at the level of the protofilament. The X-ray pattern of one of these fibrils, the Val30Met transthyretin amyloid, has been analysed in detail to generate a novel molecular structure, which has been described (Blake & Serpell, 1996; Blake *et al.*, 1996), and it is reasonable to suppose that its basic structural elements are representative of the other amyloid fibrils examined here. In this molecular model the protofilaments that make up the observed fibrils are composed of a number of β-sheets (four in the case of transthyretin fibrils; but this number may be particular to transthyretin amyloid) running parallel to the axis of the protofilament, with their component β-strands closely perpendicular to this axis. The regular orientation of the strands and sheets with respect to the fibril axis may account for the magnetic anisotropy observed in amyloid fibril samples, which allows samples of fibrils to be aligned in a magnetic field (Inouye *et al.*, 1993). The diamagnetic anisotropy of the planar peptide bond has the effect that β-sheets, in which the plane of the peptide bond is parallel to the sheet, have a tendency to orient parallel to an applied magnetic field (Worcester, 1978).

The meridional reflections from these diverse amyloids are all consistent with the model of the continuous β-sheet helix described in detail for the Val30Met amyloid fibril (Blake & Serpell, 1996). For all of the amyloids, the lowest-order reflection, at 4.8 Å, is the 24th order of the 115.5 Å repeat, suggesting that the amyloid core contains 24 β-strands in each 115.5 Å-long repeating unit along the fibril axis (Figure 3). A twist of the β-sheet through 360° in 115.5 Å generates a relative twist of 15° between neighbouring β-strands if there are 24 β-strands in the helical repeat. Most β-sheet structures in folded proteins are twisted rather than planar and have a right-handed twist of 0° to 30° between strands. The right-handed twisted conformation represents the lowest energy conformation of the β-sheet structure (Pauling & Corey, 1951; Chothia, 1973). This model of the amyloid protofilament core incorporates the most likely, lower energy, right-handed twisted β-sheets but the data do not differentiate between left and right-handed helices. In this model, the twisting of the β-sheets around a common helical axis, which is parallel to the axis of the protofilament, accounts for the repeating unit of approximately 115.5 Å that is observed in all the amyloid fibrils studied here. The model is therefore an elaboration of the classical cross-β molecular structure, which permits the incorporation of the favourable twisted β-sheet structures (Pauling & Corey, 1951; Chothia, 1973). The helical structure of the protofilament enables the hydrogen bonding between the β-strands to be extended over the total length of the amyloid fibrils, thereby accounting for their characteristic rigidity and stability. The extended order in this dimension of the fibrils is responsible for the pseudo-crystalline sharpness of the meridional reflections.

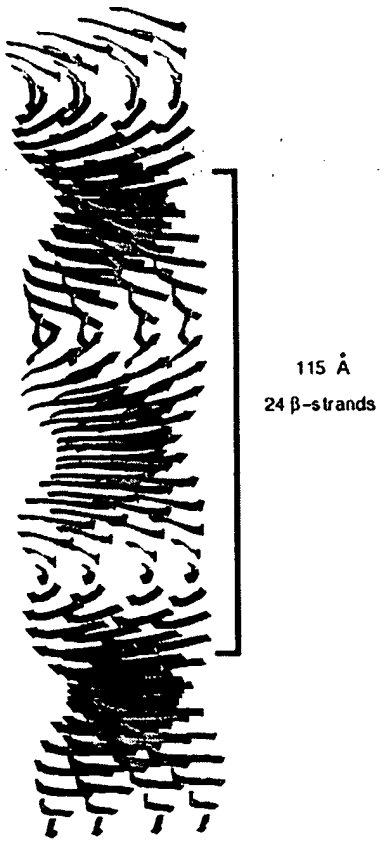

Figure 3. Model of the generic amyloid fibril structure. Molecular model of the common core protofilament structure of amyloid fibrils. A number of β-sheets (four illustrated here) make up the protofilament structure. These sheets run parallel to the axis of the protofilament, with their component β-strands perpendicular to the fibril axis. With normal twisting of the β-strands, the β-sheets twist around a common helical axis that coincides with the axis of the protofilament, giving a helical repeat of 115.5 Å containing 24 β-strands (this repeat is indicated by the boxed region).

The present X-ray results support the view that this model represents the core molecular structure of all of the amyloid fibrils studied here, irrespective of the number or arrangement of protofilaments, and demonstrate the independence of the 115.5 Å helical repeat from the nature of precursor protein. The ability of this single structure to accommodate different length polypeptide chains may be understood in the following way. Very short peptide chains, say six to ten residues, are able to form a single β-strand, which can act as the basic unit to be repeated along the fibre axis. Longer polypeptides will be able to form a larger number of β-strands by folding their chains back and forth. In this way the cross-β amyloid structure may be independent of the length of the polypeptide chains forming it. The features of the structure that may vary and be dependent on characteristics of the precursor are mainly expressed in directions perpendicular to the fibre axis, where loops of varying length or other structures can be accommodated without affecting the core β-sheet structure. These variations would be expected to be reflected in variability of the spacings and intensities of the equatorial reflections. In contrast, the common β-sheet helical structure should result in a constant pattern for the spacings and intensities of meridional reflections. These characteristics are exactly what is observed in the diffraction patterns from different amyloid fibrils.

Fibrillogenesis and a structural conversion

Table 1 lists the known or predicted structures of the amyloid fibril subunit precursors in their non-fibrillar form. The amyloidogenic proteins display a wide range of native folds, yet the present analysis has demonstrated that all amyloid fibrils have the same cross-β molecular skeleton. Proteins such as the immunoglobulin light chain (Schormann *et al.*, 1995), transthyretin (Blake *et al.*, 1978; Terry *et al.*, 1993; Hamilton *et al.*, 1993; Sebastião *et al.*, 1996) and β_2-microglobulin (Becker & Reeke, 1985) have similar, mainly β-sheet native structures but, even so, must sustain significant structural changes when they are deposited in the cross-β amyloid form (Blake & Serpell, 1996; Blake *et al.*, 1996), and it is known that the form of transthyretin that is amyloidogenic has a non-native conformation (Colon & Kelly, 1992; McCutchen *et al.*, 1993, 1995; Kelly, 1996). Proteins such as insulin (Adams *et al.*, 1969), cystatin C (Bode *et al.*, 1988), the amyloidogenic variants of lysozyme (Pepys *et al.*, 1993; Booth *et al.*, 1997), and the prion protein (Riek *et al.*, 1996), which have extensive native α-helical structure, may undergo even larger conformational changes when they form amyloid fibrils.

Such a structural conversion has been demonstrated for the amyloidogenic variants of human lysozyme (Booth *et al.*, 1997), which show an increase in β-sheet content and a loss of α-helical structure during fibril formation *in vitro*, and it is also associated with infectivity in the prion spongiform encephalopathies (Pan *et al.*, 1993; Gasset *et al.*, 1992, 1993; Harrison *et al.*, 1997). Studies of various peptides corresponding to regions of the Alzheimer's disease Aβ peptide have also demonstrated that structural plasticity is related to fibril formation (Hilbich *et al.*, 1991; Barrow *et al.*, 1992; Talafous *et al.*, 1994; Sticht *et al.*, 1995; Soto *et al.*, 1995).

The present work demonstrates that, although the amyloidogenic proteins have very different precursor structures, they can all undergo a structural conversion, perhaps along a similar pathway, to a misfolded form that is the building block of the β-sheet helix protofilament. This mechanism of structural conversion and the generic structure of

the amyloid protofilament offer two distinct targets for therapeutic molecules: compounds that could interfere with the transition from precursor to β-structured fold and agents that might inhibit or reverse the packing of protofilaments into fibrils.

Acknowledgements

We thank Drs G. A. Tennent, V. Bellotti and W. L. Hutchinson for preparing fibrils, and S. Lee for assistance with preparation of Figures. We thank Professor E. Lundgren and Dr G. Sangren, University of Umeå, Sweden, for providing variant transthyretin Val30Met fibrils extracted from vitreous humor. L.C.S. was supported by the Oxford Centre for Molecular Sciences, and P. E. F. by the Alzheimer's Society of Ontario and the Ontario Mental Health Foundation. This work was supported in part by MRC Programme grant (G7900510) to M.B.P. and MRC Project grants to M.B.P. and C.C.F.B. We dedicate this paper to the memory of the late Dr George Glenner, the champion of β-fibrillosis.

References

Adams, M. J., Blundell, T. L., Dodson, E. J., Dodson, G. G., Vijayan, M., Baker, E. N., Harding, M. M., Hodgkin, D. C., Rimmer, B. & Sheat, S. (1969). The structure of rhombohedral 2 zinc insulin crystals. *Nature*, **224**, 491–495.

Arnott, S., Dover, S. & Elliot, A. (1967). Structure of β-poly-L-alanine: refined atomic co-ordinates for an anti-parallel beta-pleated sheet. *J. Mol. Biol.* **30**, 201–208.

Barrow, C. J., Yasuda, A., Kenny, P. T. M. & Zagorski, M. G. (1992). Solution conformations and aggregational properties of synthetic amyloid β-peptides of Alzheimer's disease. *J. Mol. Biol.* **225**, 1075–1093.

Becker, J. & Reeke, G. (1985). Three-dimensional structures β_2-microglobulin. *Proc. Natl Acad. Sci USA*, **82**, 4225–4229.

Blake, C. C. F. & Serpell, L. C. (1996). Synchrotron X-ray studies suggest that the core of the transthyretin amyloid fibril is a continuous β-sheet helix. *Structure*, **4**, 989–998.

Blake, C. C. F., Geisow, M. J., Oatley, S. J., Rerat, B. & Rerat, C. (1978). Structure of prealbumin: secondary, tertiary and quaternary interactions determined by Fourier refinement at 1.8 Å. *J. Mol. Biol.* **121**, 339–356.

Blake, C. C. F., Serpell, L. C., Sunde, M. & Lundgren, E. (1996). A molecular model of the amyloid fibril. In *CIBA Symposium No. 199, The Nature and origin of Amyloid Fibrils*, pp. 6–21, John Wiley & Sons Ltd, Chichester, UK.

Bode, W., Engh, R., Musil, D., Thiele, U., Huber, R., Karshikov, A., Brzin, J., Kos, J. & Turk, V. (1988). The 2.0 Å X-ray crystal structure of chicken egg white cystatin and its possible mode of interaction with cysteine proteinases. *EMBO J.* **7**, 2593–2599.

Bonar, L., Cohen, A. S. & Skinner, M. (1967). Characterization of the amyloid fibril as a cross-β Protein. *Proc. Soc. Expt. Biol. Med.* **131**, 1373–1375.

Booth, D. R., Soutar, A. K., Hawkins, P. N., Reilly, M., Harding, A. & Pepys, M. B. (1994). Three new amyloidogenic transthyretin gene mutations: advantages of direct sequencing. In *Amyloid and Amyloidosis 1993* (Kisilevsky, R., Benson, M. D., Frangione, B., Gauldie, J. T., Muckle, J. & Youngs, I. D., eds), pp. 456–458, Parthenon Publishing, New York, Pearl River.

Booth, D. R., Sunde, M., Bellotti, V., Robinson, C. V., Hutchinson, W. L., Fraser, P. E. *et al.* (1997). Instability, unfolding and fibrillogenesis in amyloidogenic lysozyme variants. *Nature*, **385**, 787–793.

Bradbury, E. M., Brown, L., Downie, A. R., Elliott, A., Fraser, R. D. B., Hanby, W. E. & Macdonald, T. R. R. (1960). The "cross-beta" structure in polypeptides of low molecular weight. *J. Mol. Biol.* **2**, 276.

Burge, R. E. (1959). X-ray scattering by bundles of cylinders. *Acta Crystallog.* **12**, 285–289.

Burge, R. E. (1963). Equatorial X-ray diffraction by fibrous proteins: short range order in collagen, feather keratin and f-actin. *J. Mol. Biol.* **7**, 213–224.

Burke, M. J. & Rougvie, M. A. (1972). Cross-β protein structures I. Insulin fibrils. *Biochemistry*, **11**, 2435–2439.

Burtnick, L. D., Robinson, R. C. & Koepf, E. K. (1996). The structure of horse plasma gelsolin to 2.5 Å. *Biophys. J.* **70**, Pt. 2, pSUA12.

Chothia, C. (1973). Conformations of twisted β-sheets in proteins. *J. Mol. Biol.* **75**, 295–302.

Cohen, A. S., Shirahama, T. & Skinner, M. (1981). Electron microscopy of amyloid. In *Electron Microscopy of Protein* (Harriss, I., ed.), vol. 3, pp. 165–205, Academic Press, London.

Colon, W. & Kelly, J. W. (1992). Partial denaturation of transthyretin is sufficient for amyloid fibril formation in vitro. *Biochemistry*, **31**, 8654–8660.

Come, J. H., Fraser, P. E. & Lansbury, P. T. (1993). A kinetic model for amyloid formation in the prion diseases: importance of seeding. *Proc. Natl Acad. Sci. USA*, **90**, 5959–5963.

Damas, A., Sebastião, M. P., Domingues, F. S., Costa, P. P. & Saraiva, M. J. (1995). Structural studies on FAP fibrils: removal of contaminants is essential for the interpretation of X-ray data. *Amyloid: Int. J. Exp. Clin. Invest.* **2**, 173–1278.

Eanes, E. D. & Glenner, G. G. (1968). X-ray diffraction studies on amyloid filaments. *J. Histochem. Cytochem*, **16**, 673–677.

Filshie, B. K., Fraser, R. D. B., MacRae, T. P. & Rogers, G. E. (1964). X-ray diffraction and electron microscope observations on soluble derivatives of keratin. *Biochem. J.* **92**, 19–26.

Fraser, P. E., Nguyen, J. T., Surewicz, W. K. & Kirschner, D. A. (1991). pH dependent structural transitions of Alzheimer's amyloid peptides. *Biophys. J.* **60**, 1190–1201.

Gasset, M., Baldwin, M. A., Lloyd, D. H., Gabriel, J.-M., Holtzman, D. M., Cohen, F. E., Fletterick, R. & Prusiner, S. B. (1992). Predicted α-helical regions of the prion protein, when synthesized as peptides, form amyloid. *Proc. Natl Acad. Sci. USA*, **89**, 10940–10944.

Gasset, M., Baldwin, M., Fletterick, R. & Prusiner, S. (1993). Perturbation of secondary structure of the scrapie prion protein under conditions that alter infectivity. *Proc. Natl Acad. Sci. USA*, **90**, 1–5.

Geddes, A. J., Parker, K. D., Atkins, E. D. T. & Beighton, E. (1968). "Cross β" conformation in protein. *J. Mol. Biol.* **32**, 343–358.

Gilchrist, P. & Bradshaw, J. (1993). Amyloid formation by salmon calcitonin. *Biochim. Biophys. Acta,*, 111–114.

Glenner, G. G. (1080a). Amyloid deposits and amyloidosis. The beta-fibrilloses (part one). *New Eng. J. Med.* **302**, 1283–1292.

Glenner, G. G. (1980b). Amyloid deposits and amyloidosis. The beta-fibrilloses (part two). *New Eng. J. Med.* **302**, 1333–1343.

Glenner, G. G. & Wong, C. W. (1984). Alzheimer's disease: initial report of the purification and characterization of a novel cerebrovascular amyloid protein. *Biochem. Biophys. Res. Commun.* **120**, 885–890.

Gorevic, P., Castano, E., Sarma, R. & Frangione, B. (1987). Ten to fourteen residue peptides of Alzheimer's disease protein are sufficient for amyloid fibril formation and its characteristic X-ray diffraction pattern. *Biochem. Biophys. Res. Commun.* **147**, 854–862.

Hamilton, J., Steinrauf, L., Braden, B., Liepnieks, J., Benson, M., Holmgren, G., Sandgren, O. & Steen, L. (1993). The X-ray crystal structure refinements of normal human transthyretin and the amyloidogenic Val-30-Met variant to 1.7 Å resolution. *J. Biol. Chem.* **268**, 2416–2424.

Harrison, P. M., Bamborough, P., Daggett, V., Prusiner, S. B. & Cohen, F. E. (1997). The prion folding problem. *Curr. Opin. Struct. Biol.* **7**, 53–59.

Hilbich, C., Kisters-Woike, B., Reed, J., Masters, C. & Beyreuther, K. (1991). Aggregation and secondary structure of synthetic amyloid βA4 peptides of Alzheimer's disease. *J. Mol. Biol.* **218**, 149–163.

Inouye, H., Fraser, P. E. & Kirschner, D. A. (1993). Structure of β-crystallite assemblies by Alzheimer β-amyloid protein analogues: analysis by X-ray diffraction. *Biopys. J.* **64**, 502–519.

Jarvis, J. A., Craik, D. J. & Wilce, M. C. J. (1993). X-ray diffraction studies of fibrils formed from peptide fragments of transthyretin. *Biochem. Biophys. Res. Commun.* **192**, 991–998.

Kelly, J. W. (1996). Alternative conformations of amyloidogenic proteins govern their behaviour. *Curr. Opin. Struct. Biol.* **6**, 11–17.

Kelly, J. W. (1997). Amyloid fibril formation and protein misassembly: a structural quest for insights into amyloid and prion diseases. *Structure*, **5**, 595–600.

Kirschner, D. A., Abraham, C. & Selkoe, D. A. (1986). X-ray diffraction from intraneuronal paired helical filaments and extra-neuronal amyloid fibres in Alzheimer's disease indicates crossβ conformation. *Proc. Natl Acad. Sci. USA*, **83**, 503–507.

Kirschner, D. A., Inouye, H., Duffy, L., Sinclair, A., Lind, M. & Selkoe, D. A. (1987). Synthetic peptide homologous to β-protein from Alzheimer's disease forms amyloid-like fibrils *in vitro*. *Proc. Natl Acad. Sci. USA*, **84**, 6953–6957.

Lorenz, M. & Holmes, K. C. (1993). Computer processing and analysis of X-ray diffraction data. *J. Appl. Crystallog.* **26**, 82–91.

McCutchen, S., Colon, W. & Kelly, J. W. (1993). Transthyretin mutation Leu-55-Pro significantly alters tetramer stability and increases amyloidogenicity. *Biochemistry*, **32**, 12119–12127.

McCutchen, S. L., Lai, Z., Miroy, G. J., Kelly, J. W. & Colon, W. (1995). Comparison of lethal and nonlethal transthyretin variants and their relationship to amyloid disease. *Biochemistry*, **34**, 13527–13536.

Nelson, S., Lyon, M., Gallager, J., Johnson, E. & Pepys, M. B. (1991). Isolation and characterisation of the integral glycosaminoglycan constitutents of human amyloid A and monoclonal light-chain amyloid fibrils. *Biochem. J.* **275**, 67–74.

Nguyen, J. T., Inouye, H., Baldwin, M. A., Fletterick, R., Cohen, F. E., Prusiner, S. B. & Kirschner, D. A. (1995). X-ray diffraction from scrapie prion rod and PrP peptides. *J. Mol. Biol.* **252**, 412–422.

Nolte, R. T. & Atkinson, D. (1992). Conformational analysis of apolipoprotein A-1 and E-3 based on primary sequence and circular dichroism. *Biophys. J.* **63**, 1221–1239.

Pan, K.-M., Baldwin, M. A., Nguyen, J. T., Gaseet, M., Serban, A., Groth, D., Mehlhorn, I., Huang, Z., Fletterick, R. J., Cohen, F. E. & Prusiner, S. B. (1993). Conversion of α-helices into β-sheets features in the formation of the scrapie prion proteins. *Proc. Natl Acad. Sci. USA*, **90**, 10962–10966.

Pauling, L. & Corey, R. (1951). Configuration of polypeptide chains with favoured orientation around single bonds: two new pleated sheets. *Proc. Natl Acad. Sci. USA*, **37**, 729–739.

Pepys, M. B. (1996). Amyloidosi. In *The Oxford Textbook of Medicine* (Weatherall, D. J., Ledingham, J. G. G. & Warell, D. A., eds), 3rd edit., vol. 2, pp. 1512–1524, Oxford University Press, Oxford.

Pepys, M. B., Hawkins, P. N., Booth, D. R., Vigushin, D. M., Tennet, G. A., Soutar, A. K., Totty, N., Nguyen, O., Blake, C. C. F., Terry, C. J., Feest, T. G., Zalin, A. M. & Hsuan, J. J. (1993). Human lysozyme gene mutations cause hereditary systemic amyloidosis. *Nature*, **362**, 553–557.

Riek, R., Hornemann, S., Wider, G., Billeter, M., Glockshuber, R. & Wüthrich, K. (1996). NMR structure of the mouse prion protein domain PrP(121–231). *Nature*, **382**, 180–182.

Schormann, N., Murrell, J. R., Liepnieks, J. & Benson, M. (1995). Tertiary structure of an amyloid immunoglobulin light chain protein: a proposed model for amyloid fibril formation. *Proc. Natl Acad. Sci. USA*, **92**, 9490–9494.

Sebastião, P., Dauter, Z., Saraiva, M. J. & Damas, A. M. (1996). Crystallization and preliminary X-ray diffraction studies of Leu55Pro variant transthyretin. *Acta Crystallog. sect. D*, **52**, 566–568.

Serpell, L. C., Sunde, M., Fraser, P. E., Luther, P. K., Morris, E., Sandgren, O., Lundgren, E. & Blake, C. C. F. (1995). The examination of the structure of the transthyretin amyloid fibril by image reconstruction from electron micrographs. *J. Mol. Biol.* **254**, 113–118.

Shirahama, T. & Cohen, A. S. (1967). High resolution electron microscopic analysis of the amyloid fibril. *J. Cell Biol*, **33**, 679–706.

Shirahama, T., Benson, M. D., Cohen, A. S. & Tanaka, A. (1973). Fibrillar assemblage of variable segments of immunoglobulin light chains: an electron microscopic study. *J. Immunol.* **110**, 21–30.

Soto, C., Castano, E., Frangione, B. & Inestrosa, N. (1995). The α-helical to β-sheet transition in the amino-terminal fragment of the amyloid β-peptide modulates amyloid formation. *J. Biol. Chem.* **270**, 3063–3067.

Sticht, H. P., Bayer, P., Willbold, D., Dames, S., Hilbich, C., Beyreuther, K., Frank, R. & Rosch, P. (1995). Structure of amyloid A4(1-40)-peptide of Alzheimer's disease. *Eur. J. Biochem.* **233**, 293–298.

Soutar, A. K., Hawkins, P. N., Vigushin, D. M., Tennent, G. A., Booth, S., Hutton, T., Nguyen, O., Totty, N., Feest, T. G., Hsuan, J. J. & Pepys, M. B. (1992). Apolipoprotein A-1 mutation Arg-60 causes autosomal dominant amyloidosis. *Proc. Natl Acad. Sci. USA*, **89**, 7389–7393.

Tagliavini, F., Prelli, F., Verga, L., Giaccone, G., Jarma, R., Gorevic, P., Ghetti, B., Passerini, F., Ghibaudi, E., Forloni, G., Salmona, M., Bugiani, O. & Frangione, B. (1993). Synthetic peptides homologous to prion protein residues 106–147 form amyloid-like fibrils *in vitro*. *Proc. Natl Acad. Sci. USA*, **90**, 9678–9682.

Talafous, J., Marcinowski, K., Klopman, G. & Zagorski, M. (1994). Solution structure of residues 1–28 of the amyloid β-peptide. *Biochemistry*, **33**, 7788–7796.

Tan, S. Y., Pepys, M. B. & Hawkins, P. N. (1995). Treatment of amyloidosis. *Am. J. Kidney Dis.* **26**, 267–285.

Terry, C. J., Damas, A. M., Oliviera, P., Saraiva, M. J. M., Alves, A. L., Costa, P. P., Matias, P. M., Sakaki, Y. & Blake, C. C. F. (1993). Structure of Met30 variant of transthyretin and its amyloidogenic variations. *EMBO J.* **12**, 735–741.

Turnell, W., Sarra, R., Baum, J. O., Caspi, D., Baltz, M. L. & Pepys, M. B. (1986a). X-Ray scattering and diffraction by wet gels of AA amyloid fibrils. *Mol. Biol. Med.* **3**, 409–424.

Turnell, W., Sarra, R., Glover, I. D., Baum, J. O., Caspi, D., Baltz, M. L. & Pepys, M. B. (1986b). Secondary structure preduction of human SAA_1, presumptive identification of calcium and lipid binding sites. *Mol. Biol. Med.* **3**, 387–407.

Worcester, D. L. (1978). Structural origins of diamagnetic anisotropy in proteins. *Proc. Natl Acad. Sci. USA*, **75**, 5475–5477.

Edited by F. E. Cohen

(Received 8 May 1997; received in revised form 5 August 1997; accepted 5 August 1997)

American Journal of Pathology, Vol. 141, No. 2, August 1992

Effect of Serum Amyloid P Component Level on Transthyretin-derived Amyloid Deposition in a Transgenic Mouse Model of Familial Amyloidotic Polyneuropathy

Tatsufumi Murakami,*‡ Shigehiro Yi,†‡ Shuichiro Maeda,* Fumi Tashiro,‖ Ken-ichi Yamamura,‖ Kiyoshi Takahashi,† Kazunori Shimada,* and Shukuro Araki‡

From the Departments of Biochemistry and Pathology,† the First Department of Internal Medicine,‡ and the Institute for Medical Genetics,‖ Kumamoto University Medical School, Kumamoto, Japan*

To elucidate the pathogenesis of amyloid deposition associated with familial amyloidotic polyneuropathy (FAP), we developed several transgenic mouse lines carrying the human mutant transthyretin (TTR) gene. We found that human TTR and mouse serum amyloid P component (SAP) are deposited as amyloid in tissues of these mouse lines. Because SAP is a major acute-phase reactant in mice, we asked whether repeated injections of* Escherichia coli *lipopolysaccharide (LPS) would enhance the amyloid deposition in one of these transgenic mouse lines. During the course of repeated LPS injections, serum levels of SAP in the transgenic mice remained between severalfold to about 50-fold higher than seen in the absence of stimulation. As no significant difference was detected in the onset, progression, and tissue distribution of TTR-derived amyloid (ATTR) deposition between the LPS-stimulated and unstimulated transgenic mice, the induction of SAP synthesis by acute inflammation probably does not affect the onset and extent of ATTR deposition. (Am J Pathol 1992, 141: 451–456)

Familial amyloidotic polyneuropathy (FAP) is an autosomal dominantly inherited systemic amyloidosis.[1] The amyloid deposits derived from the Japanese, Portuguese, and Swedish types of FAP all consist of the same variant transthyretin (TTR) with a single amino-acid substitution of methionine for valine at position 30.[2–4] These amyloids also contain a small but significant amount of serum amyloid P component (SAP).[5] We reported evidence for a direct link between a point mutation in the TTR gene and FAP.[6–10] However, the wide span of age at onset suggests the presence of factor(s), other than a mutation in the TTR gene, which affect amyloid deposition.[11] One such factor may be SAP, because all known types of amyloid deposits so far studied contain SAP.[12] SAP is a major acute-phase reactant in the mouse,[13] and Baltz et al[14] considered that in the mouse there may be a relationship between the sustained high levels of SAP and the deposition of casein-induced amyloid. The rate of synthesis of SAP in individuals with systemic amyloidosis was shown to be increased up to 10-fold higher than that in control subjects.[15]

In an attempt to elucidate the molecular pathogenesis of FAP, we constructed several transgenic mouse lines carrying and expressing the human mutant TTR gene. In these mouse lines, we found that human TTR and mouse SAP deposit as amyloid.[11,16] To investigate the relationship between SAP and amyloidogenesis in FAP, we examined whether sustained high serum levels of SAP induced by repeated intraperitoneal injections of *Escherichia coli* lipopolysaccharide (LPS) enhance the amyloid deposition in one of these transgenic mouse lines.

Materials and Methods

Mice and Induction of Acute Inflammation

Acute inflammation was induced in groups of male C57BL/6 mice by the intraperitoneal injection of LPS. At different times after the injection of 1 μg of LPS/g body weight, blood samples were taken from the ether-anesthetized animals.

A transgenic mouse line used in this study was developed as follows.[11,16,17] First, we prepared a 7.8-kb

Supported in part by a grant-in-aid for scientific research from the Ministry of Education, Science, and Culture, Japan.

Accepted for publication February 5, 1992.

Dr. Shimada's current address is Research Institute for Microbial Diseases, Osaka University, Osaka, Japan.

Address reprint requests to Dr. Shuichiro Maeda, Department of Biochemistry, Kumamoto University Medical School, Kumamoto 860, Japan.

BEST AVAILABLE IMAGES

Defective images within this document are accurate representations of the original documents submitted by the applicant.

Defects in the images may include (but are not limited to):

- BLACK BORDERS
- TEXT CUT OFF AT TOP, BOTTOM OR SIDES
- FADED TEXT
- ILLEGIBLE TEXT
- SKEWED/SLANTED IMAGES
- COLORED PHOTOS
- BLACK OR VERY BLACK AND WHITE DARK PHOTOS
- GRAY SCALE DOCUMENTS

IMAGES ARE BEST AVAILABLE COPY.

As rescanning documents *will not* correct images, please do not report the images to the Image Problem Mailbox.

*Stu*I-*Eco*RI fragment, in which the promoter region of the mouse metallothionein-I (MT-I) gene was ligated to the structural gene of human mutant TTR gene (MT-hTTR30met), for an adequate expression of the human mutant TTR gene. This DNA construct was microinjected into fertilized eggs of C57BL/6 mice and several transgenic mice, expressing the human TTR gene were thus obtained. In one of these transgenic mouse lines, amyloid began to deposit in the alimentary tract when the mice were 6 months old. At 12 months of age, amyloid deposits remarkably increased in the same organs and also appeared in the kidneys, heart, and thyroid of most of the transgenic mice examined. The amyloid deposits constantly increased with aging, and in mice aged 15 months, they were observed in most of the organs examined.[11,16,18] In the current study, we used the transgenic mice of this line for the following experiments. Groups of the male transgenic mice of the same litter were given injections of LPS every 5 to 6 days, as initiated at the age of 2 months.

Specific Protein Assays

To examine the serum levels of SAP, blood samples were taken from ether-anesthetized mice and the sera were analyzed by single radial immunodiffusion and Western blot analyses, using rabbit anti-mouse SAP antiserum (Calbiochem, La Jolla, CA). The serum levels were calibrated with mouse SAP standard serum (Calbiochem).

Histochemical Analysis

After repeated injections of LPS, transgenic mice were killed after ether anesthetization at 5.5, 7, 13, and 18 months of age. Various tissues were excised, fixed in 10% neutral buffered formalin, and embedded in paraffin for histochemical analyses. At each time point, two male transgenic mice given repeated LPS injections as well as two male and one female unstimulated transgenic mice of the same litter were also examined. Tissue sections were stained with Congo red and examined under polarized light for the presence of amyloid deposits.

Immunohistochemistry

For immunohistochemical demonstration of the major components of amyloid deposits, tissue sections were immunostained by the avidin-biotin complex (ABC) method, using antisera. The antisera used were anti-human TTR (Behringwerke; Marburg, FRG), and anti-mouse amyloid A protein (AA) (provided by Prof. S. Migita, Cancer Research Institute, Kanazawa University, Japan).

Results

Changes of Serum Levels of SAP After an Intraperitoneal Injection of LPS in C57BL/6 Mice

Male C57BL/6 mice were given 1 μg of LPS/g body weight intraperitoneally. At 0, 24, 48, 69, and 96 hours after inducing an acute inflammation, the mice were killed and serum levels of SAP were examined by single radial immunodiffusion and Western blot analyses. The results are shown in Figure 1. There was a progressive increase in the serum level of SAP and a peak was reached within 24–48 hours. At the maximum level, the serum level of SAP was approximately 160 μg/ml and 50-fold higher than that of the control level. The elevated level then gradually decreased, but the original unstimulated level was not reverted to even at 96 hours after the administration of LPS. We also noted that the serum level of SAP in the control female mice was severalfold higher than in the control male mice (Figure 1). Based on these findings, we repeated the injections of LPS every 5 to 6 days, and examined whether each one of the repeated injections caused a similar change in the serum level of SAP. Groups of two male mice were given LPS every 5 days for up to 20 days and sera were taken from two mice of one group at 24 hours after each injection. Serum levels of SAP were examined using the single radial immunodiffusion method. Similar changes in the serum levels of SAP were observed after each one of the repeated injections of LPS (data not shown).

Induction of SAP Synthesis in a Transgenic Mouse Model of FAP

To examine whether the sustained high serum levels of SAP would enhance amyloid deposition, we injected LPS every 5 to 6 days into four groups of male transgenic mice.[11,16] The injections were initiated when the mice were 2 months old. We measured the serum level of SAP in each one of the transgenic mice at 24 hours after the last LPS injection and confirmed that it was essentially identical to that observed in the control male C57BL/6 mice. Figure 2 shows the results of Western blot analysis of the serum levels of SAP in 13- and 18-month-old transgenic mice at 24 hours after the last LPS injection. As shown in Figure 3, the serum level of human TTR in these transgenic mice also increased up to about 16-fold within 10 hours after the injection of LPS. The serum level of

A

47 —

33 —

24 —

Figure 1
and Me
indicate
standar
C57BL/
Molecul
radial i
SAP sta

humar
was a
male t
Aft
month
exami
its, as
pare
betwe

Figu
in th
from
seru
F; 0.
geni
stim

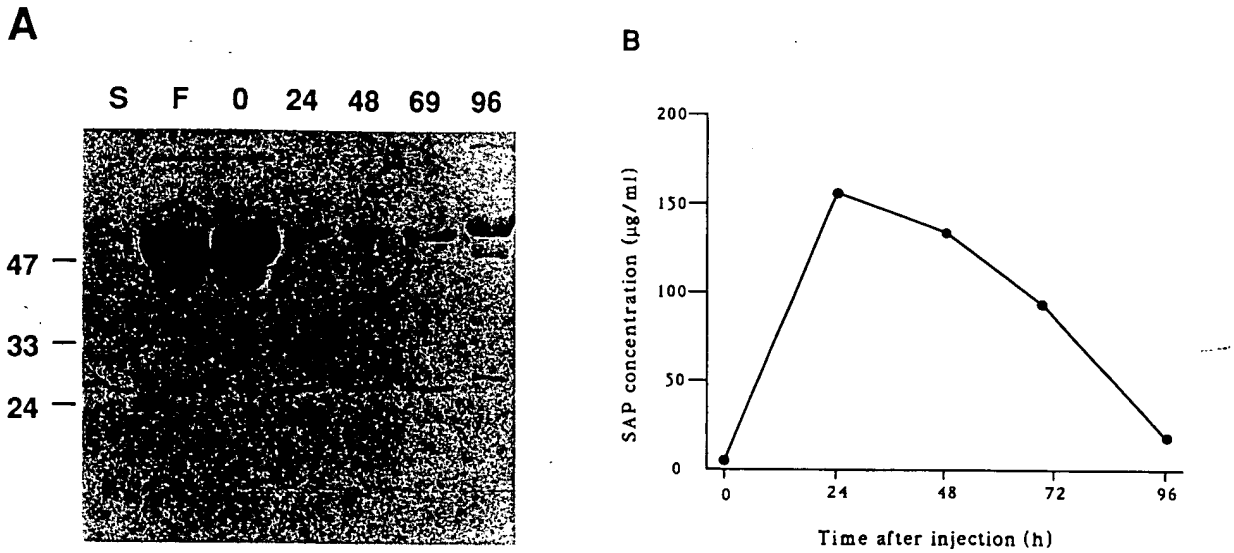

Figure 1. *SAP responses to LPS injection in C57BL/6 mice. The serum samples were prepared from the mice, as described under the Materials and Methods, and analyzed by Western blot analysis* (A) *and single radial immunodiffusion method* (B). A: *Numbers above the lanes indicate the time (in hr) after the LPS injection. At each time point, the two mice were examined. Lane S; 0.8 μl (9.4 μg/ml) of mouse SAP standard serum (Calbiochem); lane F; 0.8 μl of serum from unstimulated female C57BL/6 mouse, lanes 0, 24, 48, 69, 96; serum from male C57BL/6 stimulated mice, lane 0; 0.8 μl of serum, lanes 24, 48, 69; 0.8 μl of 1/10 diluted serum, lane 96; 0.8 μl of 1/5 diluted serum. Molecular mass in kilo daltons is indicated on the left of the panel. An arrowhead indicates SAP.* B: *The SAP level was measured by single radial immunodiffusion method using anti-mouse SAP antiserum and 1.2% agarose gel. The serum levels were calibrated with the mouse SAP standard serum.*

human TTR in the unstimulated female transgenic mice was about four-fold higher than that in the unstimulated male transgenic mice (Figure 3).

After repeated LPS injections and at 5.5, 7, 13, and 18 months of age, two male transgenic mice were killed and examined for distribution and degree of amyloid deposits, as described under Materials and Methods. To compare the distribution and degree of amyloid deposition between the LPS stimulated and unstimulated transgenic mice, we also histochemically examined two male and one female unstimulated transgenic mice of the same litter for amyloid deposition. Amyloid deposits were not

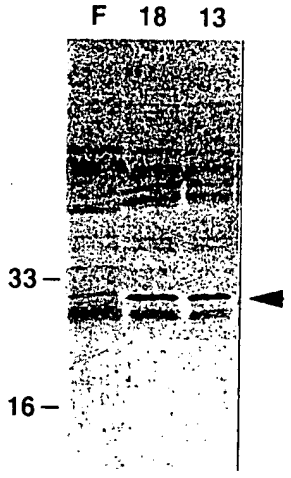

Figure 2. *The acute-phase response of SAP to the last LPS injection in the transgenic mouse aged 13 and 18 month-8. Sera were taken from the transgenic mice at 24 hr after the last LPS injection and serum levels of SAP were analyzed by Western blot analysis. Lane F; 0.8 μl of serum from unstimulated 18 month-old female transgenic mouse, lanes 18, 13; 0.8 μl of 1/5 diluted serum from LPS-stimulated 18- and 13-month–old transgenic mice, respectively.*

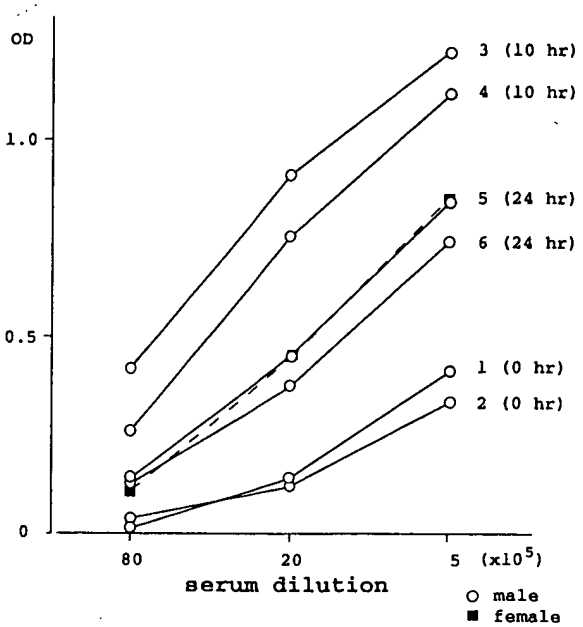

Figure 3. *Effect of acute inflammation on serum level of human TTR in transgenic mice. Acute inflammation was induced in male transgenic mice at 13 months of age by a single intraperitoneal injection of LPS (1 μg LPS/g body weight) and the serum samples were prepared from the two mice/timepoint at 0 and at 10-, and 24-hr intervals. The plasma levels of human TTR were analyzed by enzyme-linked immunosorbent assay and dilution curves were made. 1, 2; 0 hr, 3, 4; 10 hr, 5, 6; 24 hr. The dilution curve of an unstimulated female transgenic mouse serum was also made.*

detected in any one of the 5.5- and 7-month-old transgenic mice (Table 1). At 13 months of age, amyloid deposits were observed in the heart, liver, spleen, stomach, intestine, thyroid gland, and skin (Table 1). We detected similar amyloid deposits in similar tissues of two male mice and one female unstimulated mouse of the same litter. However, we found no amyloid deposits in the liver and spleen of these unstimulated transgenic mice (Table 1). At 18 months of age, amyloid deposits appeared more remarkably in the same tissues and also in kidneys and lymph nodes (Table 1). The amyloid deposits in the liver, spleen, and lymph nodes were evident only in the stimulated mice (Table 1, Figure 4a, b). There was no significant difference in the degree of the amyloid deposition in the other tissues between the unstimulated and stimulated transgenic mice (Figure 4c, d). The components of amyloid deposits were examined using the ABC method. The amyloid deposits in the liver and spleen of the 18-month-old stimulated mice did not react with anti-human TTR antisera, but did react with anti-mouse AA antisera (Figure 5a, b). On the other hand, the amyloid deposits in the kidneys, heart, stomach, intestine, thyroid gland, and lymph nodes of the 18-month-old stimulated mice reacted with anti-human TTR antisera, but not with anti-mouse AA antisera (Figure 5c, d). We confirmed that the amyloid deposits in various tissues of the 18-month-old unstimulated mice reacted with anti-human TTR and anti-mouse SAP antisera but not with anti-mouse AA antisera (data not shown).

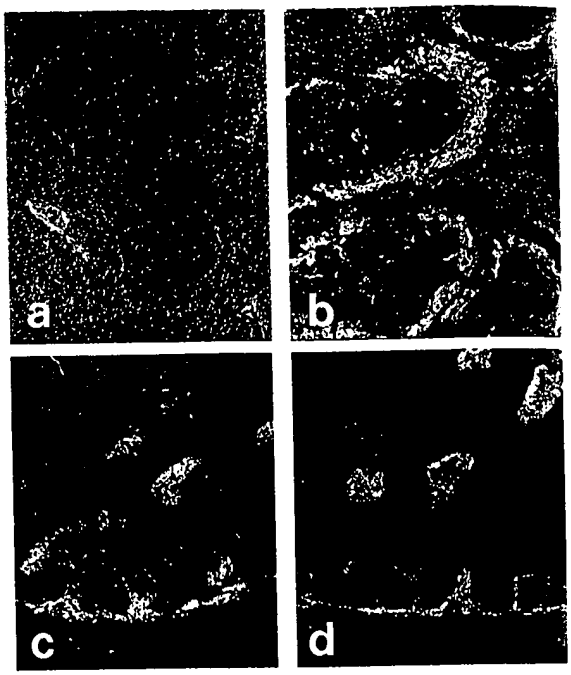

Figure 4. *Histochemical analysis of spleen and small intestine of the 18-month-old transgenic mice. Tissues were stained with Congo red, then viewed through cross polar. The amyloid deposits stained with Congo red give the bright green birefringence characteristic of amyloid;* (a, b), *spleen (×30);* (c, d), *small intestine (×50),* (a, c), *unstimulated transgenic mice;* (b, d), *LPS-stimulated transgenic mice.*

Discussion

Our observations strongly suggest that the sustained high serum level of SAP caused by the repeated acute inflammation does not affect the onset and extent of TTR-derived amyloid (ATTR) deposition. SAP is a major acute-phase reactant in mice.[13] In C57BL/6 male mice, serum levels of SAP increased about fifty-fold at 24 hours after the injection of LPS (Figure 1), decreased gradually but remained severalfold higher than that of the unstimulated

Table 1. *Histochemical Tissue Distribution of Amyloid Deposits in Transgenic Mice Carrying the MT-hTTR30met Gene*

Organs	LPS	Transgenic mice: age examined (months)							
		5.5		7		13		18	
		(−)	(+)	(−)	(+)	(−)	(+)	(−)	(+)
Brain		−	−	−	−	−	−	−	−
Choroid plexus		−	−	−	−	−	−	−	−
Sciatic nerve		−	−	−	−	−	−	−	−
Heart		−	−	−	−	+	±	+	+ +
Lung		−	−	−	−	−	−	−	−
Liver		−	−	−	−	−	±	−	+
Spleen		−	−	−	−	−	+	−	+ +
Pancreas		−	−	−	−	−	−	−	−
Kidney		−	−	−	−	−	−	+	+ +
Stomach		−	−	−	−	+	+	+ +	+ +
Intestine		−	−	−	−	+ +	+	+ + +	+ +
Lymph node		−	−	−	−	−	−	−	+
Thyroid gland						+	+	+	+ +
Skin		−	−	−	−	+	+	+	+

Amyloid deposits are absent, −; limited to the wall of small vessels, ±; observed in the small vessels and their surrounding regions, +; moderate in the interstitium, + +; marked in the interstitium and parenchyma, + + +.

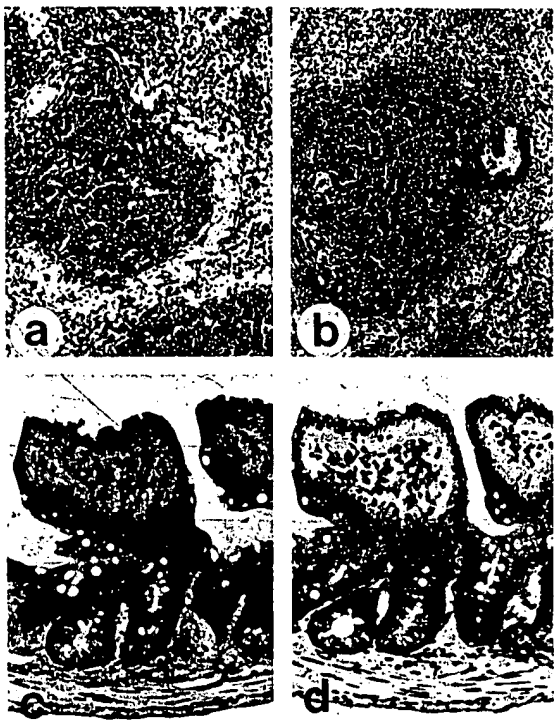

Figure 5. *Immunohistochemistry of spleen and small intestine of the LPS-stimulated 18-month-old transgenic mice;* (a, b), *spleen (×60);* (c, d), *small intestine (×75). The specimens were treated with anti-human TTR* (a, c) *or anti-mouse AA* (b, d).

level even at 96 hours after the administration of LPS (Figure 1). Kinetics of changes in the serum levels of SAP correlated with that of the mouse liver SAP mRNA.[19] We repeatedly injected LPS into the transgenic mice for 3.5 to 16 months. Even after 16 months of these repeated LPS injections, the acute phase response of SAP to the LPS injection was essentially identical with that observed after the first LPS injection (Figure 2). Thus, the serum levels of SAP in the transgenic mice remained between several-fold to about fifty-fold higher than that in the unstimulated mice during the course of the repeated LPS injections.

The LPS injection also increased the serum level of human TTR in the transgenic mice (Figure 3). We expected this increase, because transcription of the human TTR gene in these transgenic mice is under the control of the promoter of the mouse MT-I gene, and because a similar increase in the level of mouse liver MT-I mRNA was already evident after the injection of LPS.[20] We also noted that the serum level of human TTR in the unstimulated female transgenic mice was about fourfold higher than that in the unstimulated male transgenic mice (Figure 3).

After 3.5 and 5 months of repeated LPS injections, amyloid deposits were not detected in any one of these transgenic mice, a finding that suggests that repeated induction of SAP synthesis by acute inflammation does not lead to an early deposition of ATTR. After 11 months of repeated LPS injections, amyloid deposits appeared, but the degree of deposition was much the same as that in the unstimulated transgenic mice, except for the presence of amyloid in the liver and the spleen. After 16 months of repeated LPS injections, the amyloid deposits were more extensive. However, there was no significant difference in the degree and distribution of ATTR deposition in tissues between the stimulated and unstimulated 18-month–old transgenic mice. The amyloid deposition in the liver and the spleen of the stimulated mice reacted with anti-mouse AA antisera but not with anti-human TTR antisera. Repeated administration of an inflammatory stimulus into mice induces deposition of amyloid fibrils mainly consisting of AA proteins derived from circulating serum amyloid A protein.[21] Accordingly, the induction of systemic AA amyloidosis indicated that repeated LPS injections effectively induced an acute phase responses in the transgenic mice.

The serum levels of both SAP and human TTR in the unstimulated female transgenic mice were severalfold higher than those in the unstimulated male mice. However, there was no significant difference in the onset and extent of amyloid deposition between the male and female unstimulated transgenic mice. Snel et al reported data on systemic AA amyloidosis in hamsters, in which AA and female protein (FP), the hamster counterpart of mouse SAP, are deposited as amyloid.[22] Systemic AA amyloidosis was induced in female, male, and castrated male hamsters by repeated injection of casein. The SAA responses of the three groups of hamsters to the repeated casein injection were indistinguishable, but castrated males had about a three-fold higher serum FP level than did control males though still lower than in females. There was no significant difference in the onset and extent of AA amyloid deposition between the three groups by casein injection alone.[22] These findings are similar to ours described herein. However, when AA amyloidosis was induced by injecting amyloid enhancing factor[23] followed by casein, amyloid deposition occurred sooner and was more extensive in both females and castrated males than in control males.[22] This observation supports the possibility that FP plays some role in the AA amyloid deposition.

Our findings suggest that the induction of SAP synthesis by acute inflammation does not affect the onset and extent of ATTR deposition in the transgenic mouse model of FAP. However, these findings do not rule out the possibility that SAP has a crucial role in ATTR deposition. Normal serum levels of SAP may be sufficient for the deposition of ATTR. In that case, targeted disruption of the SAP gene in mouse embryo-derived stem cells to generate mutant mice[24] should make way for the evaluation of the role of SAP in cases of amyloid deposition.

Acknowledgment

The authors thank M. Ohara for pertinent comments.

References

1. Andrade C: A peculiar form of peripheral neuropathy: Familial atypical generalized amyloidosis with special involvement of the peripheral nerves. Brain 1952, 75:408–427
2. Tawara S, Nakazato M, Kangawa K, Matsuo H, Araki S: Identification of amyloid prealbumin variant in familial amyloidotic polyneuropathy (Japanese type). Biochem Biophys Res Commun 1983, 116:880–888
3. Saraiva MJM, Birken S, Costa PP, Goodman DS: Amyloid fibril protein in familial amyloidotic polyneuropathy, Portuguese type. J Clin Invest 1984, 74:104–119
4. Dwulet FE, Benson MD: Primary structure of an amyloid prealbumin and its plasma precursor in a heredo-familial polyneuropathy of Swedish origin. Proc Natl Acad Sci USA 1984, 81:694–698
5. Skinner M, Sipe JD, Yood RA, Shirahama T, Cohen AS: Characterization of P-component (AP) isolated from amyloidotic tissue: Half-life studies of human and murine AP. Ann NY Acad Sci 1982, 389:190–198
6. Mita S, Maeda S, Shimada K, Araki S: Cloning and sequence analysis of cDNA for human prealbumin. Biochem Biophys Res Commun 1984, 124:558–564
7. Mita S, Maeda S, Ide M, Tsuzuki T, Shimada K, Araki S: Familial amyloidotic polyneuropathy diagnosed by cloned human prealbumin cDNA. Neurology 1986, 36:298–301
8. Ide M, Mita S, Ikegawa S, Maeda S, Shimada K, Araki S: Identification of carriers of mutant prealbumin gene associated with familial amyloidotic polyneuropathy type I by Southern blot procedures: study of six pedigrees in the Arao district of Japan. Hum Genet 1986, 73:281–285
9. Maeda S, Mita S, Araki S, Shimada K: Structure and expression of the mutant prealbumin gene associated with familial amyloidotic polyneuropathy. Mol Biol Med 1986, 3:329–338
10. Shimada K, Maeda S, Araki S: Genetic basis for familial amyloidotic polyneuropathy. Bioessays 1986, 4:208–212
11. Shimada K, Maeda S, Murakami T, Nishiguchi S, Tashiro F, Yi S, Wakasugi S, Takahashi K, Yamamura K: Transgenic mouse model of familial amyloidotic polyneuropathy. Mol Biol Med 1989, 6:333–343
12. Pepys MB, Baltz ML: Acute phase proteins with special reference to C-reactive protein and related proteins (pentaxins) and serum amyloid A protein. Adv Immunol 34. Edited by FJ Dixon, HG Kunkel. New York, Academic Press, 1983, pp 141–211
13. Pepys MB, Baltz M, Gomer K, Davies AJS, Doenhoff M: Serum amyloid P-component is an acute-phase reactant in the mouse. Nature 1979, 278:259–261
14. Baltz ML, Gomer K, Davies AJS, Evans DJ, Klaus GGB, Pepys MB: Differences in the acute phase responses of serum amyloid P-component (SAP) and C3 to injections of casein or bovine serum albumin in amyloid-susceptible and -resistant mouse strains. Clin Exp Immunol 1980, 39:355–360
15. Hawkins PN, Myers MJ, Lavender JP, Pepys MB: Diagnostic radionuclide imaging of amyloid: biological targeting by circulating human serum amyloid P component. Lancet 1988, i:1413–1418
16. Wakasugi S, Inomoto T, Yi S, Naito M, Uehira M, Iwanaga T, Maeda S, Araki K, Miyazaki J, Takahashi K, Shimada K, Yamamura K: A transgenic mouse model of familial amyloidotic polyneuropathy. Proc Japan Acad 1987, 63(B):344–347
17. Yamamura K, Tashiro F, Wakasugi S, Yi S, Maeda S, Shimada K: Transgenic mouse model of an autosomal dominant disease: familial amyloidotic polyneuropathy, Molecular mechanisms of aging. Edited by K Beyreuther, G Schettler. Heidelberg, Springer-Verlag, 1990, pp 146–154
18. Yi S, Takahashi K, Naito M, Tashiro F, Wakasugi S, Maeda S, Shimada K, Yamamura K, Araki S: Systemic amyloidosis in transgenic mice carrying the human mutant transthyretin (Met30) gene: pathologic similarity to human familial amyloidotic polyneuropathy, type I. Am J Pathol 1991, 138:403–412
19. Murakami T, Ohnishi S, Nishiguchi S, Maeda S, Araki S, Shimada K: Acute-phase response of mRNAs for serum amyloid P component, C-reactive protein and prealbumin (transthyretin) in mouse liver. Biochem Biophys Res Commun 1988, 155:554–560
20. Durnam DM, Hoffman JS, Quaife CJ, Benditt EP, Chen HY, Brinster RL, Palmiter RD: Induction of mouse metallothionein-I mRNA by bacterial endotoxin is independent of metals and glucocorticoid hormones. Proc Natl Acad Sci USA 1984, 81:1053–1056
21. Husby G, Sletten K: Amyloid proteins. Amylodosis. Edited by J Marrink, MHV Rijswijk. Dordrecht, Nijhoff, 1986, pp 23–34
22. Snel FWJJ, Niewold ThA, Baltz ML, Hol PR, Van Ederen AM, Pepys MB, Gruys E: Experimental amyloidosis in the hamster: correlation between hamster female protein levels and amyloid deposition. Clin Exp Immunol 1989, 76:296–300
23. Varga J, Flinn MSM, Shirahama T, Rodgers OG, Cohen AS: The induction of accelerated murine amyloid with human splenic extract: probable role of amyloid enhancing factor. Virchows Arch (B) 1986, 51:177–185
24. Capecchi MR: The mouse genetics: altering the genome by gene targeting. Trends Genet 1989, 5:70–76

BEST AVAILABLE IMAGES

Defective images within this document are accurate representations of the original documents submitted by the applicant.

Defects in the images may include (but are not limited to):

- BLACK BORDERS
- TEXT CUT OFF AT TOP, BOTTOM OR SIDES
- FADED TEXT
- ILLEGIBLE TEXT
- SKEWED/SLANTED IMAGES
- COLORED PHOTOS
- BLACK OR VERY BLACK AND WHITE DARK PHOTOS
- GRAY SCALE DOCUMENTS

IMAGES ARE BEST AVAILABLE COPY.

As rescanning documents *will not* correct images, please do not report the images to the Image Problem Mailbox.

American Journal of Pathology, Vol. 150, No. 4, April 1997

Animal Model

Analysis of Amyloid Deposition in a Transgenic Mouse Model of Homozygous Familial Amyloidotic Polyneuropathy

Kyoko Kohno,* Joana. A. Palha,†‡ Kazuhisa Miyakawa,§ Maria J. M. Saraiva,† Sadahiro Ito,* Tadashi Mabuchi,* William S. Blaner,‖ Hiroyuki Iijima,¶ Shigeo Tsukahara,¶ Vasso Episkopou,# Max E. Gottesman,‡ Kazunori Shimada,** Kiyoshi Takahashi,§ Ken-ichi Yamamura,†† and Shuichiro Maeda*

From the Departments of Biochemistry and Ophthalmology,¶ Yamanashi Medical University, Yamanashi, Japan; Instituto de Ciências Biomédicas Abel Salazar e Centro de Estudos da Paramiloidose,† Universidade do Porto, Porto, Portugal; the Institute of Cancer Research‡ and the Institute of Human Nutrition,‖ Columbia University, New York, New York; the Department of Pathology§ and Institute of Molecular Embryology and Genetics, ††Kumamoto University School of Medicine, Kumamoto, Japan; the Embryology Group,# Royal Postgraduate Medical School, Hammersmith Hospital, London, United Kingdom; and the Department of Medical Genetics,** Research Institute for Microbial Diseases, Osaka University, Osaka, Japan*

Amyloid fibrils derived from the Japanese, Portuguese, and Swedish types of familial amyloidotic polyneuropathy all consist of a variant transthyretin (TTR) with a substitution of methionine for valine at position 30 (TTR Met 30). In an attempt to establish an animal model of TTR Met-30-associated homozygous familial amyloidotic polyneuropathy and to study the structural and functional properties of human TTR Met 30, we generated a mouse line carrying a null mutation at the endogenous ttr locus ($ttr^{-/-}$) and the human mutant ttr gene (6.0-hMet 30) as a transgene. In these mice, human TTR Met-30-derived amyloid deposits were first observed in the esophagus and stomach when the mice were 11 months of age. With advancing age, amyloid deposits extended to various other tissues. Because no significant difference was detected in the onset, progression, and tissue distribution of amyloid deposition between the ttr−/− and ttr+/+ transgenic mice expressing 6.0-hMet 30, endogenous normal mouse TTR probably does not affect the deposition of human TTR Met-30-derived amyloid in mice. TTR is a tetramer composed of four identical subunits that binds thyroxine (T_4) and plasma retinol-binding protein. The introduction of 6.0-hMet 30 into the $ttr^{-/-}$ mice significantly increased their depressed serum levels of T_4 and retinol-binding protein, suggesting that human TTR Met 30 binds T_4 and retinol-binding protein in vivo. The T_4-binding ability of human TTR Met 30 was confirmed by the analysis of T_4-binding proteins in the sera of $ttr^{-/-}$ transgenic mice expressing 6.0-hMet 30. The T_4-binding studies also demonstrated the

Supported by grants-in-aids for Scientific Research on Priority Areas (05275101), for Scientific Research (05454579), and for International Scientific Research Program (07044242) from the Ministry of Education, Science, Sports, and Culture, Japan, to S. Maeda, by a grant from the Ministry of Health and Welfare, Japan, to S. Maeda, by a grant-in-aid for International Scientific Research Program (04044111) from the Ministry of Education, Science, Sports, and Culture, Japan, to K. Shimada, by grants JNICT-STRDA 33892 and NATO-CRG920215 to M. J. M. Saraiva, and by a grant from the Markey Foundation to M. E. Gottesman. J. A. Palha was the recipient of a Ph.D. fellowship from Junta Nacional de Investigação Científica e Technológica, Portugal.

Accepted for publication December 19, 1996.

Address reprint requests to Dr. Shuichiro Maeda, Department of Biochemistry, Yamanashi Medical University, 1110 Shimokato, Tamaho-cho, Nakakoma-gun, Yamanashi 409-38, Japan.

J. A. Palha's present address: Instituto Superior de Ciências da Saúde, Paredes, Portugal.

presence of hybrid tetramers between mouse and human TTR subunits in the ttr$^{+/+}$ transgenic mice expressing 6.0-hMet 30. (Am J Pathol 1997, 150:1497–1508)

Familial amyloidotic polyneuropathy (FAP) is an autosomal dominantly inherited disorder, characterized by extracellular deposition of fibrillar amyloid protein and by a progressive neuropathy leading predominantly to sensory and autonomic dysfunction.[1] The amyloid is mainly composed of variant transthyretin (TTR) with single amino acid substitutions. Many distinct TTR point mutations have been identified in association with FAP.[2] Substitution of methionine for valine at amino acid position 30 of TTR (TTR Met 30) predominates over other mutations in the Japanese and is the sole mutation found associated with FAP in Sweden and Portugal.[3–6] To investigate the molecular pathogenesis of TTR Met-30-associated FAP, we generated transgenic mice carrying the human mutant *ttr* gene.[7–9] In the transgenic mice, human TTR deposited as amyloid fibrils in many of the same tissues where amyloid deposition is commonly observed in FAP patients. However, a difference in the pattern of amyloid deposition was observed between the transgenic mice and FAP patients. For example, the transgenic mice had no amyloid deposition in the peripheral nervous tissues, the characteristic site of amyloid deposition in FAP patients.[7–9]

TTR is a tetramer composed of four identical subunits.[10] A possible reason for the difference in the pattern of amyloid deposition might be that the endogenous normal mouse TTR affects amyloid deposition by forming hybrid tetramers with the human variant TTR. Although formation of hybrid tetramers between mouse and human TTR in the transgenic mice carrying the human mutant *ttr* gene had not been clearly demonstrated, previous immunological analyses of the mice sera with anti-human TTR antiserum were consistent with this possibility.[11]

In this report, we describe experiments designed to study the effect of endogenous mouse TTR on human variant TTR-derived amyloid deposition. We have investigated the relationship between the levels of expression of the human mutant *ttr* gene and amyloid deposition and studied the structural and functional properties of human TTR Met 30. These experiments used two lines of mice: a TTR-deficient ($ttr^{-/-}$) mouse generated through gene targeting[12] and a wild-type transgenic mouse carrying the human mutant *ttr* gene with its cognate 6-kb upstream region (6.0-hMet 30).[13] The transgene, 6.0-hMet 30, was expressed in the liver, choroid plexus, kidney, and yolk sac, precisely the same tissues as the endogenous mouse *ttr* gene, and the levels of expression were equivalent to those of the endogenous mouse *ttr* gene.[13] The two lines were crossed to generate transgenic mice that lacked endogenous mouse TTR and expressed 6.0-hMet 30. We compare in this manuscript the onset and tissue distribution of amyloid deposition of this transgenic mouse line with that of the wild-type transgenic mouse line expressing both the endogenous mouse *ttr* and human mutant *ttr* genes.

TTR possesses high-affinity binding sites for both thyroxine (T_4)[14] and plasma retinol-binding protein (RBP)[15,16] and plays an important role in the plasma transport of thyroid hormone and retinol (vitamin A). The $ttr^{-/-}$ mice have significantly depressed serum levels of T_4[12,17] and RBP.[12,18] We show that expression of 6.0-hMet 30 affects serum T_4 and RBP binding in these mice.

Materials and Methods

Animals

Transgenic mice producing human variant TTR and lacking endogenous mouse TTR were generated as follows. A male C57BL/6 mouse carrying 6.0-hMet 30[13] was mated with $ttr^{-/-}$ outbred female mice.[12] The heterozygous ($ttr^{+/-}$) F1 male mice carrying 6.0-hMet 30 were mated with the heterozygous ($ttr^{+/-}$) F1 female mice carrying 6.0-hMet 30. Homozygous mutant ($ttr^{-/-}$) F2 mice carrying 6.0-hMet 30 ($ttr^{-/-}$–6.0-hMet $30^{+/-}$) were then selected. Homozygous mutant ($ttr^{-/-}$) F2 male mice carrying 6.0-hMet 30 ($ttr^{-/-}$–6.0-hMet $30^{+/-}$) were mated with the homozygous mutant ($ttr^{-/-}$) F2 female mice carrying 6.0-hMet 30 ($ttr^{-/-}$–6.0-hMet $30^{+/-}$). The F3 progenies were used in the present study. The F3 transgenic mice were maintained in cages housing four to six mice each, on separate racks in the same room, kept under a 12-hour light cycle. Regular rodent's chow (Oriental Yeast, Tokyo, Japan) and tap water were freely available.

Blood samples collected from the eye artery or from the heart after ether anesthesia were centrifuged, and serum was immediately frozen for further analysis. Genotype analysis for each animal was carried out by polymerase chain reaction on DNA from tails purified with phenol, chloroform, and ethanol precipitation, as described.[12]

Light Microscopy and Histochemistry

Transgenic mice were killed after anesthesia with ether. The ages of the mice were 5, 7, 11, 14, and 18 months. Various tissues were excised, fixed in 10% buffered neutral formalin, and embedded in paraffin. At each time point, six $ttr^{-/-}$ transgenic mice carrying 6.0-hMet 30 and six $ttr^{+/+}$ transgenic mice carrying 6.0-hMet 30 were examined. Paraffin sections were stained with hematoxylin and eosin for light microscopy and with Congo red for histochemical demonstration of amyloid. To confirm amyloid deposition in Congo-red-positive material, apple-green birefringence was determined under a polarization microscope.

Immunohistochemistry

For immunohistochemical analysis, portions of the tissues were fixed in 2% periodate-lysine-paraformaldehyde fixative at 4°C for 4 hours, washed with phosphate-buffered saline (PBS) containing 10, 15, and 20% sucrose at 4°C for 4 hours, and embedded in OCT compound (Miles, Eikhart, IN). After freezing in dry ice/acetone, the tissues were cut into 6-μm-thick sections on a cryostat (Bright, Huntington, UK). After inhibition of endogenous peroxidase activity by the method of Isobe et al,[19] the cryostat sections were immunostained by the indirect immunoperoxidase method using rabbit anti-human TTR antibody (Behringwerke, Marburg, Germany) and rabbit anti-mouse serum amyloid P component (SAP) antibody (Behring Diagnostic, La Jolla, CA). As secondary antibody, a donkey anti-rabbit immunoglobulin horseradish-peroxidase-linked $F(ab')_2$ fragment (Amersham, Little Chalfont, UK) was used. After visualization with 3,3'-diaminobenzidine and H_2O_2, the sections were stained with hematoxylin and mounted with resin.

Western Blot Analysis of Human TTR Levels

A 2-μl aliquot of each mouse serum diluted 1:40 in 0.9% NaCl were mixed with 8 μl of loading buffer (125 mmol/L Tris/HCl, pH 6.8, 4% sodium dodecyl sulfate (SDS), 20% glycerol, 0.005% bromophenol blue, and 10% 2-mercaptoethanol), and denatured at 95°C for 5 minutes, followed by SDS-polyacrylamide gel electrophoresis (8 to 16% gradient SDS-polyacrylamide gel, TEFCO, Matsumoto, Japan) at a constant current of 18 mA for 1.5 hours. The proteins were transferred onto Immobilon-P membrane (Millipore, Bedfold, MA) at a constant voltage of 25 V for 1.25 hours. As internal standard, 25 and 50 ng of human TTR standard (Calbiochem, La Jolla, CA) were also run in each gel. Nonspecific binding on the blot was blocked by incubation in 10% nonfat dry milk in blocking solution (Tris-buffered saline (TBS) containing 10 mmol/L Tris/HCl, pH 7.4, and 150 mmol/L NaCl) with 0.05% Tween 20 (Bio-Rad, Richmond, CA) for 3 hours. The blots were then incubated overnight in binding solution (2% nonfat dry milk and 0.05% Tween 20 in TBS) containing rabbit anti-human TTR antibody (Behringwerke) at a dilution of 1:250. After washing five times (10 minutes each) with washing solution (0.1% Nonidet P-40 (BRL, Bethesda, MD) and 0.05% Tween 20 in TBS), the blots were incubated in the binding solution containing ^{125}I-labeled protein A (2.3 MBq/μg; Cal-Rad, Santa Ana, CA) at a dilution of 1:10,000 for 3 hours. After washing, the blots were air dried, exposed to imaging plates (Fuji Photo Film, Tokyo, Japan), and scanned with the BAS 2000 system (Fuji). There was an approximately linear relationship between the amounts of human TTR standard and the autoradiographic intensity of the bands in the range of 25 to 100 ng. The amount of human TTR was estimated by the sum of the autoradiographic intensities of TTR monomers and dimers.

Southern Blot Analysis of the Copy Number of the Human ttr *Gene*

Genomic DNA extracted from mice livers was digested with *Bam*HI, separated by 0.9% agarose gel electrophoresis, and transferred onto nylon membranes (Hybond-N+, Amersham). The membranes were cross-linked by exposure to ultraviolet light (UV Stratalinker 1800, Stratagene, La Jolla, CA) and hybridized with the following two ^{32}P-labeled probes: an 850-bp *Pvu*II fragment of mouse SAP cDNA[20] and a 160-bp *Xba*I-*Pst*I fragment of human TTR cDNA.[21] The copy number of 6.0-hMet 30 was estimated from the relative intensity of the hybridizing band to that of the *sap* band using the BAS 2000 system.

Measurement of Serum Thyroxine Levels

Serum total T_4 levels were measured by radioimmunoassay (RIA), as described.[17]

Thyroxine Binding to Serum Proteins

Aliquots of 5 μl of serum samples and of isolated TTR preparations (1 to 2 μg) were incubated for 30 minutes at room temperature with 15 μl of a 1:15 [^{125}I]T_4 (21.1 MBq/μg) (DuPont, Wilmington, DE) dilution in

glycine/acetate buffer (200 mmol/L glycine, 130 mmol/L sodium acetate, pH 8.6)[22] and electrophoresed on 8% native polyacrylamide gels, using the same glycine/acetate as gel and running buffer, for 3 to 5 hours at 40 mA and room temperature. The migration of albumin was followed with a serum sample incubated with bromophenol blue. Gels were dried and exposed for autoradiography.

Purification of Mouse and Human TTR

Human RBP, isolated from plasma, and retinol were mixed in a 1:1.2 molar ratio in PBS for 12 hours in the dark at 4°C and then dialyzed against coupling buffer (100 mmol/L sodium hydrogen carbonate, 500 mmol/L sodium chloride, pH 8.3) for 6 hours in the dark. Coupling to cyanogen-bromide-activated Sepharose CL-4B (Pharmacia, Uppsala, Sweden) was performed at 4°C following the instructions of the supplier. Mouse serum samples of 200 μl were diluted in 400 μl of TBS and recirculated in the RBP column; after washing with TBS, the RBP-Sepharose-bound fraction was eluted with H_2O, pH 10.4.[23] Both fractions were concentrated to the initial volumes by centrifugation on Centricon-10 filters (Amicon, Beverly, MA).

Human TTR Met 30 and human normal TTR were isolated from recombinant bacteria as previously described.[24] Quantification of human native TTR by radial immunodiffusion was performed using a kit from The Binding Site (Birmingham, UK).

Hybrid Tetramer Formation between Mouse TTR and Human Variant or Normal TTR in Vitro

One hundred micrograms of mouse TTR, recombinant human TTR Met 30, and recombinant human normal TTR were individually denatured by agitation in 1 ml of 6 mol/L guanidine for 16 hours at 37°C. Solutions containing mouse TTR and human TTR Met 30 or mouse TTR and human normal TTR molecules were then mixed for 1 hour at 37°C, followed by dialysis in glycine/acetate buffer. The same denaturing/renaturing treatment was applied to one hundred micrograms of recombinant human TTR Met 30 and to one hundred micrograms of recombinant normal human TTR preparations. The dialyzed solutions were concentrated in Centricon-10 filters (Amicon).

Measurement of Serum RBP Levels

Serum RBP levels were measured by RIA, as described.[18]

Statistical Analysis

Group values, expressed as the mean ± SD, were compared by Student's *t*-test. $P < 0.05$ was considered significant.

Results

Amyloid Deposition

Six $ttr^{-/-}$ transgenic mice carrying 6.0-hMet 30 were killed at 5, 7, 11, 14, and 18 months of age and examined for the occurrence and tissue distribution of amyloid deposits, as described under Materials and Methods. To compare the onset, progression, and tissue distribution of amyloid deposition between the $ttr^{-/-}$ and $ttr^{+/+}$ transgenic mice carrying 6.0-hMet 30, we also examined histochemically six $ttr^{+/+}$ transgenic mice. Amyloid deposits were not detected in any of the 5- and 7-month-old transgenic mice. As shown in Table 1, amyloid deposits were first observed at 11 months of age in the esophagus and stomach. With advancing age, these deposits extended to various other tissues. There was no significant difference in the onset, progression, and tissue distribution of amyloid deposition between the $ttr^{-/-}$ and $ttr^{+/+}$ transgenic mice carrying 6.0-hMet 30. This result suggests that endogenous normal mouse TTR does not affect the deposition of human TTR-derived amyloid in the transgenic mice. No amyloid deposits were detected in peripheral nervous tissues in the transgenic mice up to age 24 months. Thus, deposition of human TTR Met-30-derived amyloid in the peripheral nervous tissues of the transgenic mice could not be induced by eliminating normal mouse TTR.

Amyloid deposits in the $ttr^{-/-}$ transgenic mice carrying 6.0-hMet 30 were stained with Congo red (Figure 1, a, c, and e) and emitted an apple-green birefringence under polarized light (Figure 1, b, d, and f). The amyloid deposits in the $ttr^{-/-}$ transgenic mice carrying 6.0-hMet 30 reacted with anti-human TTR antibody (Figure 2, a–c), indicating that human variant TTR deposits as amyloid fibrils in transgenic mice.

Amyloid deposits of all types have been shown to contain SAP.[25] As indicated in Figure 2d, the amyloid deposits in the $ttr^{-/-}$ transgenic mice carrying 6.0-hMet 30 reacted with anti-mouse SAP antibody. This result clearly demonstrates that murine SAP binds to human TTR Met-30-derived amyloid.

To investigate the relationship between amyloid deposition and serum levels of human TTR, TTR

Table 1. *Tissu*
Carr

Age examin (months)
11
14
18

–/–, homo
2 means appr

serum leve
detailed u
The levels
mice varie
level of h
(36 ± 13
$ttr^{+/+}$ tran
wide varia
appear to
acute infl
correlatec
(Table 1).
hMet 30
Materials
mice wer

Table 1. *Tissue Distribution of Amyloid Deposits in TTR-Deficient ($ttr^{-/-}$) and Wild-Type ($ttr^{+/+}$) Transgenic Mice Carrying the Human Mutant ttr Gene (6.0-hMet 30)*

Age examined (months)	Genotype	Amyloid deposit	Tissue	Serum level of human TTR (mg/dl)	Copy number
11	−/−	+	Esophagus	39	2
		+	Esophagus	24	1
		+	Esophagus, stomach	32	2
		−		32	2
		−		22	1
		−		40	2
	+/+	+	Esophagus	30	1
		−		33	1
		−		40	1
		−		79	2
		−		58	2
		−		39	1
14	−/−	+	Esophagus, heart, lung, bladder	48	2
		+	Esophagus, heart, stomach, intestine, liver	33	1
		−		26	1
		−		26	1
		−		67	2
		−		27	1
	+/+	+	Esophagus, heart, stomach, intestine	41	2
		+	Esophagus, heart, stomach, intestine	29	1
		−		46	2
		−		26	1
		−		30	1
		−		65	2
18	−/−	+	Heart, intestine, kidney	23	1
		+	Esophagus, lung, intestine, spleen	25	1
		+	Esophagus, heart, stomach, intestine, liver, spleen, thyroid	27	1
		−		58	2
		−		59	2
		−		36	2
	+/+	+	Kidney	22	1
		+	Esophagus, lung, intestine	26	1
		+	Esophagus, stomach, intestine	60	2
		+	Heart, intestine, spleen	28	2
		−		34	1
		−		37	1

−/−, homozygous for the mutant *ttr* gene; +/+ wild-type; −, amyloid deposit is absent; +, amyloid deposit is present. For copy number, 2 means approximately 60 copies and 1 means approximately 30 copies of 6.0-hMet 30.

serum levels were measured by Western blotting, as detailed under Materials and Methods (Figure 3). The levels of human TTR in the serum of transgenic mice varied from 22 to 79 mg/dl. The mean serum level of human TTR in the $ttr^{-/-}$ transgenic mice (36 ± 13 mg/dl) was nearly equivalent to that in the $ttr^{+/+}$ transgenic mice (40 ± 15 mg/dl) (Table 1). The wide variation in serum levels of human TTR did not appear to be due to environmental factors, such as acute inflammation and starvation[26,27] but instead correlated well with the copy number of 6.0-hMet 30 (Table 1). The copy number of the integrated 6.0-hMet 30 was estimated by Southern blotting (see Materials and Methods). Because the transgenic mice were generated by interbreeding of F2 mice hemizygous for 6.0-hMet 30 (6.0-hMet $30^{+/-}$), they are expected to be either hemizygous (6.0-hMet $30^{+/-}$) or homozygous (6.0-hMet $30^{+/+}$) for 6.0-hMet 30. The result of this analysis showed that the approximate copy numbers of 6.0-hMet 30 of hemizygous (6.0-hMet $30^{+/-}$) and homozygous (6.0-hMet $30^{+/+}$) mice were 30 and 60, respectively (data not shown). The mean serum level of human TTR in the hemizygous (6.0-hMet $30^{+/-}$) and homozygous (6.0-hMet $30^{+/+}$) transgenic mice was 29 ± 5.3 mg/dl (n = 20) and 49 ± 14 mg/dl (n = 16), respectively. As expected, there was a correlation between the serum levels of human TTR and the copy number of the transgene 6.0-hMet 30. However, no correlation was observed between the copy number of 6.0-hMet

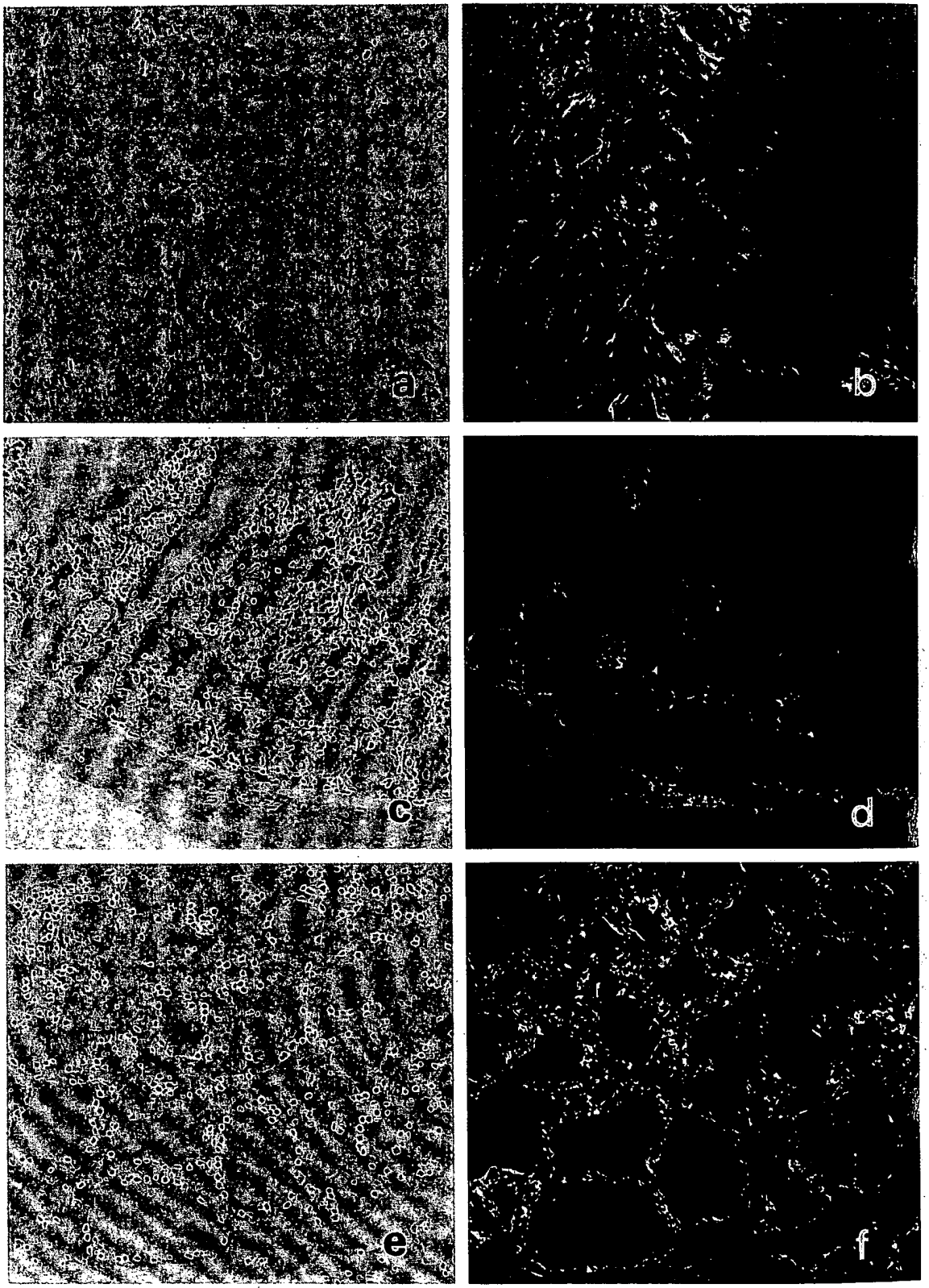

Figure 1. *Congo-red-positive deposits are present in the myocardium of heart* (a), *in the mucosal and submucosal layers of small intestine* (c), *and in the interstitium of thyroid gland* (e) *of* tv^{I-} *transgenic mice carrying 6.0-hMet 30. In the same sections, these deposits are seen emitting apple-green birefringence in polarized light* (b, d, *and* f). *Congo red stain; magnification,* ×40 (a *and* b), ×320 (c *to* f).

Figure 2. *Hist completely ref Amyloid depo* b); *indirect i*

1

Figure 3. *W ttr*$^{-/-}$ *transg indicate the tively.* Lane *μl each of m TTR plasma and monon cross-reacti*

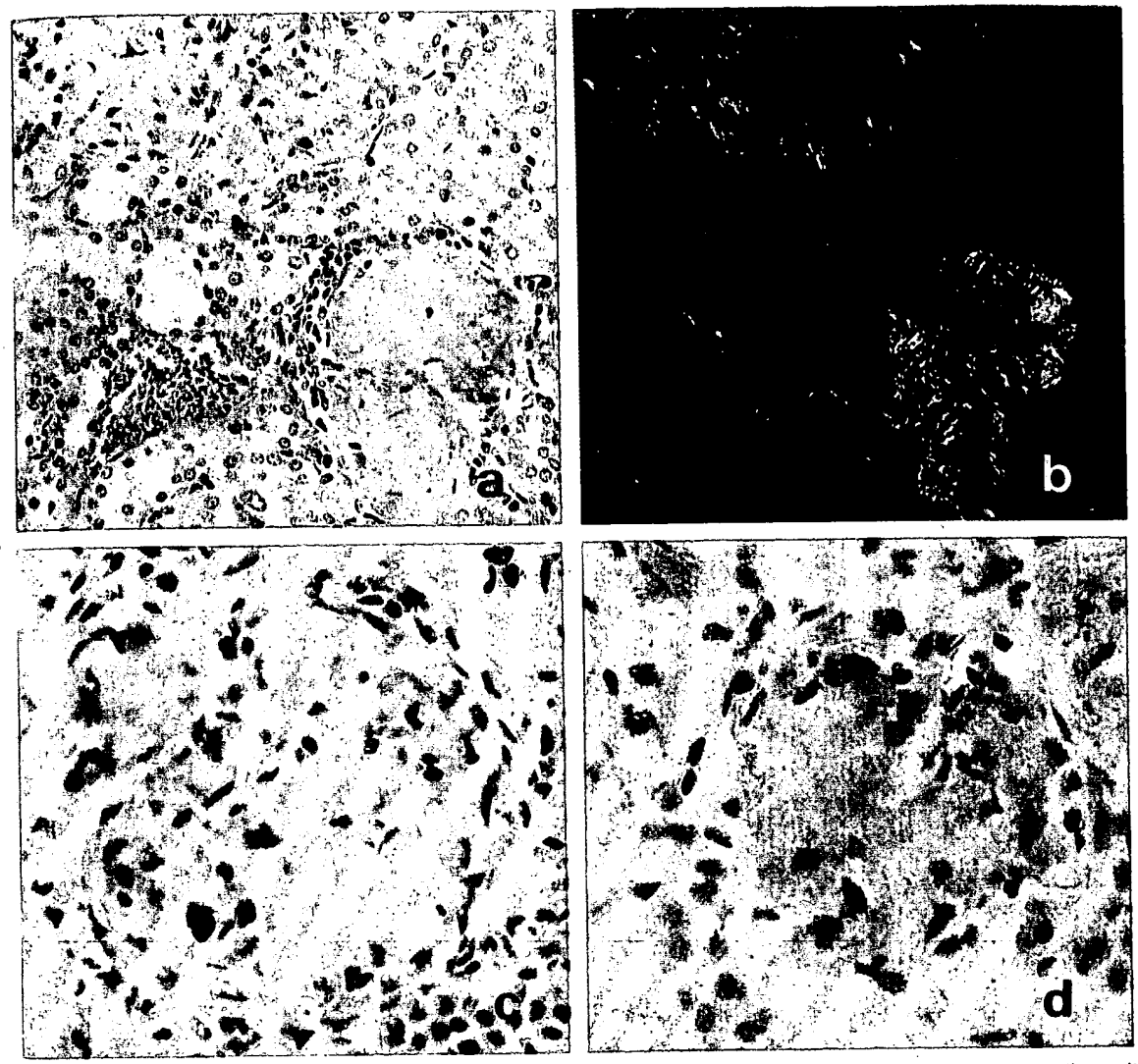

Figure 2. *Histochemical and immunohistochemical findings of renal tissues from the ttr*$^{-/-}$ *transgenic mice carrying 6.0-hMet 30. Glomeruli are completely replaced by Congo-red-positive amorphous deposits* (a), *which emit apple-green birefringence under a polarized light microscope* (b). *Amyloid deposits in the glomeruli show positive reactions for anti-human TTR antibody* (c) *and anti-mouse SAP antibody* (d). *Congo red stain* (a *and* b); *indirect immunoperoxidase method* (c *and* d); *magnification,* ×100 (a *and* b) *and* ×200 (c *and* d).

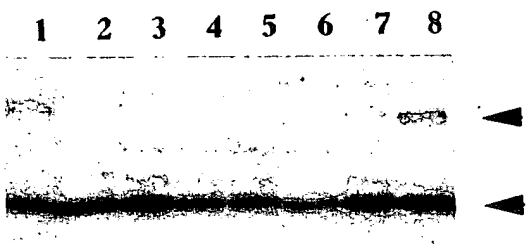

Figure 3. *Western blot analysis of serum levels of human TTR in the ttr*$^{-/-}$ transgenic mice. The upper *and* lower arrowheads *on the right indicate the locations of the human TTR dimer and monomer, respectively.* Lane 1, *25 ng of standard human TTR plasma;* lanes 2 *to* 7, *2 μl each of mouse serum diluted 1:40;* lane 8, *50 ng of standard human TTR plasma. The intermediate bands between the human TTR dimer and monomer, which appear in* lanes 2 *to* 7 *represent nonspecific cross-reacting material also present in the sera of nontransgenic mice.*

30 or the serum levels of human variant TTR and the onset and extent of amyloid deposition in these transgenic mice (Table 1).

Serum Total Thyroxine Levels

To analyze the potential of human TTR Met 30 to bind T_4, serum total T_4 levels were assayed by RIA in 11 $ttr^{-/-}$ and 10 $ttr^{+/+}$ mice and in 12 $ttr^{-/-}$ and 10 $ttr^{+/+}$ transgenic mice carrying 6.0-hMet 30 (Table 2). Serum total T_4 levels in the $ttr^{-/-}$ nontransgenic mice were reduced to 41% of that of the wild-type mice. The $ttr^{-/-}$ transgenic mice carrying 6.0-hMet 30 had 38% higher total T_4 levels compared with $ttr^{-/-}$ nontransgenic mice. This result suggests that

Table 2. *Serum Total T4 and RBP Levels*

Genotype	T4 (μg/dl)	n	RBP (mg/dl)	n
$ttr^{-/-}$	1.69 ± 0.41	11	0.11 ± 0.09*	6
$ttr^{-/-}$, 6.0-hMet 30	2.34 ± 0.54	12	2.94 ± 0.91	8
$ttr^{+/+}$, 6.0-hMet 30	4.15 ± 0.73	10	3.52 ± 0.70	8
$ttr^{+/+}$	4.16 ± 0.65	10	3.41 ± 1.21*	5

All values are given as mean ± SD. Then n values refer to number of mice used.
*These values were presented by Wei et al.[18]

human TTR Met 30 binds T_4. Serum total T_4 levels did not differ between wild-type transgenic and nontransgenic mice (Table 2).

Thyroxine Binding to Serum Proteins

The different electrophoretic mobilities of mouse TTR and human TTR on native polyacrylamide gels allowed us to detect the presence of mouse/human hybrid TTR tetramers in the sera of $ttr^{+/+}$ transgenic mice carrying 6.0-hMet 30. These hybrid tetramers are expected to bind T_4, as total serum T_4 levels in the $ttr^{+/+}$ transgenic mice were similar to wild-type nontransgenic mice (Table 2). Mouse/human hybrid TTR tetramers should, therefore, display as T_4-binding proteins with mobilities intermediate between that of mouse and human TTR. Consistent with this prediction, we found a smear of [^{125}I]T_4-binding protein in the $ttr^{+/+}$ transgenic mice (lane 3 of Figure 4) between bands representing mouse TTR (lane 4) and human TTR Met 30 (lower band of lane 2). Serum from a human homozygous for the mutant *ttr* gene showed no labeled T_4 in the TTR fraction (lane 1). However, TTR Met 30 does, in fact, have the ability to bind T_4, as seen in lane 2, where serum from a $ttr^{-/-}$ transgenic mouse carrying 6.0-hMet 30 was applied. Recombinant human TTR Met 30 likewise has a very low capacity for T_4 (lane 6). Lane 5 shows that mouse TTR/human TTR Met 30 hybrid tetramers formed *in vitro* (see below) bind T_4 efficiently. Similarly, mouse TTR/normal human TTR hybrid tetramers formed *in vitro* bind T_4 (lane 7).

Taken together, these data show that human TTR Met 30 binds T_4 and forms hybrid tetramers with mouse TTR, and that these hybrid tetramers bind T_4 efficiently. The level of native human TTR in the serum of the $ttr^{+/+}$ transgenic mice carrying 6.0-hMet 30, as determined by radial immunodiffusion using human TTR-specific antibody, was nearly twice that of the $ttr^{-/-}$ transgenic mice carrying 6.0-hMet 30 (data not shown). This difference could not be accounted for by differential expression of the human mutant *ttr* gene in the two strains, as Western blot analysis indicated that the serum levels of human TTR monomers were similar in both groups of mice (Figure 3). This result suggests that the formation of mouse/human hybrid TTR tetramers increases the number of immunoreactive TTR tetramers in the serum of the $ttr^{+/+}$ transgenic mice. Further support for this notion comes from the analysis by radial immunodiffusion of mouse/human hybrid TTR tetramers formed *in vitro*.

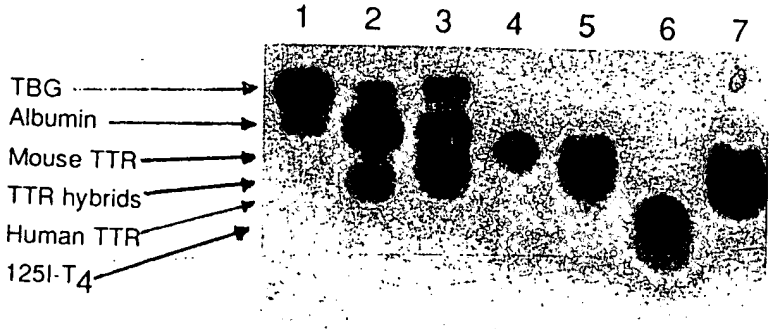

Figure 4. In vivo *and* in vitro *formed mouse and human TTR tetramers were electrophoresed on native PAGE after incubation with* [^{125}I]T_4. Lane 1 , *serum from a homozygous human TTR Met 30;* lane 2, *serum from a* $ttr^{-/-}$ *transgenic mouse carrying 6.0-hMet 30;* lane 3, *serum from a* $ttr^{+/+}$ *transgenic mouse carrying 6.0-hMet 30;* lane 4, *purified mouse TTR;* lane 5, in vitro *formed hybrid tetramers between purified mouse TTR and purified recombinant human TTR Met 30;* lane 6, *purified recombinant human TTR Met 30;* lane 7, in vitro *formed hybrid tetramers between purified mouse TTR and purified recombinant human normal TTR; free* [^{125}I]T_4 *migrates where indicated.*

In Vitro *Mouse/Human Hybrid TTR Tetramer Formation*

Mouse TTR and human TTR Met 30 monomers were prepared by denaturing the native TTRs. Equal concentrations of monomers were mixed and renatured in an attempt to form hybrid tetramers (Figure 4; see Materials and Methods). As a control, a sample of human TTR Met 30 alone was denatured and renatured. Corresponding amounts of untreated human TTR Met 30 were applied to the radial immunodiffusion plates. A similar value for native TTR concentration was found for the treated and untreated human TTR Met 30 solutions, showing that human TTR Met 30 was able to return to its initial configuration after denaturation. As predicted, the mixed and renatured mouse/human TTR preparation yielded twice as many immunoreactive native human TTR molecules (data not shown). Interestingly, we found that no hybrid tetramers formed unless the human and mouse TTRs were first reduced to monomers.

Serum RBP Levels

To examine the potential of human TTR Met 30 to bind RBP, serum RBP levels were measured by RIA in eight $ttr^{-/-}$ and in eight $ttr^{+/+}$ transgenic mice carrying 6.0-hMet 30. As shown in Table 2, the mean serum RBP level in the $ttr^{-/-}$ nontransgenic mice was reduced to 3% of that of the wild-type mice. The expression of 6.0-hMet 30 in these mice increased RBP levels to 86% of the wild-type mice. We conclude that human variant TTR binds RBP. Serum RBP levels were equivalent in wild-type transgenic and nontransgenic mice.

Discussion

We used $ttr^{-/-}$ and $ttr^{+/+}$ transgenic mice expressing 6.0-hMet 30 to examine the effect of endogenous mouse TTR on human TTR Met-30-derived amyloid deposition and to determine the relationship between the levels of expression of the human mutant *ttr* gene and amyloid deposition. The properties of human TTR Met 30 were also investigated. We found that the presence of endogenous normal mouse TTR does not affect human variant TTR-derived amyloid deposition. We also demonstrated that TTR Met 30 binds both T_4 and RBP and forms hybrid tetramers with mouse TTR *in vivo*.

We observed no correlation in these mice between the serum levels of human variant TTR and the time of appearance, extent, or tissue distribution of amyloid deposition. We previously generated two lines of transgenic mice carrying a human mutant *ttr* transgene; one carries a DNA fragment containing approximately 0.6 kb of the upstream region and the entire human gene (0.6-hMet 30), and the other carries a fragment in which the promoter region of the mouse metallothionein-I gene was fused to the entire human gene (MT-hMet 30).[8] The presence of mouse/human hybrid TTR tetramers in the serum of these transgenic mice was suggested by analyzing the antigenicity of TTR produced in the mice.[11] The analysis of [^{125}I]T_4-binding proteins in the serum of the $ttr^{+/+}$ transgenic mice carrying 6.0-hMet 30 showed TTR molecular species with mobilities intermediate between mouse TTR and human TTR Met 30 (Figure 4). This experiment provided direct evidence for the presence of mouse/human hybrid TTR tetramers in the transgenic mice. As hybrid TTR tetramers form *in vitro* solely by renaturation of previously denatured mouse and human TTR tetramers, we propose that mouse/human hybrid TTR tetramers form in the liver before secretion.

Although the serum levels of human TTR in the two transgenic lines were similar, amyloid deposits were more prominent in the MT-hMet 30 line than in the 0.6-hMet 30 line. The serum level of homotetramers composed of human variant TTR was expected to be higher in the MT-hMet 30 line than in the 0.6-hMet 30 line, as a significant fraction of the human TTR produced in the former derived from heart, skeletal muscle, kidney, and lung, organs in which TTR is not normally synthesized.[8] We speculated, therefore, that the human variant homotetramers were more amyloidogenic than the mouse/human hybrid TTR tetramers.[8] This notion was supported by the observations of McCutchen et al,[28] who reported that human TTR Met 30 was more amyloidogenic than wild-type TTR, which in turn was more amyloidogenic than a variant TTR with a substitution of methionine for threonine at position 119 (TTR Met 119), a nonpathogenic variant in the Portuguese population. Moreover, the TTR Met 119 mutation appears to protect individuals who also carry the TTR Met 30 mutation in different monomeric subunits within the TTR tetramer from developing amyloidosis.[29] This result suggested that amyloid deposits would be more prominent in the $ttr^{-/-}$ transgenic mice expressing 6.0-hMet 30 than in the $ttr^{+/+}$ transgenic mice expressing 6.0-hMet 30, because the serum level of the homotetramers composed of human TTR Met 30 should be significantly higher in the former than in the latter. However, we found no significant difference in the onset, progression, and tissue distribution of amyloid deposition between the $ttr^{-/-}$

and $ttr^{+/+}$ transgenic mice carrying 6.0-hMet 30 (Table 1). Our observation is consistent with the finding that the age of onset and severity of clinical symptoms of the FAP patients homozygous for the TTR Met 30 mutation are the same as those seen among FAP patients heterozygous for the mutation.[30]

The onset and progression of amyloid deposition between two independent lines of MT-hMet 30 transgenic mice have been compared.[31] The serum level of human TTR Met 30 in one line was approximately 5 mg/dl, ie, fivefold higher than the other. In good correlation with the serum levels of human variant TTR, amyloid deposits were more prominent in the former line than in the latter.[31] The serum levels of human TTR Met 30 were significantly higher in the transgenic mice used in the present study than in either of the MT-hMet 30 lines, and unlike the earlier study, there was no correlation between amyloid deposition and the serum levels of human TTR Met 30 (Table 1). These findings suggest that, although variant TTR is necessary for amyloid deposition, concentrations of variant TTR above a threshold serum level do not further enhance amyloid deposition.

No amyloid deposits were detected in the peripheral nervous tissues of transgenic mice expressing 6.0-hMet 30 up to age 24 months. A specific interaction between human variant TTR and the component(s) of peripheral nerve may be necessary for amyloid deposition in these tissues. Myelin P_2 protein, a minor component of myelin, a structure unique to the nervous tissues, is specifically associated with TTR-derived amyloid fibrils from FAP patients.[32] Amyloid deposition in the peripheral nervous tissues might require a specific interaction between human TTR Met 30 and human myelin P_2 protein. Construction of transgenic mice carrying and expressing both the human mutant *ttr* gene and human myelin P_2 protein gene will aid in testing this hypothesis.

Amyloid deposition in the gastrointestinal tract is more prominent in transgenic mice than in FAP patients, and in the stomach of transgenic mice, it is more prominent in the nonglandular side than in the glandular side.[9] These observations suggest that the absence of amyloid deposition in peripheral nervous tissues of the transgenic mice might reflect fine anatomic structural differences between mice and humans, including the blood-nerve barrier.[33]

Immunohistochemical analysis of amyloid deposits in the $ttr^{-/-}$ transgenic mice carrying 6.0-hMet 30 demonstrated that human TTR and mouse SAP are deposited as amyloid fibrils (Figure 2). We previously reported that amyloid deposits in $ttr^{+/+}$ transgenic mice carrying 6.0-hMet 30 reacted with anti-mouse SAP antibody.[9] Because both variant and normal TTR are present in amyloid deposits of FAP patients[5,34] and we demonstrated the presence of mouse/human hybrid TTR tetramers in the serum of the transgenic mice, amyloid deposits in the $ttr^{+/+}$ transgenic mice are likely to be composed of both human variant and mouse normal TTR. Thus, it was not clear whether mouse SAP bound to human variant or mouse normal TTR in the amyloid deposits. Because the mice lack endogenous mouse TTR, the results described here clearly indicate that mouse SAP binds to human TTR-derived amyloid deposits. This observation is consistent with the report that SAP recognizes a protein conformation specific for amyloid fibrils.[35]

The introduction of 6.0-hMet 30 into the $ttr^{-/-}$ mice increased the total serum T_4-binding capacity of $ttr^{-/-}$ mice by 38% (Table 2), suggesting that TTR Met 30 homotetramers bind T_4 *in vivo*. The analysis of T_4-binding proteins in the sera of $ttr^{-/-}$ transgenic mice confirmed the T_4-binding ability of human TTR Met 30 homotetramers (Figure 4). Recombinant human TTR Met 30 homotetramers have been reported to bind T_4 *in vitro*.[24] On the other hand, Rosen et al[36] detected no T_4 bound to TTR Met 30 homotetramers in the serum of homozygous FAP patients. In humans, thyroxine-binding globulin is the major plasma carrier of T_4, whereas TTR is the major carrier in rodents.[37] We think it likely that the T_4-binding ability of TTR Met 30 homotetramers in the serum of homozygous FAP patients is masked by thyroxine-binding globulin. In mice, thyroxine-binding globulin is much less abundant and has less affinity for T_4 than in humans. The analysis of [^{125}I]T_4-binding proteins in the serum of the $ttr^{+/+}$ transgenic mice carrying 6.0-hMet 30 provided direct evidence for the presence of mouse/human hybrid TTR tetramers in the transgenic mice. It indicates, furthermore, that such hybrid tetramers bind T_4. However, despite the increased number of circulating TTR molecules, the serum total T_4-binding capacity of the $ttr^{+/+}$ transgenic mice carrying 6.0-hMet 30 was equivalent to the $ttr^{+/+}$ nontransgenic mice. This finding suggests that the mouse/human hybrid TTR tetramer has less affinity for T_4 than the mouse TTR.

The serum RBP levels of FAP patients heterozygous for the TTR Met 30 mutation are normal,[38] whereas those of FAP patients heterozygous for the TTR Ser 84 mutation are significantly depressed.[39,40] X-ray crystallographic analysis of the structure of the complex formed by TTR and RBP indicates that position 84, but not position 30, of TTR is involved in the interaction with RBP.[41] The introduction of 6.0-hMet 30 into the $ttr^{-/-}$ mice increased the serum RBP level up to 86% of that of the wild-type mice (Table 2),

suggesting that human TTR Met 30 and mouse RBP form a complex. Formation of a complex *in vitro* between TTR and RBP from different species has been reported.[42]

The existence of mouse/human hybrid TTR tetramers in the serum of wild-type transgenic mice suggests that TTR may circulate as a hybrid tetramer composed of variant and normal TTR monomers in the serum of heterozygous FAP patients. Both variant and normal TTR are present in amyloid deposits of heterozygous FAP patients.[5,34] Whether TTR is present in the deposits as monomers, homotetramers, or hybrid tetramers is unknown. It has been proposed that the TTR tetramer dissociates into a monomeric intermediate that self-assembles into amyloid fibrils.[43] Analyses of mouse/human hybrid TTR tetramers in the serum or amyloid deposits of the transgenic mice should aid in elucidating the process of amyloid deposition. Such studies are now in progress.

In the present work, we established a transgenic mouse model of TTR Met-30-associated homozygous FAP by introducing 6.0-hMet 30 into $ttr^{-/-}$ mice generated through gene targeting.[12] The $ttr^{-/-}$ transgenic mouse carrying 6.0-hMet 30 has proved to be a better model than the wild-type transgenic mouse carrying 6.0-hMet 30 for studying the biochemistry of human TTR Met 30. The same approach should be useful in establishing mouse models of other variant TTR-associated FAP.

References

1. Andrade C: A peculiar form of peripheral neuropathy: familial atypical generalized amyloidosis with special involvement of peripheral nerves. Brain 1952, 75:408–427
2. Saraiva MJM: Transthyretin mutations in health and disease. Hum Mutat 1995, 5:191–196
3. Tawara S, Nakazato M, Kangawa K, Matsuo H, Araki S: Identification of amyloid prealbumin variant in familial amyloidotic polyneuropathy (Japanese type). Biochem Biophys Res Commun 1983, 116:880–888
4. Dwulet FE, Benson MD: Primary structure of an amyloid prealbumin and its plasma precursor in a heredofamilial polyneuropathy of Swedish origin. Proc Natl Acad Sci USA 1984, 81:694–698
5. Saraiva MJM, Birken S, Costa PP, Goodman DS: Amyloid fibril protein in familial amyloidotic polyneuropathy, Portuguese type: definition of molecular abnormality in transthyretin (prealbumin). J Clin Invest 1984, 74:104–119
6. Ide M, Mita S, Ikegawa S, Maeda S, Shimada K, Araki S: Identification of carriers of mutant prealbumin gene associated with familial amyloidotic polyneuropathy type I by Southern blot procedures: study of six pedigrees in the Arao district of Japan. Hum Genet 1986, 73:281–285
7. Wakasugi S, Inomoto T, Yi S, Naito M, Uehira M, Iwanaga T, Maeda S, Araki K, Miyazaki J, Takahashi K, Shimada K, Yamamura K: A transgenic mouse model of familial amyloidotic polyneuropathy. Proc Jpn Acad 1987, 63(B):344–347
8. Shimada K, Maeda S, Murakami T, Nishiguchi S, Tashiro F, Yi S, Wakasugi S, Takahashi K, Yamamura K: Transgenic mouse model of familial amyloidotic polyneuropathy. Mol Biol Med 1989, 6:333–343
9. Yi S, Takahashi K, Naito M, Tashiro F, Wakasugi S, Maeda S, Shimada K, Yamamura K, Araki S: Systemic amyloidosis in transgenic mice carrying the human mutant transthyretin (Met 30) gene. Am J Pathol 1991, 138:403–412
10. Blake CCF, Geisow MJ, Swan ID, Rerat C, Rerat B: Structure of human plasma prealbumin at 2.5 Å resolution: a preliminary report on the polypeptide chain conformation, quaternary structure and thyroxine binding. J Mol Biol 1974, 88:1–12
11. Yamamura K, Wakasugi S, Maeda S, Inomoto T, Iwanaga T, Uehira M, Araki K, Miyazaki J, Shimada K: Tissue-specific and developmental expression of human transthyretin gene in transgenic mice. Dev Genet 1987, 8:195–205
12. Episkopou V, Maeda S, Nishiguchi S, Shimada K, Gaitanaris GA, Gottesman ME, Robertson EJ: Disruption of the transthyretin gene results in mice with depressed levels of plasma retinol and thyroid hormone. Proc Natl Acad Sci USA 1993, 90:2375–2379
13. Nagata Y, Tashiro F, Yi S, Murakami T, Maeda S, Takahashi K, Shimada K, Okamura H, Yamamura K: A 6-kb upstream region of the human transthyretin gene can direct developmental, tissue-specific, and quantitatively normal expression in transgenic mouse. J Biochem 1995, 117:169–175
14. Blake CCF, Geisow MJ, Oatley SJ, Rerat B, Rerat C: Structure of prealbumin: secondary, tertiary and quaternary interactions determined by Fourier refinement at 1.8 Å. J Mol Biol 1978, 121:339–356
15. Jaarsveld PP van, Edelhoch H, Goodman DS, Robbins J: The interaction of human plasma retinol-binding protein and prealbumin. J Biol Chem 1973, 248:4698–4705
16. Raz A, Shiratori T, Goodman DS: Studies on the protein-protein and protein-ligand interactions involved in retinol transport in plasma. J Biol Chem 1970, 245: 1903–1912
17. Palha JA, Episkopou V, Maeda S, Shimada K, Gottesman ME, Saraiva MJM: Thyroid hormone metabolism in a transthyretin-null mouse strain. J Biol Chem 1994, 269:33135–33139
18. Wei S, Episkopou V, Piantedosi R, Maeda S, Shimada K, Gottesman ME, Blaner WS: Studies on the metabolism of retinol and retinol-binding protein in transthyre-

tin-deficient mice produced by homologous recombination. J Biol Chem 1995, 270:866–870
19. Isobe S, Nakane PK, Brown WR: Studies on translocation of immunoglobulins across intestinal epithelium. I. Improvements in the peroxidase-labeled antibody method for applications to study of human intestinal mucosa. Acta Histochem Cytochem 1977, 10:161–171
20. Nishiguchi S, Maeda S, Araki S, Shimada K: Structure of the mouse serum amyloid P component gene. Biochem Biophys Res Commun 1988, 155:1366–1373
21. Mita S, Maeda S, Shimada K, Araki S: Cloning and sequence analysis of cDNA for human prealbumin. Biochem Biophys Res Commun 1984, 124:558–564
22. Saraiva MJM, Costa PP, Goodman DS: Transthyretin (prealbumin) in familial amyloidotic polyneuropathy: genetical and functional aspect. Adv Neurol, 1988 48: 201–210
23. Navab M, Smith JE, Goodman DS: Rat plasma prealbumin-metabolic studies on effects of vitamin A status and on tissue contribution. J Biol Chem 1977, 252: 5107–5114
24. Furuya H, Saraiva MJM, Gawinowicz MA, Alves IL, Costa PP, Sasaki H, Goto I, Sakaki Y: Production of recombinant human transthyretin with biological activities toward the understanding of the molecular basis of familial amyloidotic polyneuropathy (FAP). Biochemistry 1991, 30:2415–2421
25. Pepys MB, Rademacher TW, Amatayakul-Chantler S, Williams P, Noble GE, Hutchinson WL, Hawkins PN, Nelson SR, Gallimore JR, Herbert J, Hutton T, Dwek RA: Human serum amyloid P component is an invariant constituent of amyloid deposits and has a uniquely homogeneous glycostructure. Proc Natl Acad Sci USA 1994, 91:5602–5606
26. Dickson PW, Howlett GJ, Schreiber G: Rat transthyretin (prealbumin): molecular cloning, nucleotide sequence, and gene expression in liver and brain. J Biol Chem 1985, 260:8214–8219
27. Murakami T, Onishi S, Nishiguchi S, Maeda S, Araki S, Shimada K: Acute-phase response of mRNAs for serum amyloid P component, C-reactive protein and prealbumin (transthyretin) in mouse liver. Biochem Biophys Res Commun 1988, 155:554–560
28. McCutchen SL, Lai Z, Miroy GJ, Kelly JW, Colón W: Comparison of lethal and nonlethal transthyretin variants and their relationship to amyloid disease. Biochemistry 1995, 34:13527–13536
29. Alves IL, Saraiva MJM: Comparative catabolism and stability of TTR Met 30 and TTR Met 119. Neuromuscul Disord 1996, 6:S19
30. Holmgren G, Bergstrom S, Drugge U, Lundgren E, Nording-Sikstorm C, Sandgren O, Steen L: Homozygosity for the transthyretin-Met30-gene in seven individuals with familial amyloidosis with polyneuropathy detected by restriction enzyme analysis of amplified genomic DNA sequences. Clin Genet 1992, 41:39–41
31. Yamamura K, Tashiro F, Wakasugi S, Yi S, Maeda S, Shimada K: Transgenic mouse model of autosomal dominant disease: familial amyloidotic polyneuropathy. Molecular Mechanisms of Aging. Edited by K Beyreuther, G Schttler. Heidelberg, Springer-Verlag, 1990, pp 146–154
32. Martone RL, Benson MD, Herbert J: Myelin P2 protei in transthyretin (Ser-84) vitreous amyloid. Amyloid and Amyloidosis 1990. Edited by JB Natvig, Ø Førre, G Husby, A Husebekk, B Skogen, K Sletten, P Westermark. Amsterdam, Kluwer Academic Publishers, 1991, pp 655–658
33. Wadhwani KC, Rapoport SI: Transport properties of vertebrate blood-nerve barrier: comparison with blood-brain barrier. Prog Neurobiol 1994, 43:235–279
34. Benson MD, Dwulet FE: Identification of carriers of a variant plasma prealbumin (transthyretin) associated with familial amyloidotic polyneuropathy type I. J Clin Invest 1985, 75:71–75
35. Tennent GA, Lovat LB, Pepys MB: Serum amyloid P component prevents proteolysis of the amyloid fibrils of Alzheimer disease and systemic amyloidosis. Proc Natl Acad Sci USA 1995, 92:4299–4303
36. Rosen HN, Moses AC, Murrell JR, Liepnieks JJ, Benson MD: Thyroxine interactions with transthyretin: a comparison of 10 different naturally occurring human transthyretin variants. J Clin Endocrinol Metab 1993, 77:370–374
37. Davis PJ, Spaulding SW, Gregerman RI: The three thyroxine-binding proteins in rat serum: binding capacities and effects of binding inhibitors. Endocrinology 1970, 87:978–986
38. Saraiva MJM, Costa PP, Goodman DS: Studies on plasma transthyretin (prealbumin) in familial amyloidotic polyneuropathy, Portuguese type. J Lab Clin Med 1983, 102:590–603
39. Benson MD, Dwulet FE: Prealbumin and retinol binding protein serum concentrations in the Indiana type hereditary amyloidosis. Arthritis Rheum 1983, 26:1493–1498
40. Dwulet FE, Benson MD: Characterization of a transthyretin (prealbumin) variant associated with familial amyloidotic polyneuropathy type II (Indiana/Swiss). J Clin Invest 1986, 78:880–886
41. Monaco HL, Rizzi M, Coda A: Structure of a complex of two plasma proteins: transthyretin and retinol-binding protein. Science 1995, 268:1039–1041
42. Rask L: The vitamin A transporting system in porcine plasma. Eur J Biochem 1974, 44:1–5
43. Colon W, Kelly JW: Partial denaturation of transthyretin is sufficient for amyloid fibril formation *in vitro*. Biochemistry 1992, 31:8654–8660

BEST AVAILABLE IMAGES

Defective images within this document are accurate representations of the original documents submitted by the applicant.

Defects in the images may include (but are not limited to):

- BLACK BORDERS
- TEXT CUT OFF AT TOP, BOTTOM OR SIDES
- FADED TEXT
- ILLEGIBLE TEXT
- SKEWED/SLANTED IMAGES
- COLORED PHOTOS
- BLACK OR VERY BLACK AND WHITE DARK PHOTOS
- GRAY SCALE DOCUMENTS

IMAGES ARE BEST AVAILABLE COPY.

As rescanning documents *will not* correct images, please do not report the images to the Image Problem Mailbox.

American Journal of Pathology, Vol. 138, No. 2, February 1991

Systemic Amyloidosis in Transgenic Mice Carrying the Human Mutant Transthyretin (Met30) Gene

Pathologic Similarity to Human Familial Amyloidotic Polyneuropathy, Type I

Shigehiro Yi,*† Kiyoshi Takahashi,* Makoto Naito,* Fumi Tashiro,‡ Shoji Wakasugi,‡ Shuichiro Maeda,‖ Kazunori Shimada,‖ Ken-ichi Yamamura,‡ and Shukuro Araki†

From the Second Department of Pathology, First Department of Internal Medicine,† Institute for Medical Genetics,‡ and the First Department of Biochemistry,‖ Kumamoto University Medical School, Kumamoto, Japan*

To analyze the pathologic processes of amyloid deposition in type I familial amyloidotic polyneuropathy (FAP), mice were made transgenic by introducing the human mutant transthyretin (TTR) gene. In these transgenic mice, amyloid deposition started in the gastrointestinal tract, cardiovascular system, and kidneys 6 months after birth and extended to various other organs and tissues with advancing age. At age 24 months, the pattern of amyloid deposition was similar to that observed in human autopsy cases of FAP, except for its absence in the choroid plexus and in the peripheral and autonomic nervous systems. Amyloid deposition was shown to be composed of human mutant TTR and, in addition, mouse serum amyloid P component. These results clearly indicate that human variant TTR produced in transgenic mice deposits is a major component of amyloid fibrils in various organs and tissues. Thus this animal model is useful for analyzing how amyloid deposition initiates and proceeds in FAP. (Am J Pathol 1991, 138:403–412)

Familial amyloidotic polyneuropathy (FAP) is a heredofamilial amyloidosis transmitted by an autosomal dominant trait, occurring in middle-aged adults, and running a lethal clinical course.[1] Since the first description of Portuguese patients with FAP by Andrade in 1952,[2] many similar cases have been reported in various countries. It is classified by clinical workup into at least four types: type I (Andrade type), type II (Rukavina type), type III (Van Allen type), and type IV (Meretoja type).[3] Previous studies demonstrated that amyloid precursor protein in FAP type I and II is immunologically related to a serum protein, prealbumin, recently named transthyretin (TTR).[4] Furthermore biochemical analyses revealed that these amyloid deposits consist of variant TTR molecules.[5] So far six different types of variant TTR molecules have been identified and shown to form amyloid deposits in FAP.[6]

Type I FAP predominates over the other clinical types in Japan. Several families of FAP patients reported in Kumamoto and Nagano prefectures[7,8] are classified as type I, like FAP patients in Portugal[9] and Sweden.[10] Although the average age at onset differs significantly between Japanese, Portuguese, and Swedish patients, the pathologic distribution of amyloid deposition is similar. Amyloid deposition usually occurs in the peripheral and autonomic nerve tissues, cardiovascular system, kidneys, thyroid, or small and large intestines.[11,12] In all Japanese,[5] Portuguese,[9] or Swedish[10] patients with type I FAP, biochemical studies revealed that the major component of the amyloid deposits is a variant TTR with a single amino acid substitution of valine for methionine at position 30 (hMet30). Recent molecular biologic studies demonstrated one base change from G to A in the mutant TTR gene corresponding to the single amino acid substitution at position 30.[13,14] The presymptomatic diagnosis of FAP became possible by the detection of this variant TTR in the serum or the mutant TTR gene in the

Supported in part by a grant-in-aid from the Ministry of Education, Science and Culture of Japan, a grant from the Kato Memorial Trust for Nambyo Research, and a grant from the Mitsubishi Foundation.

Accepted for publication October 2, 1990.

Address reprint requests to Dr. Kiyoshi Takahashi, Second Department of Pathology, Kumamoto University Medical School, 2-2-1 Honjo, Kumamoto 860, Japan.

chromosome.[15] All FAP patients examined so far carried at least one mutant TTR gene, suggesting that this disease is mainly caused by the presence of the mutant TTR gene. However it remains unclear why the age at onset, clinical manifestation, and degree of amyloid deposition in various tissues vary so much from one case to another.

To elucidate the pathologic processes of amyloid deposition in FAP, we produced transgenic mice by the introduction of the human mutant TTR gene and found systemic amyloidosis in them.[16] This paper describes the patterns of amyloid deposition obtained from our histochemical, immunohistochemical, and ultrastructural studies and their similarity to human FAP.

Materials and Methods

Production of Transgenic Mice

An inbred strain of mouse, C57BL/6, was chosen for DNA microinjection to minimize the possible influence of genetic background on amyloid deposition. A chromosomal DNA segment covering the entire sequence for the mutant TTR gene associated with type I FAP was cloned as described previously.[13] The 7.8-kilobase pair *StuI-EcoRI* fragment was constructed by ligating the promoter region of the mouse methallothionein-I (MT-I) gene to the entire structural gene of the human mutant TTR gene (MT-hMet30).[16]

Approximately 200 copies of these constructs (MT-hMet30) were microinjected into fertilized eggs of C57BL/6 mice according to the method described elsewhere.[17] Four of twelve mice derived from eggs microinjected with the MT-hMet30 gene integrated it, as revealed by Southern blot analysis. These transgenic offspring were used in the following studies and were kept in plastic cages in our laboratory according to the guidelines of the Ministry of Education. They were bred by brother × sister mating.

DNA Isolation and Southern Blot Analysis

When the mice were 4 weeks old, genomic DNAs were extracted from a piece of tail and used for Southern blot analysis to examine whether the MT-hMet30 gene had integrated into the mouse chromosome.[18]

Western Blot Analysis

To analyze the production of human TTR in the mice, blood was taken from each transgenic mouse before they were killed and the sera were analyzed by Western blot assay.

Preparation and Fixation of Tissues

Transgenic mice were killed using ether anesthesia at 3-month intervals up to 24 months after birth. At each time point, we examined two to six transgenic mice and excised the heart, kidneys, spleen, liver, lungs, pancreas, stomach, small and large intestines, urinary bladder, thyroid gland, lymph nodes, bone marrow, sciatic nerves, autonomic nerves, and brain. For light microscopy, tissues were fixed in 10% neutral buffered formalin and embedded in paraffin. Paraffin sections were used for histochemistry. For immunohistochemistry, part of the tissues were fixed in periodite-lysine-paraformaldehyde (PLP) fixative for 4 hours and cut by a cryostat (Bright; Huntingdon, UK). Small tissue blocks were obtained from the heart, kidneys, small intestine, and sciatic nerve, fixed in chilled 2.5% glutaraldehyde in 0.1 mol/l (molar) cacodylate buffer for 60 minutes, and submitted to electron microscopy.

Light Microscopy and Histochemistry

For light microscopy, paraffin sections were stained with hematoxylin and eosin. Semithin sections were cut from Epon-embedded blocks for electron microscopy and stained with 0.05% toluidine blue. For histochemical demonstration of amyloid, paraffin sections were stained by the Congo red method and some were treated with potassium permanganate ($KMnO_4$) before Congo red staining according to Wright's method.[19] To detect the emerald green birefringence emitted from amyloid deposits, the Congo red-stained paraffin sections were observed under a polarization microscope.

Immunohistochemistry

For immunohistochemical demonstration of the major components in amyloid deposits, formalin-fixed paraffin sections or PLP-fixed cryostat sections were immunostained by the avidin-biotin complex (ABC) method using polyclonal and monoclonal antibodies. The antibodies were anti-human TTR (Behringwerke; Marburg, FRG), anti-human serum amyloid A (SAA) (Dako; Santa Barbara, CA), anti-human serum amyloid P component (SAP) (Dako), anti-mouse SAA (supplied by Prof. S. Migita, Cancer Research Institute, Kanazawa University, Japan), and anti-mouse SAP (Behring Diagnostics; La Jolla, CA).

Electron Microscopy

After glutaraldehyde fixation, tissue blocks were post-fixed in 2% osmium tetroxide for 60 minutes, dehydrated in a graded series of ethanols, and embedded in Epok-812 (Oken; Tokyo, Japan). The blocks were cut by an ultrotome Nova (LKB, Upssala, Sweden), stained with uranyl acetate and lead citrate, and observed with an H-300 or 12-A electron microscope (Hitachi; Tokyo, Japan).

Results

Transgenic Mice

Transgenic mice showed normal appearance and good development in all lines until age 12 months. After age 15 months, hair became coarse in two lines, but no muscular atrophy or gait disturbance was found. Southern blot analysis indicated that the copy numbers of the integrated MT-hMet30 genes varied from 2 to 30 per diploid genome. The concentrations of the human mutant TTR in the blood varied among the mice and ranged from 1 to 5 mg/dl, one tenth to one half of that in FAP patients (Figure 1). When the mice were killed, no inflammatory lesions, such as pulmonary abscess or parasitic infestation, were found in any of these mice.

Amyloid Deposition

Table 1 shows the occurrence and degree of amyloid deposition in various tissues of the transgenic mice. Amyloid deposition was first found in the small intestine, stomach, and renal glomeruli at 6 months, and it occurred invariably in the gastrointestinal tract, kidneys, heart, and thyroid at 12 months and thereafter.

In the gastrointestinal tract, amyloid deposits occurred predominantly in the mucosa of the small intestine, particularly the terminal ileum. Amyloid deposition there was marked in the lamina propria of the intestinal villi and submucosal layer, and it occurred in or around the walls of small blood vessels later (Figure 2a and b). Electron microscopically, amyloid deposits were observed to consist of clusters of amyloid fibrils approximately 7 to 10 nm wide that varied in length, findings consistent with human FAP[11,12] or other types of amyloidosis (Figure 3).[20] In the initial stage, amyloid deposits were observed in the propria mucosa at the top of the intestinal villi, particularly beneath the epithelial cells. Also they were found in the basal area of the lamina propria, in the muscularis mucosae, and in the submucosa. In the submucosa, amyloid deposition occurred in the connective tissue and around small blood vessels. In the advanced stage, diffuse amyloid deposition was found in the mucosa, muscularis mucosae, submucosa, and subserosa.

In the wall of the stomach, amyloid deposits first occurred in the lamina propria of the ridge and were found in the submucosa, particularly the nonglandular part. In the large intestine, amyloid deposited in the submucosa of the cecum and anal ring.

In the kidneys, amyloid deposits occurred exclusively in the glomeruli at the initial stage, later involving the renal interstitium. Figure 4 shows the degree of amyloid deposition in the glomeruli. At age 6 months, slight amyloid deposits first were detected in the mesangial areas of about 10% of glomeruli. At 18 months, most of the glomeruli were affected by increased amyloid deposition. After 21 months, nearly 100% of the glomeruli were obliterated completely by massive amyloid deposits (Figure 2c and d). Ultrastructurally amyloid fibrils first were detected in

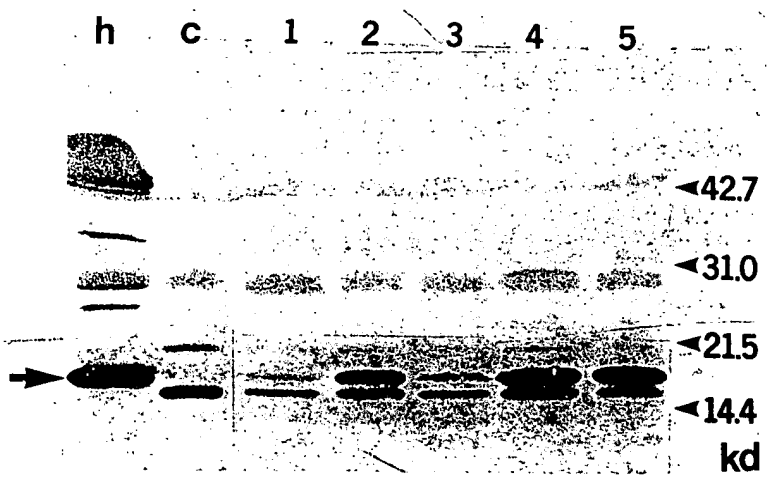

Figure 1. *Western blot analysis showing levels of expression of the MT-hMet30 gene in sera of transgenic mice. The size of the molecular weight in kilodaltons is indicated on the right of the panel. The arrow on the left indicates location of the human TTR monomer. Variable amounts of the human TTR were detected in the sera from all transgenic mice with amyloid deposits. Lane h, 0.5 μl of human serum; lane c, 1 μl of control mouse serum; lanes 1, 2, 3, 4, and 5, 1 μl of serum from each transgenic mouse at 12 months of age.*

Table 1. *Tissue Distribution of Amyloid Deposits in Transgenic Mice Carrying the MT-hMet30 Gene and Autopsy Cases of FAP[11] Determined Histochemically*

Organs	Transgenic mice: age examined (months)								Autopsy cases of FAP
	3	6	9	12	15	18	21	24	
Brain	−	−	−	−	−	−	−	−	−
Choroid plexus	−	−	−	−	−	−	−	−	+ +
Sciatic nerve	−	−	−	−	−	−	−	−	+ + +
Heart	−	−	−	+	+ +	+	+ +	+ + +	+ + +
Lung	−	−	−	−	−	−	±	±	±
Liver	−	−	−	−	−	−	±	±	±
Spleen	−	−	−	−	−	−	±	±	±
Kidney	−	+	−	+	+	+ +	+ + +	+ + +	+ + +
Pancreas	−	−	−	−	−	−	±	±	+
Thyroid gland	−	−	−	+	+	+ +	+ +	+ + +	+ + +
Stomach	−	+	−	+ +	+ +	+ +	+ +	+ + +	+
Intestine	−	+	−	+ +	+ +	+ + +	+ + +	+ + +	+
Lymph node	−	±	−	−	−	±	±	±	±

Amyloid deposits are absent, −; limited to the wall of small vessels, ±; observed in the wall of small vessels and their surrounding regions, +; moderate in the interstitium; + +; marked in the interstitium and parenchyma, + + +.
FAP, familial amyloidotic polyneuropathy.

the matrix around the mesangial cells or beneath the endothelial cells of glomerular capillaries. With age, the amount of amyloid fibrils increased and their clusters were observed in the lamina rara interna between the basal lamina and endothelial cells. At the advanced stage, clusters of amyloid fibrils were deposited massively in almost all parts of the mesangial matrix of glomeruli; the mesangial cells were swollen and the glomerular epithelial cells showed fusion of their foot processes (Figure 5). In the renal interstitium, amyloid deposition was found in the cortex after age 21 months but not in the medulla. Electron microscopically, amyloid deposition was observed to be particularly dense around the renal tubules.

In the cardiovascular system, amyloid deposits were marked. At age 12 months, slight, patchy amyloid deposition occurred in the subendocardial layer and in the superficial myocardium. Ultrastructurally clusters of amyloid fibrils in the superficial myocardium were observed initially around small blood vessels (Figure 6). After 18 months, amyloid deposits coalesced and became diffuse in the subendocardial layer and superficial myocardium (Figure 2e and f). At 24 months, the deposition extended to the deeper areas of the myocardium. On electron microscopy, myocardial cells showed atrophy and degenerative changes due to massive amyloid deposits.

In the vascular system, initial amyloid deposits were observed electron microscopically around blood capillaries or venules. Around the blood capillaries, deposits were observed beneath the basal lamina, extending to the perivascular region. Amyloid deposition in the arterial wall occurred mostly in the advanced stage, particularly in the adipose tissues and gastrointestinal tract. Also vascular amyloid deposition was found in the salivary glands, testes, lungs, and liver at age 15 months, and later in the pancreas, skeletal muscles, and splenic trabecles.

In the thyroid gland, amyloid deposits occurred around the interfollicular blood capillaries at 12 months, increased with age, and became prominent at 24 months. In the advanced stage, the thyroid follicles were compressed by marked interstitial amyloid deposition (Figure 2g and h).

In all the transgenic mice, no amyloid deposition was detected in the brain, choroid plexus, peripheral nerves, or in the hematopoietic tissues such as the bone marrow, spleen, liver, or lymph nodes. In the nontransgenic mice, no amyloid deposition was confirmed in any tissues examined up to age 24 months.

Histochemical and Immunohistochemical Features of Amyloid Deposits and Localization of Anti-human TTR in the Transgenic Mice

Amyloid deposits in the transgenic mice were stained with Congo red, showed resistance to treatment $KMnO_4$

Figure 2. *Light microscopic changes of principal organs in the transgenic mouse carrying the MT-hMet30 gene.* **a, b**: *Amyloid deposits of the terminal ileum at 12 months of age. Amyloid deposits were marked in the villous stroma and around the small vessels (×50).* **c, d**: *Amyloid deposits of the kidney at 24 months of age. All of the renal glomeruli were replaced by massive amyloid deposition (×25).* **e, f**: *Amyloid deposits of the heart at 18 months of age. Amyloid deposits were marked around the myocardial fibers (×60).* **g, h**: *Amyloid deposits of the thyroid gland at 24 months of age. Amyloid deposits were marked in the interstitium (×25). (***a, c, e,** *and* **g,** *Congo red and hematoxylin;* **b, d, f,** *and* **h,** *identical area viewed under polarizing light.)*

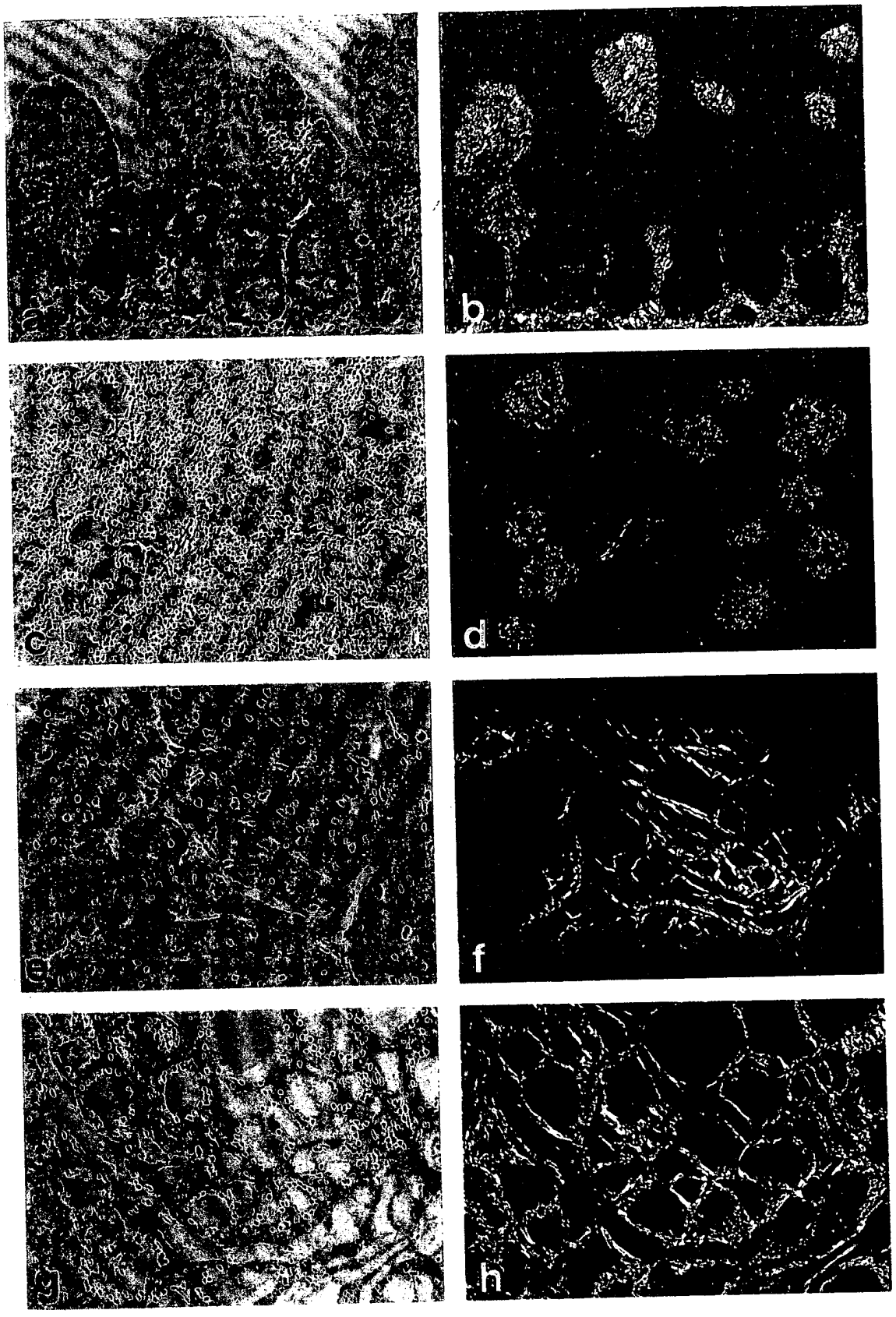
a
b
c
d
e
f
g
h

Figure 3. *Electron micrograph of submucosal tissue in the terminal ileum of the transgenic mouse at 12 months of age. Clusters of amyloid fibrils were found among collagen fibers (asterisk) in the extracellular space, but not in the cytoplasm of fibroblasts (×15,000). Inset: Higher magnification of amyloid fibrils. Amyloid fibrils measured approximately 7 to 10 nm in width (×40,000).*

by Wright's method,[18] and emitted an emerald-green birefringence under polarized light. By the ABC method, the amyloid deposits reacted with anti-human TTR (Figure 7a) and anti-mouse SAP (Figure 7b) antisera, but not with anti-mouse SAA, anti-human AA, or anti-human SAP antisera.

In the transgenic mice, liver cells, ductal epithelia of the salivary glands, pancreatic exocrine cells, epithelial cells of renal tubules at the proximal convulsion, myocardial cells, and part of the skeletal muscle cells showed immunoreactivity with anti-human TTR, but the epithelial cells of the choroid plexus were nonimmunoreactive.

The nontransgenic C57BL/6 mice demonstrated no immunoreactivity with anti-human TTR in any kind of cell.

Discussion

In this paper we demonstrated clearly that hMet30 could be deposited as amyloid fibrils in transgenic mice carrying the human mutant TTR gene (MT-hMet30). Amyloid deposition occurred predominantly in the intestinal mucosa, renal glomeruli, myocardium, small vascular walls, and thyroid. With age, amyloid deposition became marked and was found in various other organs and tissues, except for the nervous tissues. The possibility of the development of age-associated amyloid deposition in transgenic mice can be ruled out for the reasons described below.

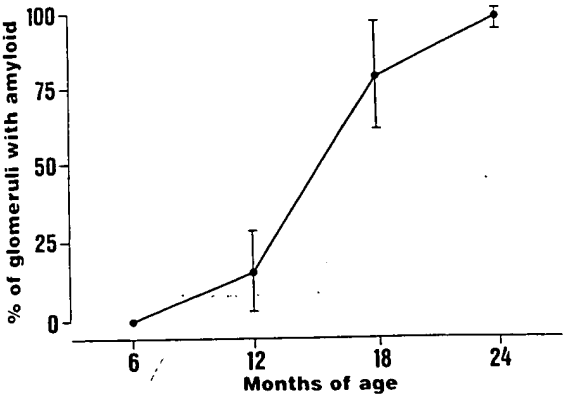

Figure 4. *Time course of amyloid deposits in renal glomeruli. Glomeruli involved in amyloid deposits suddenly increased after age 12 months. Renal amyloid deposition was expressed as the rate of affected glomeruli to total glomeruli on a section. Each point represents mean ± SD.*

Figure 5. *Electron micrograph of a renal glomerulus in the transgenic mouse at age 21 months. Amyloid fibrils (asterisk) were found in the mesangial matrix (×17,000).*

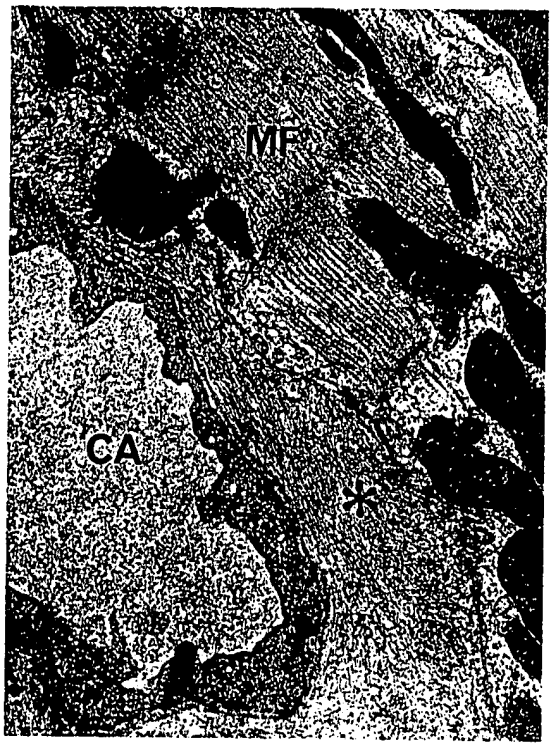

Figure 6. *Electron micrograph of the myocardium in the transgenic mouse at age 12 months. Amyloid fibrils (asterisk) were observed around small blood vessels (×17,000). CA, capillary lumen; MF, myocardial fibers.*

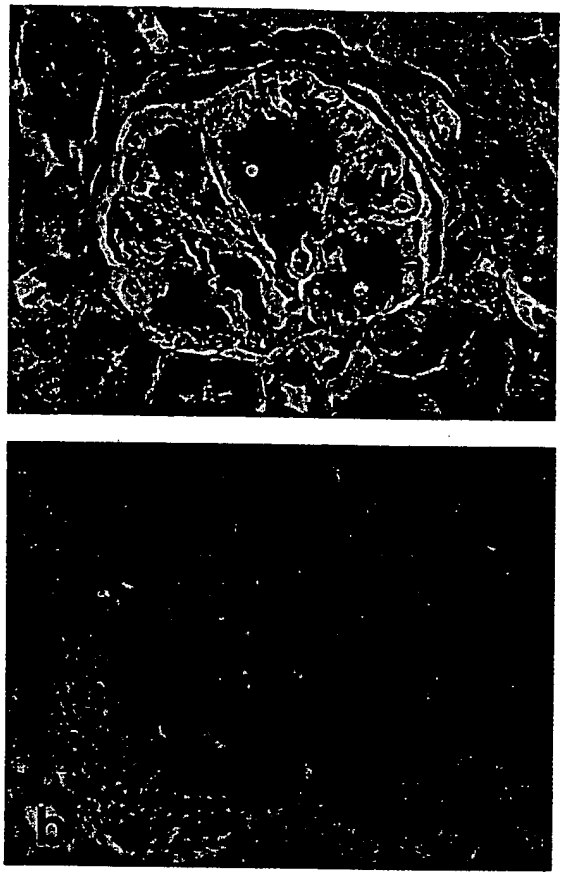

Figure 7. *Amyloid deposits in renal glomeruli showing positive staining with anti-human TTR* (a) *and anti-mouse SAP* (b) *antisera (ABC method, ×100).*

Senile amyloidosis is known to occur spontaneously in various strains of mice, including C57BL mice, and to involve the spleen, liver, heart, kidneys, or gastrointestinal tract.[21–26] In senile amyloidosis, renal amyloid deposition occurs mainly in the renal papilla or interstitium, and glomerular involvement is slight or absent.[21–25] In senile amyloidosis of C57BL mice, amyloid deposition was reported to occur in the renal papilla in 50% of the animals at age 18 months and to involve the spleen, particularly around the white splenic pulp; however glomerular amyloid involvement is slight.[21] By contrast, in transgenic mice amyloid deposition is prominent in the renal glomeruli but slight or absent in the spleen or liver. Compared to the development of spontaneous senile amyloidosis in mice,[22] in transgenic mice amyloid deposition occurs at least 6 months earlier. Another definitive difference involves amyloid precursor protein. Although the amyloid precursor protein in human senile amyloidosis is also TTR,[27,28] it has not been determined yet in mice. Non-AA[24] or apoprotein A II (Pro^5-Gln)[29] have been mentioned. In transgenic mice, however, we demonstrated clearly that the amyloid precursor protein is human variant TTR. In the following section, four subjects will be discussed in relation to the pathologic similarity and dissimilarity between the transgenic mice and human FAP autopsy cases.

First the pathologic changes of the transgenic mice correlate well with those reported in previous pathologic studies of FAP.[30–32] Some of the present authors recently reported in nine autopsy cases of type I FAP that amyloid deposition occurred predominantly in the cardiovascular system, peripheral and autonomic nervous system, choroid plexus, kidneys, thyroid, and gastrointestinal tract.[11,12] However it was slight or minimal in the pancreas, bone marrow, spleen, lymph nodes, or liver, and absent from the brain parenchyma. The major sites and pattern of amyloid deposition in the transgenic mice are similar to these human autopsy cases, except for the peripheral and autonomic nervous tissues. In the mice, cardiac amyloid deposition initially occurs in the subendocardial layer and in the superficial areas of myocardium, and then it extends deeper into the cardiac wall. This pattern is similar to that in the heart of human cases confirmed by our pathologic study.[11,12] In the kidneys of transgenic mice, amyloid deposition first occurred in the mesangial areas of the glomeruli. The number of involved glomeruli and the grade of glomerular involvement increased with age and amyloid deposition was found around the renal tubules in advanced age. These find-

ings also are almost consistent with those reported in autopsy cases of type 1 FAP.[11,12,31] Amyloid deposition in the thyroid gland of transgenic mice is prominent and its pattern closely resembles that of human cases of FAP.[11,12]

On the other hand, in the gastrointestinal tract of transgenic mice, amyloid deposition is more prominent than in the human autopsy cases of FAP and occurs predominantly in the mucosa of the terminal ileum, in the gastric submucosa at the ridge of the nonglandular part, and around the anal ring. In the mouse, the stomach is divided into two parts, the left nonglandular side and the right glandular side, by the U-shaped ridge. This ridge is formed by a thickened lamina propria. Unexpectedly amyloid deposition is more prominent in the nonglandular side, including the ridge, than in the glandular side. A similar pattern of amyloid deposition was observed around the anal ring: it was more prominent under the squamous epithelium than the glandular epithelium. It is interesting to note that such a peculiar pattern of amyloid involvement in the stomach of transgenic mice is also found in spontaneous senile amyloidosis of mice.[22,23] These results suggest that the difference of amyloid deposition in the alimentary tract between transgenic mice and FAP patients is due to the difference in anatomic structure and that such microenvironments, including the fine anatomic structure or local blood flow, are involved in the amyloid deposition.

One important question is how the amyloid deposition initiates and proceeds in the early stage of FAP. So far there has been no clear data on this subject, partly because detailed pathologic tissue analysis is only possible at autopsy. By that time a large amount of amyloid usually has accumulated in many tissues, as discussed earlier. The main target tissues for amyloid deposition in FAP patients are not the liver and the choroid plexus where the hMet30 gene is expressed. This suggests that hMet30 is transported *via* blood or lymphatic circulation into tissues to deposit as a major amyloid component *in loco*. Transgenic mice presented here made it possible to analyze the initial stage of amyloid deposition. As expected, amyloid deposition initiates around blood capillaries and extends to the perivascular region. From this point of view, it is reasonable that amyloid deposition is most prominent in tissues with a rich blood supply, such as kidneys, heart, and thyroid glands. Although the MT-hMet30 gene is expressed in a variety of tissues, the distribution pattern of amyloid deposition is not related to the tissue specificity of the MT-hMet30 gene expression.[33] This finding is consistent with the notion that amyloid fibrils are derived from the blood.

It is a well-known fact that SAP is a minor component of all types of amyloidosis.[34–36] Although its role in amyloid deposition has not been elucidated clearly yet, SAP is known to exist in the sera of various mammalian species and to have a binding capacity to specific ligands in the presence of calcium.[37] In our transgenic mice, a concomitant deposition of mouse SAP was demonstrated immunohistochemically in almost all amyloid deposits. These results suggest that the pathologic role of mouse SAP is the same as that of human SAP, although SAP is a typical acute-phase reactant in mice but not in humans. Further investigation is needed to determine whether SAP is involved in the initiation or acceleration of amyloid deposition.

Although the most striking pathologic feature of FAP is amyloid deposition in the peripheral and autonomic nervous tissues, no amyloid deposition was observed in the nervous tissues of the transgenic mice examined up to age 24 months. In all the autopsy cases of FAP, we also observed marked amyloid deposition in the choroid plexus and substantiated the histochemical localization of human TTR in the choroid plexus epithelial cells.[11,12] The choroid plexus and liver are considered the major sites of human TTR production.[38] If we consider the fact that the peripheral nerve is open-ended with respect to the subarachnoid space,[39] we can speculate that the production of human variant TTR by the choroid plexus epithelia is related to amyloid deposition in the peripheral nerve tissues. In the transgenic mice, however, we demonstrated immunohistochemically little or no production of human TTR in the epithelial cells of the choroid plexus. This could be the reason for the absence of amyloid deposition there and in the peripheral and autonomic nervous system in transgenic mice. A second possibility is the low-level expression of the hMet30 gene in these transgenic mice. To provide more definite evidence for this speculation, we are making mice transgenic that produce a high level of hMet30 in the epithelial cells of the choroid plexus. A third possibility lies in the characteristic metabolic features of the mouse itself. For example, a mutant mouse deficient for the enzyme in purine metabolism, hypoxanthine-guanine phosphoribosyl transferase (HPRT), was produced;[40,41] however no symptoms have developed yet in this mouse. In humans HPRT deficiency causes severe neurologic disorder and hyperuricemia (Lesch-Nyhan syndrome). Interestingly degenerative changes in the peripheral nerve tissues before amyloid deposition were reported in FAP patients.[11,12] Thus another intrinsic factor(s) may be involved in amyloid deposition in the nervous tissues of FAP.

Acknowledgment

The authors thank Dr. S. Migita of the Cancer Research Institute, Kanazawa University, Kanazawa, Japan, for providing the anti-mouse serum amyloid A monoclonal antibody.

References

1. Araki S: Type I familial amyloidotic polyneuropathy (Japanese type). Brain Dev 1984, 6:128–133
2. Andrade C: A peculiar form of peripheral neuropathy: Familiar atypical generalized amyloidosis with special involvement of the peripheral nerves. Brain 1952, 75:408–427
3. Glenner GG, Murphy MA: Amyloidosis of the nervous system. J Neurol Sci 1989, 94:1–28
4. Costa PP, Figueira A, Bravo F: Amyloid fibril protein related to prealbumin in familial amyloidotic polyneuropathy. Proc Natl Acad Sci USA 1978, 75:4499–4503
5. Tawara S, Nakazato M, Kangawa K, Matsuno H, Araki S: Identification of amyloid prealbumin variant in familial amyloidotic polyneuropathy (Japanese type). Biochem Biophys Res Commun 1983, 116:880–888
6. Benson MD: Familial amyloidotic polyneuropathy. Trends Neurosci 1989, 12:88–92
7. Araki S, Mawatari S, Ohta M, Nakajima A, Kuroiwa Y: Polyneuritic amyloidosis in a Japanese family. Arch Neurol 1968, 18:593–602
8. Kito S, Itoga E, Kamiya K, Kishida T, Yamamura Y: Studies in familial amyloid polyneuropathy in Ogawa Village, Japan. Eur Neurol 1980, 19:141–151
9. Saraiva MJM, Birken S, Costa PP, Googmann DS: Amyloid fibril protein in familial amyloidotic polyneuropathy, Portuguese type. J Clin Invest 1984, 74:104–119
10. Dwulet FE, Benson MD: Primary structure of an amyloid prealbumin and its plasma precursor in a heredo-familial polyneuropathy of Swedish origin. Proc Natl Acad Sci USA 1984, 81:694–698
11. Takahashi K, Kimura Y, Yi S, Araki S: Pathology of familial amyloidotic polyneuropathy occurring in Kumamoto. *In* Isobe T, Araki S, Uchino F, Kito S, Tsubura E, eds. Amyloid and Amyloidosis. New York, Plenum Press, 1988, pp 505–510
12. Takahashi K, Yi S, Kimura Y, Araki S: Type 1 familial amyloidotic polyneuropathy occurring in Kumamoto: A clinicopathologic, histochemical, immunohistochemical, and ultrastructural study. Hum Pathol 1991 (In press)
13. Mita S, Maeda S, Shimada K, Araki S: Cloning and sequence analysis of cDNA for human prealbumin. Biochem Biophys Res Commun 1984, 124:558–564
14. Sasaki H, Sakaki Y, Matsuo H, Goto I, Kuroiwa Y, Sahashi I, Takahashi A, Shinoda T, Isobe T, Takagi Y: Diagnosis of familial amyloidotic polyneuropathy by recombinant DNA techniques. Biochem Biophys Res Commun 1984, 125:636–642
15. Mita S, Maeda S, Ide M, Tsuzuki T, Shimada K, Araki S: Familial amyloidotic polyneuropathy diagnosed by cloned human prealbumin cDNA. Neurology 1986, 36:298–301
16. Wakasugi S, Inomoto T, Yi S, Naito M, Uehira M, Iwanaga T, Maeda S, Araki K, Miyazaki J, Takahashi K, Shimada K, Yamamura K: A transgenic mouse model of familial amyloidotic polyneuropathy. Proc Japan Acad 1987, 63(B):344–347
17. Yamamura K, Kikutani H, Takahashi N, Taga T, Akira S, Kawai K, Fukuchi K, Kumahara Y, Honjo T, Kishimoto T: Introduction of human γl immunoglobulin genes into fertilized mouse eggs. J Biochem (Tokyo) 1984, 96:357–365
18. Southern EM: Detection of specific sequences among fragments separated by gel electrophoresis. J Mol Biol 1975, 98:503–517
19. Wright JR: Potassium permanganate reaction in amyloidosis. Lab Invest 1977, 36:274–281
20. Glenner GG, Eanes ED, Bladen HA, Linke RP, Termine JD: β-Pleated sheet fibrils; a comparison of native amyloid with synthetic protein fibrils. J Histochem Cytochem 1974, 22:1141–1158
21. Thung PJ: Senile amyloidosis in mice. Gerontologia 1957, 1:259–279
22. Dunn TB: Relationship of amyloid infiltration and renal disease in mice. J Natl Cancer Inst 1944, 5:17–28
23. West WT, Murphy ED: Sequence of deposition of amyloid in strain a mice and relationship to renal disease. J Natl Cancer Inst 1965, 35:167–174
24. Scheinberg MA, Cathcart ES, Eastcott JW, Skinner M, Benson MD, Shirahama T, Bennett M: The SJL/J mouse: A new model for spontaneous age-associated amyloidosis. Lab Invest 1976, 35:47–54
25. Chai CK: Spontaneous amyloidosis in LLC mice. Am J Pathol 1978, 90:381–398
26. Higuchi K, Matsumura A, Honma A, Takeshita S, Hashimoto K, Hosokawa M, Yasuhira K, Takeda T: Systemic senile amyloid in senescence-accelerated mice: A unique fibril protein demonstrated in tissue from various organs by the unlabeled immunoperoxidase method. Lab Invest 1983, 48:231–240
27. Sletten K, Westermark P, Natvig JB: Senile cardiac amyloid is related to prealbumin. Scand J Immunol 1980, 12:503–506
28. Cornwell III GG, Sletten K, Johansson B, Westermark P: Evidence that the amyloid fibril protein in senile systemic amyloidosis in derived from normal prealbumin. Biochem Biophys Res Commun 1988, 154:648–653
29. Yonezu T, Tsunasawa S, Higuchi K, Kogishi K, Naiki H, Handa K, Sakiyama F, Takeda T: A molecular-pathologic approach to murine senile amyloidosis. Serum precursor-apolipoprotein A-II variant (Pro^5-Gln) presents only in the senile amyloidosis-prone SAM-P/1 and SAM-P/2 mice. Lab Invest 1987, 57:65–70
30. Guimarraes A, Monteiro L, Coutinho P: Pathology of the autonomic nervous system in Andrade type of familial amyloidotic polyneuropathy: Study of 11 postmortem cases, Amyloid and Amyloidosis. Edited by GG Glenner, PP Costa, AF de Freitas. Amsterdam, Excerpta Medica, 1979, pp 139–146
31. Horta JDS, Filipe I, Duarte S: Portuguese polyneuritic familial type of amyloidosis. Pathol Microbiol (Basel) 1964, 27:809–825
32. Ikeda S, Hanyu N, Hongo M, Yoshioka J, Oguchi H, Yanagisawa N, Kobayashi T, Tsukagoshi H, Ito N, Yokota T: Hereditary generalized amyloidosis with polyneuropathy. Clinico-pathological study of 65 Japanese patients. Brain 1987, 110:315–337
33. Shimada K, Maeda S, Murakami T, Nishiguchi S, Tashiro F,

Yi S, Wakasugi S, Takahashi K, Yamamura K: Transgenic mouse model of familial amyloidotic polyneuropathy. Mol Biol Med 1989, 6:333–343

34. Skinner M, Cathcart ES, Cohen AS, Benson MD: Isolation and identification by sequence analysis of experimentally induced guinea pig amyloid fibrils. J Exp Med 1974, 140:871–876
35. Skinner M, Cohen AS, Shirahama T, Cathcart ES: P-component (pentagonal unit) of amyloid: Isolation, characterization, and sequence analysis. J Lab Clin Med 1974, 84:604–614
36. Pepys MB, Dyck RF, De Beer FC, Skinner M, Cohen AS: Binding of serum amyloid P-component (SAP) by amyloid fibrils. Clin Exp Immunol 1979, 38:284–293
37. Pepys MB, Balz ML, de Beer FC, Dyck RF, Holford S, Breathnach SM, Black MM, Tribe CR, Evans DJ, Freinstein A: Biology of serum amyloid P component. Ann NY Acad Sci 1982, 389:286–298
38. Herbert J, Wilcox JN, Pham K-TC, Fremeau RT Jr, Zeviani M, Dwork A, Soprano DR, Makover A, Goodmann DS, Zimmerman EA, Roberts JL, Schon EA: Transthyretin: A choroid plexus-specific transport protein in human brain. Neurology 1986, 36:900–911
39. McCabe JS, Low FN: The subarachnoid angle: An area of transition in peripheral nerve. Anat Rec 1969, 164:15–34
40. Hooper M, Hardy K, Handyside A, Hunter S, Monk M: HPRT-deficient (Lesch-Nyhan) mouse embryos derived from germline colonization by cultured cells. Nature 1987, 326:292–295
41. Kuehn MR, Bradley A, Robertson EJ, Evans MJ: A potential animal model for Lesch-Nyhan syndrome through introduction of HPRT mutation into mice. Nature 1987, 326:295–298

BEST AVAILABLE IMAGES

Defective images within this document are accurate representations of the original documents submitted by the applicant.

Defects in the images may include (but are not limited to):

- BLACK BORDERS
- TEXT CUT OFF AT TOP, BOTTOM OR SIDES
- FADED TEXT
- ILLEGIBLE TEXT
- SKEWED/SLANTED IMAGES
- COLORED PHOTOS
- BLACK OR VERY BLACK AND WHITE DARK PHOTOS
- GRAY SCALE DOCUMENTS

IMAGES ARE BEST AVAILABLE COPY.

As rescanning documents *will not* correct images, please do not report the images to the Image Problem Mailbox.

(19) Europäisches Patentamt
European Patent Office
Office européen des brevets

(11) EP 0 783 104 A1

(12) EUROPEAN PATENT APPLICATION

(43) Date of publication:
09.07.1997 Bulletin 1997/28

(51) Int. Cl.[6]: G01N 33/68, G01N 33/577, C07K 16/18, C07K 14/47

(21) Application number: 96120269.4

(22) Date of filing: 17.12.1996

(84) Designated Contracting States:
DE FR GB

(30) Priority: 27.12.1995 JP 351296/95

(71) Applicant: ORIENTAL YEAST CO., LTD.
Tokyo (JP)

(72) Inventors:
- Taniguchi, Yoshiyuki
Osaka-fu (JP)
- Fujita, Tuyosi
Ikeda-shi, Osaka-fu (JP)
- Matuo, Yuhsi
Suita-shi, Osaka-fu (JP)

(74) Representative: Thomsen, Dieter, Dr.
Patentanwalt
Postfach 70 19 29
81319 München (DE)

187

(54) Method for assaying soluble amyloid precursor protein

(57) The present invention relates to a method for assaying soluble APP, comprising using an antibody against amyloid β protein (Aβ) or amyloid precursor protein (APP).
In accordance with the present invention, soluble APP can be accurately assayed. Additionally, an assay system composed of a monoclonal antibody recognizing the N-terminus of Aβ and a monoclonal antibody recognizing soluble APP in combination can definitely diagnose the presence or absence of Alzheimer disease.

FIG. 1

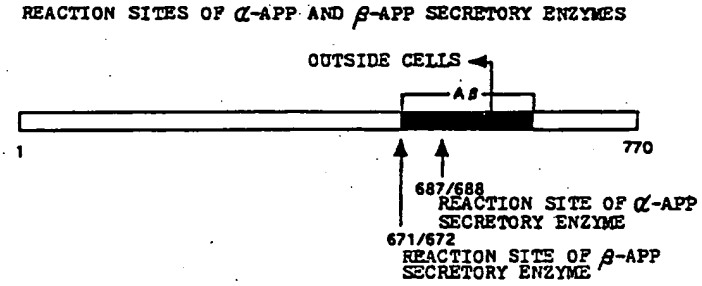

EP 0 783 104 A1

Description

Detailed Description of the Invention

Field of the Invention

The present invention relates to an assay system of amyloid precursor protein (sometimes referred to as "APP" hereinbelow), in particular soluble amyloid precursor protein (sometimes referred to as "sAPP" hereinafter).

The substance sAPP is involved in the generation of amyloid β protein (sometimes referred to as "Aβ" hereinafter) as a component of senior plaque frequently observed in patients with Alzheimer disease. The present invention is highly promising as a useful diagnostic system for Alzheimer disease.

Prior Art

Alzheimer disease, one of the diseases involving dementia due to the denaturation of nervous cells, is observed in the early stage of aging and thereafter, and therefore, the disease has been drawing social concerns in recent years with the increase in the aged population. A great number of senior plaque is observed in the brain of Alzheimer patients, and the senior plaque is primarily composed of Aβ.

A part of the amyloid precursor protein (APP) is cleaved at the proximity of the cell transmembrane region with an APP secretory enzyme to generate Aβ, which is a protein of 39 to 43 amino acids. Fig. 1 schematically depicts the site of the membrane-binding type APP with which the APP secretory enzyme reacts.

α- and β-APP secretory enzymes cleave APP at the sites shown in the figure to discharge α-sAPP and β-sAPP, respectively, outside the cells. It is suggested that after discharge of sAPP, the C-terminus of APP, left on the cell membrane, is incorporated into the inside of the cells and is then decomposed with lysozyme. For processing with the β-APP secretory enzyme, the entire length of Aβ remains on the cell membrane so that the entire length of Aβ is secreted through the decomposition with lysozyme. For processing with the α -APP secretory enzyme, alternatively, the amino acid sequence of the first to the 16-th amino acids from the N-terminus of Aβ is released as a part of sAPP. Therefore, the complete form of Aβ is not secreted. In other words, because of the processing of APP with the α-APP secretory enzyme, APP is metabolized with no generation of Aβ which is the component of senior plaque.

Fig. 2 depicts the amino acid sequence of Aβ(1-40), composed of 40 amino acids. In the figure, the arrow shows the cleavage site between the 16th amino acid (Lys) and the 17th amino acid (Leu) from the N-terminus.

Herein, APP is present in various isomers, primarily including APP 770 described above, APP 751 similarly carrying the Knitz-type protease inhibitor region (KPI region), and APP 695 without the KPI region, all of them being known. In accordance with the present invention, the term "APP" includes all these isomers, but APP 770 is used as one representative example hereinbelow to describe the present invention.

A method for assaying sAPP comprising the combination of Western blotting and immunostaining by the use of antibody and measuring the spot detected on the blotting membrane by means of a scanner, has been examined. From the respect of antibody reactivity, the substance herein assayed is possibly the total of α-sAPP and β-sAPP, but no apparent difference has been found between the sAPP level in clinical samples from normal subjects and that level in samples from Alzheimer patients.

Lannfeld et al. recently carried out the assay of α-sAPP by using the combination of Western blotting and immunostaining by using an antibody reactive with the amino acid sequence of the first to the 15-th amino acids of Aβ. Consequently, they indicated that α-sAPP might possibly serve as a highly specific diagnostic marker of Alzheimer disease, because the level of α-sAPP is significantly lower in the cerebro-spinal fluid of a carrier group with the variation in the amino acid sequence of APP 670/671 known as one of the genetic variants as the etiology of familial Alzheimer disease than the level in the cerebro-spinal fluid of a normal group (Lannfeld L. et al., Nature medicine 1, 829-832 (1995)). However, the assay procedure in the report is very complex, comprising electrophoretic separation of a sample as described above, transfer of the protein on a membrane by Western blotting, immunostaining with an antibody and the detection and assay of α-sAPP by means of a scanner.

Problems to be Solved by the Invention

It is believed that sAPP, in particular α-sAPP from the cleavage with the α-APP secretory enzyme, may potentially be a marker effective for diagnosis of Alzheimer disease, but because the sAPP assay procedure by means of the combination of Western blotting and immunostaining with an antibody as described above is very complex, the sAPP assay is not suitable for practical use. Thus, the inventors have established an sAPP assay system capable of assaying sAPP in a simple manner by using an antibody against sAPP. The assay system provides a practical method for diagnosis of Alzheimer disease.

Brief Description of Drawings

Fig. 1 depicts the reaction sites of Aβ with α- and β-APP secretory enzymes;

Fig. 2 depicts th amino acid sequence of Aβ (1-40); and

Fig. 3 shows th results of sAPP assay.

Means for Solving the Problems

So as to overcome the problems described above, the present inventors have made investigations to prepare a plurality of antibodies against sAPP and establish the immunoassay of sAPP by means of their combinations.

The preparation of antibodies to be used for such assay is carried out according to already known methods. More specifically, immunizing an animal with an immunogen sAPP or a peptide having a part of the amino acid sequence of sAPP, a polyclonal antibody having the reactivity with sAPP is generated in the serum. More preferably, resecting the spleen of the immunized animal, hybridizing an antibody-generating cell contained in the spleen with a myeloma cell to prepare a hybridoma followed by cloning, a homogeneous monoclonal antibody can be recovered at a large scale.

The immunogen to be used for immunizing animals is purified from the culture supernatant of an established cell line from a human nervous cell; otherwise, a part of human APP is prepared by peptide synthesis on the basis of the well known amino acid sequence of human APP, which is then used as such immunogen.

Animals such as goat, sheep, horse, rabbit, rat, and mouse are used for immunization. So as to prepare a monoclonal antibody, generally, mouse or rat is used from the respect of the compatibility with myeloma cells for fusion.

For immunization, an immunogen may be mixed with a variety of adjuvants so as to promote immune response; particularly when a synthetic peptide is to be used as such immunogen, the peptide preliminarily should be cross-linked with carrier proteins such as BSA (bovine serum albumin) and KLH (keyhole limpet hemocyanine) for such use.

The preparation of a hybridoma generating a monoclonal antibody is carried out according to the method described in Koehler, G. and Milstein, C., Nature 256, 495 (1975). More specifically, a splenocyte resected from an immunized animal is mixed and fused with a myeloma cell in the presence of polyethylene glycol. The hybridoma generated is selectively grown in a HAT medium (containing 1×10^{-4} M hypoxanthine, 4×10^{-7} M aminopterin, and 1.6×10^{-3} M thymidine), and the cell involving the secretion of an antibody into the culture supernatant under observation is cloned by the limited dilution method.

The thus prepared hybridoma can generate a monoclonal antibody from the culture supernatant or the ascites fluid recovered from the transplant of the hybridoma into the animal from which the myeloma cell is derived.

The anti-serum of the immunized animal, the cultur supernatant of th hybridoma, and th antibody from the ascites fluid may be purified by known purification methods such as ammonium sulfate salting out, ion exchange chromatography, and affinity chromatography.

The immunoassay of sAPP in accordance with the present invention comprises immobilizing one antibody onto an insoluble carrier, capturing a subjective assaying substance in a sample onto the antibody, thereafter reacting the other labeling substance-bound antibody with the subjective substance and detecting the activity of the labeling substance bound onto the insoluble carrier thereby assaying the subjective substance. The insoluble carrier to be used for immobilizing the antibody includes those of forms such as tube, beads, ball, and well, and as the material thereof, use may be made of plastics, glass, silicon, and latex.

Alternatively, the labeling substance is bound to the antibody to detect the antigen captured on the insoluble carrier. The labeling substance includes enzyme, radioactive substance, fluorescent substance, luminescent substance and the like, and the assay of the activity of the labeling substance can yield the measurement of the level of the antigen captured.

If desired, still further, biotin may be bound to the antibody to prepare a biotin-labeled antibody, with which avidin labeled with a labeling substance reacts to assay the antigen level, in addition to the direct binding of the labeling substance to the antibody.

So as to carry out the assay method of the present invention, for example, an anti-sAPP antibody is immobilized on a carrier, and onto the immobilized antibody is captured the sAPP antigen in a sample, and a labeled anti-Aβ antibody reacts with the resulting antigen-antibody complex. If the amino acid sequence of the sAPP antigen contains the amino acid sequence corresponding to Aβ (for example, α-sAPP), the labeled anti-A β antibody is bound to the sAPP antigen. Then, by activating and assaying the labeling substance through color development or fluorescent emission, the sAPP antigen is assayed quantitatively and qualitatively.

The present invention is to provide not only an assay method of sAPP, but also an sAPP assay kit including a variety of antibodies, buffer solutions, labeling and activating reagents, and other necessary substances to be used for the assay, and a kit for detecting Alzheimer disease, and the like. A kit incorporating an anti-sAPP monoclonal antibody and an anti-Aβ monoclonal antibody is useful for establishing the diagnosis of Alzheimer disease, and the application thereof is highly promising for health check programs for aged people.

The present invention will now be described in detail in examples hereinbelow, but these examples are not intended to limit the present invention only to sAPP derived from APP 770, excluding other isomers.

Example 1

Preparation of monoclonal antibodies against Aβ and sAPP

1. Materials

Immunogen

Regarding Aβ, a peptide having the amino acid sequence of the first to the 40-th amino acids of Aβ was prepared by peptide synthesis, which was used as an immunogen. Regarding sAPP, culturing a human urinary bladder cancer cell EJ-1 in a serum-free RPMI 1640 medium, sAPP was purified from the culture supernatant by activated Red Sepharose column chromatography and Sephadex QA 824 column chromatography.

2. Immunization

The immunization procedure for preparing Aβ antibody will be described below. To a solution (0.9 ml) containing Aβ (1 mg) was added an equal amount of Freund complete adjuvant, for sufficient mixing to prepare an emulsion, which was then injected intraperitoneally at 1.8 ml/mouse into a Balb/c mouse for immunization. Then, an emulsion of a solution containing the solution (0.6 ml) containing Aβ (1 mg) and incomplete adjuvant was injected subcutaneously as an immunogen at 1.2 ml/mouse every three weeks. After such immunization procedure was repeated several times, a PBS solution containing Aβ (100 μg) was boosted intraperitoneally into the mouse at 0.2 ml/mouse as the final immunization.

The immunization procedure for preparing sAPP antibody will be described below. To a solution (0.75 ml) containing sAPP (150 μg) was added an equal amount of Freund complete adjuvant, for sufficient mixing to prepare an emulsion, which was then injected intraperitoneally at 1.5 ml/mouse into a Balb/c mouse for immunization. Then, an emulsion of a solution containing the solution (0.4 ml) containing sAPP (75 μg) and incomplete adjuvant was injected as an immunogen subcutaneously at 0.8 ml/mouse every three weeks. After such immunization procedure was repeated several times, a PBS solution containing sAPP (62.5 μg) was boosted intraperitoneally into the mouse at 0.3 ml/mouse as the final immunization.

3. Cell fusion

Fusion

Three days after the final immunization, spleen was aseptically resected from the mous , which was finely chopped int small pieces for cell extrusion. The extruded cells after passing through nylon mesh were then washed several times in an RPMI 1640 medium for re-suspension to prepare a suspension of the spleen cells. P3-X63-Ag8-653 was used as a murine myeloma cell for fusion. The myeloma cells to be used for such purpose include for example P3-X63-Ag8-U1 and P3-Ns-1/Ag4-1, which are all known and commercially available.

Cell fusion was carried out according to the method of Koehler. G. et al. More specifically, spleen cells and the suspension of murine myeloma cells, preliminarily washed three times in a serum-free RPMI 1640 medium, were mixed together at a cellular ratio of 5:1. The cells were precipitated by centrifuging to remove the supernatant medium, and the remaining cells were mildly loosened, to which was then gradually mixed 50 % polyethylene glycol 6000 (1 ml; manufactured by Boehringer, Co. Ltd.) for fusion. Furthermore, adding gradually an RPMI 1640 medium (10 ml) containing 10 % serum to dilute the resulting mixture followed by centrifuging, the resulting supernatant was discarded. The cells were suspended in a HAT medium (50 ml) containing 1×10^{-4} M hypoxanthine, 4×10^{-7} M aminopterin, and 1.6×10^{-3} M thymidine, and the resulting suspension was divided at 0.5 ml/well into a 48-well culturing plate.

Antibody screening of the culture supernatant

After the initiation of the culturing in the HAT medium, the medium was exchanged to fresh such medium or fresh medium was added at an appropriate time. About 10 days later, screening of antibodies in the culture supernatant was conducted. After adding and immobilizing an antigen solution (5-10 μg/ml) into a microtiter plate for ELISA, 1 % bovine serum albumin was used for blocking. Supernatants sampled from the culture plate were added at 100 μl into the microtiter plate, which was then left to stand at room temperature for 2 hours. After washing, 100 μl of horse radish peroxidase (POD)-labeled rabbit anti-mouse IgG antibody (10 μg/ml) was added into each well, which was then left to stand at room temperature for 2 hours. After washing the plate, 100 μl each of a substrate solution(100 mM phosphate buffer solution, pH 6.0; 1 mg/ml o-phenylene diamine, 1 μl/ml H_2O_2) was added into the well for reaction for an appropriate period of time, followed by addition of 100 μl of 4N HCl to terminate the reaction. The absorbance at 492 nm of each well of the plate was measured to identify antibodies contained in each sample on the basis of the measurement.

Cloning

Cloning of the thus recovered hybridoma by the method described above was carried out by limited dilution. For cloning, a suspension of the spleen cells from a Balb/c mouse to a final concentration of about 1×10^6 cells /ml was used as a feeder cell, and the hybridoma was diluted with the feeder cell suspension to 0.5 cell/ml. The hybridoma diluting solution was divided at

0.1 ml into a 96-well culture plate, and about one week later, the formation of colonies was confirmed under microscopic observation. Then, a well of monoclones was confirmed of its antibody generation by the method described above. Single clone of each of antibody-generating hybridomas of Aβ and sAPP, was confirmed.

The thus recovered hybridomas were both new fused cells and named individually as mouse-mouse hybridoma β AP/OM16 and mouse-mouse hybridoma APP/OM84. These hybridomas were then deposited internationally as FERM BP-4673 and FERM BP-4672 in the Bioengineering and Industrial Technology Research Institute, the Agency of Industrial Science and Technology, Japan.

Example 2

Characterization of antibodies

The cells of the new hybridomas prepared as described above were intraperitoneally administered (1 to 3 x 10^6 cells/mouse) to mice preliminarily given mineral oil (0.5 ml) intraperitoneally. Six to 20 days later, ascites fluid containing antibodies was collected to purify monoclonal antibodies from the ascites fluid by using a protein-A column according to a routine method.

The characterization of the generated monoclonal antibodies brings about the results as follows;

anti-Aβ antibody;	subclass IgG2b/χ
specificity;	reactivity with both of Aβ and sAPP (recognizing the amino acid sequence of the first to the 16-th amino acids from the N-terminus of Aβ, the amino acid sequence being common to both of Aβ and sAPP.)
anti-sAPP antibody;	subclass IgG2a/χ
specificity;	specific reactivity with sAPP (recognizing the amino acid sequence present in sAPP, excluding the amino acid sequence of the first to the 16-th amino acids from the N-terminus of Aβ; thus, recognizing β-sAPP and β-sAPP-containing substance (α-sAPP)).

Example 3

Antibody labeling with biotin

So as to establish the assay of sAPP using the generated antibodies, the antibodies were labeled with biotin. Firstly, the concentration of the antibodies was adjusted to about 5 mg IgG/ml, which was then dialyzed against 100 mM carbonate buffer solution, pH 9.0. A biotin-labeling reagent (NHS-LC-Biotin II, manufactured by PIERCE Company) was dissolved in dimethyl formamide to a final concentration of 30 mg/ml, which was then added at 10 µl into 1 ml of the antibody solution for thorough mixing. The resulting solution was left to stand in ice for 2 hours for reaction. The solution was then dialyzed against PBS to remove the unreactiv biotin-labeling reagent.

Example 4

Assaying of soluble APP

Anti-sAPP antibody was diluted to 10 µg/ml by using PBS, which was then divided at 50 µl each into a 96-well microtiter plate, and the plate was left to stand overnight at 4 °C. After discarding the solution in the wells, each well was filled with PBS containing 0.1 % BSA (0.1 % BSA-PBS) and was then left to stand at room temperature for 3 hours. Each well was washed in PBS containing 0.1 % Tween-20 (0.1 % Tween-PBS) five times, to which was then added 50 µl of sAPP antigen diluted with 0.1 % BSA-PBS to 10, 5, 1, 0.5, 0.1, 0.05, and 0.01 µg/ml. Each well was left to stand at room temperature for 2 hours, prior to washing in 0.1 % Tween-PBS five times. 50 µl of each of biotin-labeled anti-Aβ antibodies diluted to 10 µg/ml by using 0.1 % Tween-PBS was added to each well, which was then left to stand at room temperature for 2 hours.

After washing each well five times in 0.1 % Tween-PBS, 50 µl of Vectastain ABC kit Elite PK-6100 (manufactured by Vector Company) diluted to 150- fold by using 0.1 % Tween-PBS was added to each well, which was then left to stand at room temperature for one hour. After washing each well five times in 0.1 % Tween-PBS, 100 µl of a substrate solution (100 mM phosphate buffer solution, pH 6.0, 1 mg/ml o-phenylene diamine, 1 µl/ml H_2O_2) was added to each well for reaction at room temperature for an appropriate period of time, followed by addition of 100 µl of 4N HCl to each well to terminate the reaction. The absorbance of each well at 492 nm was measured with a plate reader.

The results of the measurement are shown in Fig. 3. The results indicate that sAPP antigen level can be measured accurately.

Effects of the Invention

In accordance with the present invention, sAPP can be measured accurately at a higher sensitivity in a simple manner. An immunoassay system composed of the anti-sAPP monoclonal antibody and the anti-Aβ monoclonal antibody in combination can screen accurately Alzheimer patients, so the immunoassay system can be effectively used for diagnosis of Alzheimer disease.

Claims

1. A method for assaying soluble APP, comprising using an antibody against amyl id β-protein or sol-

uble amyloid precursor protein (APP).

2. A method for assaying soluble APP according to claim 1, using an antibody having the antigen recognition site which is the amino acid sequence in common to amyloid β-protein and soluble APP or which is a specific amino acid sequence to soluble APP.

3. A method for assaying soluble APP according to any one of claims 1 and 2, wherein the assaying subject is soluble APP having a part of the amino acid sequence of amyloid β-protein at the amino terminus thereof.

4. A method for assaying soluble APP according to any one of claims 1 to 3, wherein the assaying subject is APP solubilized through the cleavage of the amyloid β-protein between the 16-th lysine and the 17-th leucine from the amino terminus thereof.

5. A method for assaying soluble APP according to any one of claims 1 to 4, comprising immobilizing one antibody onto an insoluble carrier, capturing a subjective assaying substance in a sample onto the antibody, thereafter reacting the other labeling substance-bound antibody with the subjective substance and detecting the activity of the labeling substance bound onto the insoluble carrier thereby assaying the subjective substance.

6. A method for assaying soluble APP according to any one of claims 1 to 5, wherein soluble APP is measured for diagnosing Alzheimer disease.

7. A method for assaying soluble APP according to any one of claims 1 to 6, wherein the antibody to be used is a monoclonal antibody.

8. A monoclonal antibody specifically recognizing the amino acid sequence of amyloid β-protein from the first to the 16-th amino acids from the amino terminus thereof.

9. A monoclonal antibody recognizing a part of the amino acid sequence of amyloid β protein present on soluble APP, excluding the amino acid sequence thereof from the first to the 16-th amino acids from the amino terminus thereof.

10. A method for assaying soluble APP according to claim 7, wherein the monoclonal antibody is a monoclonal antibody according to claims 8 or 9.

11. Hybridoma cells, mouse-mouse hybridoma β AP/OM16 and mouse-mouse hybridoma APP/OM84, generating a monoclonal antibody according to claims 8 or 9, and the generated antibodies.

12. A method for assaying soluble APP, comprising immobilizing one antibody of th monoclonal antibodies generated by hybridoma cells according to claim 11 onto an insoluble carrier, capturing a subjective assaying substance in a sample onto the antibody, thereafter reacting the other labeling substance-bound antibody with the subjective substance and detecting the activity of the labeling substance bound onto the insoluble carrier thereby assaying the subjective substance.

13. A kit for detecting Alzheimer disease, containing a monoclonal antibody according to claims 8 or 9.

FIG. 1

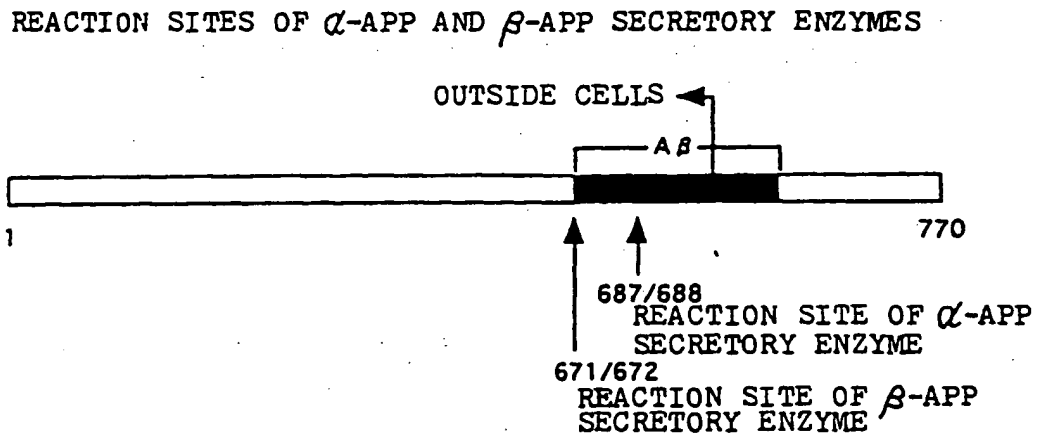
REACTION SITES OF α-APP AND β-APP SECRETORY ENZYMES
OUTSIDE CELLS
Aβ
1
770
687/688
REACTION SITE OF α-APP
SECRETORY ENZYME
671/672
REACTION SITE OF β-APP
SECRETORY ENZYME

FIG. 2

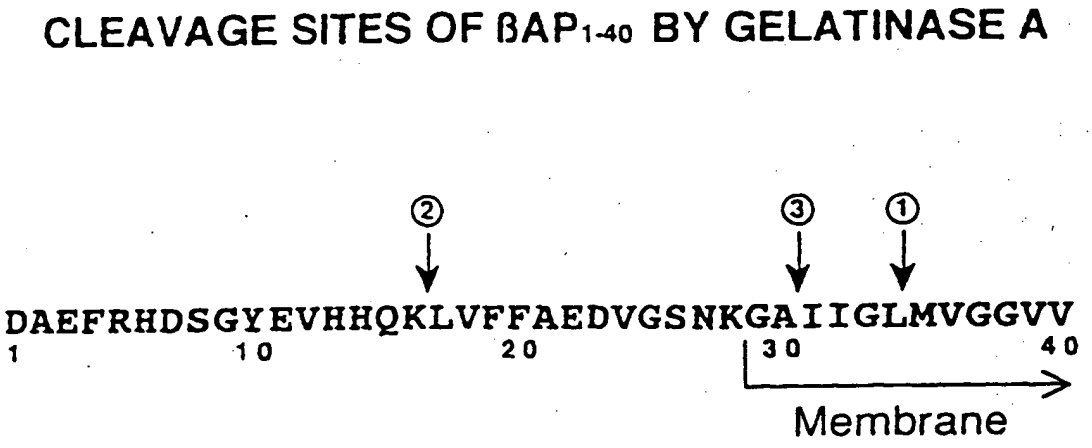
CLEAVAGE SITES OF βAP1-40 BY GELATINASE A
②
③
①
DAEFRHDSGYEVHHQKLVFFAEDVGSNKGAIIGLMVGGVV
1
10
20
30
40
Membrane

FIG. 3

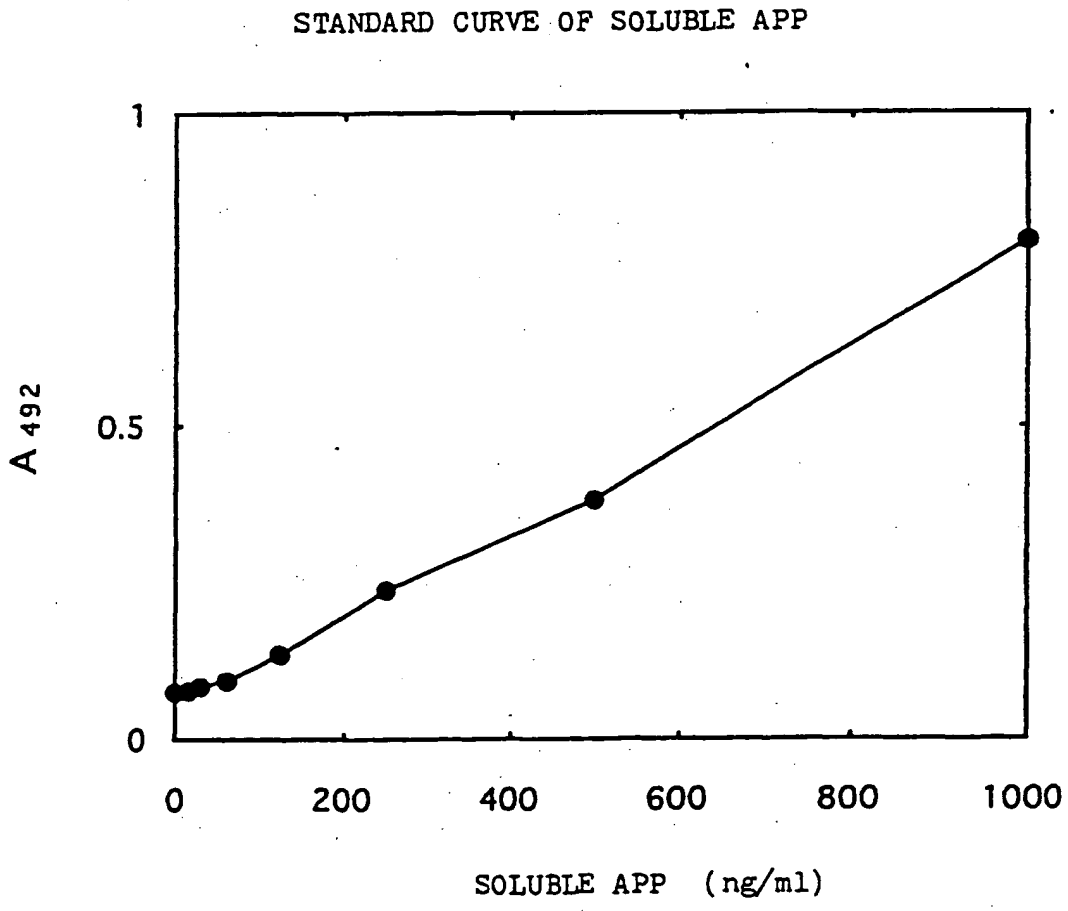
STANDARD CURVE OF SOLUBLE APP
A 492
1
0.5
0
0
200
400
600
800
1000
SOLUBLE APP (ng/ml)

European Patent Office

EUROPEAN SEARCH REPORT

Application Number
EP 96 12 0269

DOCUMENTS CONSIDERED TO BE RELEVANT

Category	Citation of document with indication, where appropriate, of relevant passages	Relevant to claim	CLASSIFICATION OF THE APPLICATION (Int.Cl.6)
X	NAT. MED. (N. Y.) (1995), 1(8), 829-32 CODEN: NAMEFI;ISSN: 1078-8956, 1995, XP002029703 LANNFELT, LARS ET AL: "Decreased. alpha.-secretase -cleaved amyloid precursor protein as a diagnostic marker for Alzheimer 's disease" * page 831, right-hand column, paragraph 2 * * the whole document *	1-13	G01N33/68 G01N33/577 C07K16/18 C07K14/47
Y	SCIENCE, vol. 255, no. 5045, 7 February 1992, pages 728-730, XP000573983 GOLDE T E ET AL: "PROCESSING OF THE AMYLOID PROTEIN PRECURSOR TO POTENTIALLY AMYLOIDOGENIC DERIVATIVES" * figure 3 *	1-13	
X	WO 94 07144 A (US ARMY) 31 March 1994 * page 23; claims *	8,11	TECHNICAL FIELDS SEARCHED (Int.Cl.6)
A	* page 2, paragraph 2 - page 2, paragraph 3 *	1-13	G01N C07K
A	WO 93 21526 A (ATHENA NEUROSCIENCES INC ;LILLY CO ELI (US)) 28 October 1993 * the whole document *	1-13	
A	SCIENCE, vol. 255, no. 5045, 7 February 1992, pages 726-728, XP000573982 ESTUS S ET AL: "POTENTIALLY AMYLOIDOGENIC, CARBOXYL-TERMINAL DERIVATIVES OF THE AMYLOID PROTEIN PRECURSOR" * the whole document *	1-13	

The present search report has been drawn up for all claims

Place of search	Date of completion of the search	Examiner
THE HAGUE	21 April 1997	Hoekstra, S

CATEGORY OF CITED DOCUMENTS

X : particularly relevant if taken alone
Y : particularly relevant if combined with another document of the same category
A : technological background
O : non-written disclosure
P : intermediate document

T : theory or principle underlying the invention
E : earlier patent document, but published on, or after the filing date
D : document cited in the application
L : document cited for other reasons

& : member of the same patent family, corresponding document

EPO FORM 1503 03.82 (P04C01)